The Development of a Sample Controlled Differential Scanning Calorimeter and its Application to the Study of Different Reaction Types

James. J. Rooney BSc (Hons)

A thesis submitted in partial fulfilment of the requirements for the degree of Master of Philosophy

School of Applied Science

The University of Huddersfield

July 2015

Contents

Page number

Chapter 3 Reactions that take place with a change in mass

Chapter 4 Reactions that take place without a change in mass

Chapter 5 Conclusions and Suggestions for Further Work

Chapter 6 References

Chapter 7 Conferences Attended, Presentations and Publications

Acknowledgements and Thanks

I would like to thank Professor Ted Charsley for his continued support throughout my working life. His patience and guidance has put me on the right path when on many occasions I may have drifted. Likewise, Dr Gareth Parkes deserves thanks for his efforts with this project, without which my thesis would not have been possible. Thanks are also due to Professor Peter Laye for his helpful comments.

A mention must also be made to the support from Hayley Markham whose constant worry always made me feel I was in a better place.

Extreme gratitude is directed towards my parents and family. Without their continued support and help in following my goal, I would not be where I am today.

To my father, Jim Rooney. your industry and passion for everything you do are what I look up to. The greatest role model I could ever need. Thank you for your support over the years.

To my children, Christopher and Kathryn, you are always an inspiration to me. The unconditional love and support you give me makes me a proud father. Always strive to do better than me! Never give up.

To Jeni and Katy, thank you for the major role in keeping me focussed during this project. The support offered has been invaluable.

Finally, this thesis is dedicated to the memory of my mother, Loraine Rooney who passed away at the start of this study. Her attitude and thirst for life is unmeasurably missed.

Abstract

A new sample controlled DSC (SC-DSC) system has been developed, which for the first time has enabled the benefits of sample controlled thermal analysis to be extended to the widely used technique of DSC. The system was based on a heat flux DSC cell interfaced to an in-house control and data processing system. Careful optimisation of the instrument parameters during the development stages minimised the potential problem of shifts in the DSC baseline when the temperature programme is changed. This has enabled the rate of heating to be controlled directly from the DSC signal and has also allowed controlled cooling to be incorporated. The difficulty of making baseline corrections in sample controlled experiments has been resolved by the implementation of the facility to replay the temperature programme for an experiment.

The potential of the new SC-DSC system was evaluated by studying a wide range of reaction types. The first group consisted of reactions taking place with a change in mass, including endothermic dehydration, dehydroxylation and decomposition reactions and exothermic decomposition and oxidation reactions. The results were compared with those obtained by sample controlled thermogravimetry. Similar profiles were obtained using both techniques and the ability of SC-DSC to provide direct information on reaction mechanisms was demonstrated

The second group included both endothermic and exothermic reactions that occurred without any significant mass change and which therefore could not be studied by existing sample controlled techniques. Although it proved difficult to control the rapid fusions of metal and organic DSC standards with the present equipment, promising results were obtained for the fusion of both organic and inorganic phase change materials which occur over a broader temperature range.

SC-DSC was found to be successful in preventing the ignition reactions in number of exothermic reactions which could occur under linear heating condition, thus providing a means to investigate the systems in more detail than is possible with conventional thermal analysis techniques. In addition, the ability to control the curing reaction of an epoxy resin should allow the development of temperature profiles to enable samples to be cured at a selected rate.

List of Figures and Tables

Figures

Tables

Chapter 1 Introduction

1.1 Overview of Thermal Analysis Techniques

Thermal analysis methods form a family of powerful techniques for the characterisation of a wide range of materials. In conventional thermal analysis a property of a sample is monitored as the sample is heated or cooled at a linear rate. A wide range of properties may be measured and the most important of these are summarised in Table 1.1.

Table 1.1 – Thermal Analysis Techniques

Property	**Technique**	**Abbreviation(s)**
Temperature Difference	Differential Thermal Analysis	DTA
Heat Flow Rate	Differential Scanning Calorimetry	DSC
Mass	Thermogravimetry	TG
Gas flow	Evolved Gas Analysis	EGA
Dimensional and Mechanical	Dynamic Mechanical Analysis Thermomechanical Analysis Thermodilatometry	DMA TMA TD
Electrical	Dielectric Thermal Analysis Thermally Stimulated Current	DEA TSC
Optical	Thermoptometry	
Structure	Thermodiffractometry Thermospectrometry	
Magnetism	Thermomagnetometry	TM
Sound	Thermosonimetry	TS

Differential scanning calorimetry (DSC) is by far the most widely used technique since it can study any reaction that takes place with a change in energy [1] These include solid-solid phase transitions, fusion, crystallisation, curing and decomposition reactions. The most important areas of application are in the study of polymers [2] and pharmaceuticals [3,4] but the technique has also been extensively used in the study of a wide range of materials including catalysts, coals and carbons, fuels, inorganics, liquid crystals, minerals and superconductors.

When a reaction takes place, there must be a change in the energy processes of the transformation regardless of any mass changes that can occur. Processes that take place can be endothermic whereby the sample absorbs energy or exothermic in which the sample emits energy. A plot indicating both these types of reactions is shown in Fig. 1.1.

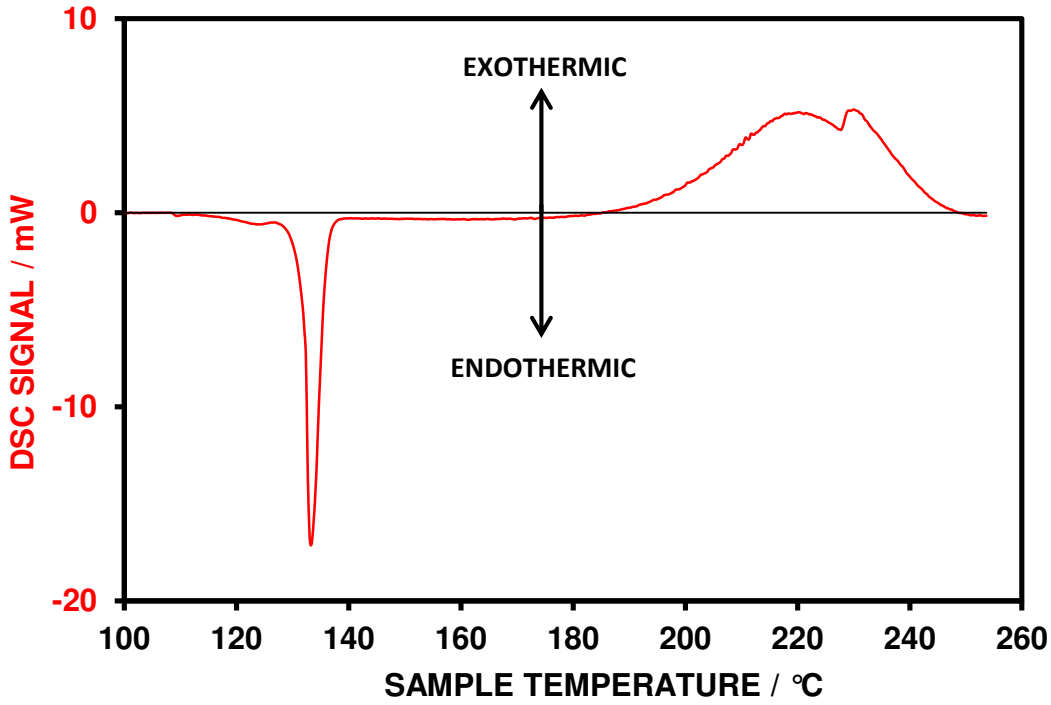

Fig. 1.1 Example plot indicating Exothermic and Endothermic Transitions by DSC

1.2 Principles of Differential Scanning Calorimetry (DSC)

The forerunner of the DSC was known as a differential thermal analysis (DTA). The concept of the modern DTA was introduced by W. C. Roberts-Austen (1899) [5] when he produced an instrument in which the sample and reference material could be heated in close proximity within the same temperature environment. This ensured that the temperature difference between the sample and reference (ΔT = Ts-Tr) was minimised. The advantage of this arrangement meant that as the sample reacted, it either absorbed heat or released heat depending on its transition thus creating a difference in ΔT. When the transition of the sample was complete, then the Ts-Tr would be reduced to that of its pre-transitional state. Fig. 1.2 shows a typical response of both the sample and reference thermocouples during the endothermic fusion reaction of aluminium.

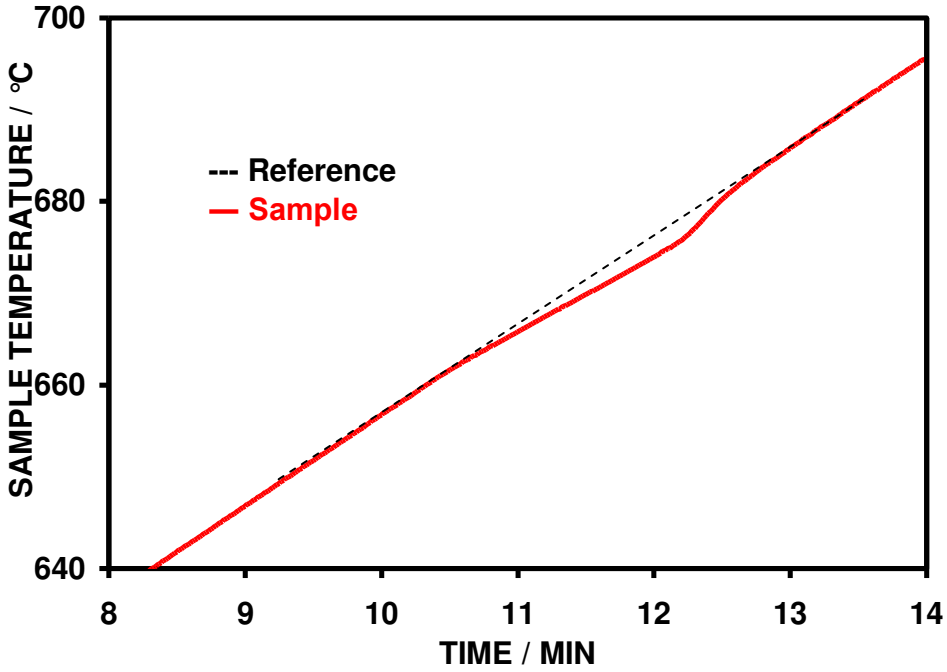

Fig. 1.2 The Response of the Sample and Reference Thermocouples during the melting of aluminium

In early DTA apparatus, a single block with symmetrical cavities for the sample and reference was heated in the furnace. The block acted as a suitable heat-sink, with the sample and reference materials in sample holders of low thermal conductivity placed within the cavities [6]. The thermocouple for the sample and reference were

placed directly into the sample holder contents and ΔT can then be determined. A typical ΔT curve is shown in Fig. 1.3 as the net response of the sample and reference thermocouples.

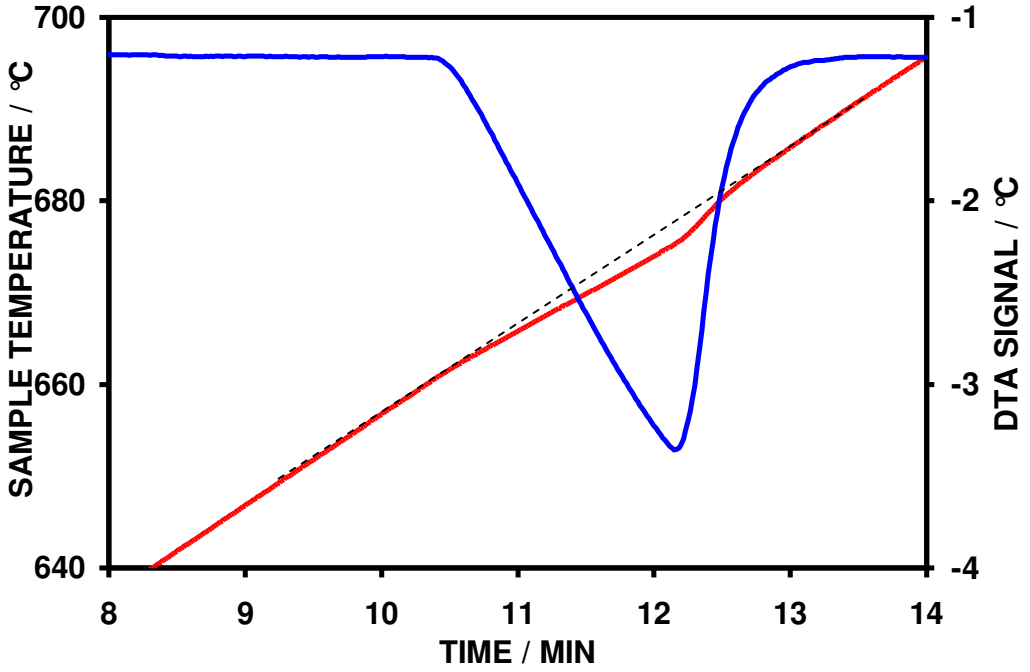

Fig. 1.3 Response of the sample thermocouple during the melting of a sample and the resultant DTA signal (sample – reference temperatures)

There are a few considerations when using this type of apparatus. The reference material should undergo no thermal events over the temperature range of investigation. Also, there should be no reaction between the sample and reference materials with the sample holder and ideally the thermal conductivity and heat capacity of the sample and reference should be similar. Other factors such as sample density, packing in the crucible, particle size etc., can create thermal events which can affect the quality of the baseline.

The considerations outlined above were in the main overcome by the developments of calorimetric DTA, also referred to as Boersma DTA [7]. Boersma suggested that the heat of reaction measured outside of the sample be led away from the sample chamber using thermocouple wires from which ΔT can be determined with the heat of reaction conducted through the sample holder using a conductive plate material. This configuration had the advantage that the output signal (ΔT) was less dependent

on the thermal properties and interactions of the sample but as the thermocouple system was isolated from direct contact with the sample, the response was much slower.

There are two types of DSC apparatus commonly used which operate using different modes of action. In power-compensated DSC, the sample and reference temperatures are maintained so that ΔT remains zero throughout the temperature controlled programme. The power-compensated DSC instrument is a measure of the power difference that is supplied to both the sample and reference system. To accommodate this, the sample and reference are required to have their own individual heaters beneath the sample base and the DSC signal is directly related to the difference in power between the sample and reference heaters in maintaining ΔT = 0. In heat flux DSC, the sample and reference are connected by a low resistance heat flow path (a metal disc). The assembly is enclosed in a single furnace. Enthalpy or heat capacity changes in the sample cause a difference in its temperature relative to the reference that can be measured with thermocouples situated beneath the sample and reference platforms.

1.3 Overview of Sample Controlled Thermal Analysis

In conventional thermal analysis it is often necessary to use slow heating rates and small sample masses in order to avoid the deleterious effects of thermal gradients or self-generated atmospheres on the experimental resolution. This is particularly true of gas-solid reactions e.g. the oxidation of coals and chars, or of finely divided metals where self-heating can lead to ignition.

These limitations have led to the development of an alternative approach called sample controlled thermal analysis (SC-TA) [8] where the rate of change of a property of a sample is made to follow a pre-determined programme and this controls the heating of the sample. This approach has the advantage of reducing both temperature and concentration gradients in a sample and is of particular value in minimising self-heating in oxidation reactions.

Fig. 1.4 shows a schematic comparison of conventional TA and SC-TA. In conventional TA the behaviour of the sample has no effect on the heating rate while in a SC-TA experiment there is feedback from the rate of some monitored process of the sample to the furnace temperature.

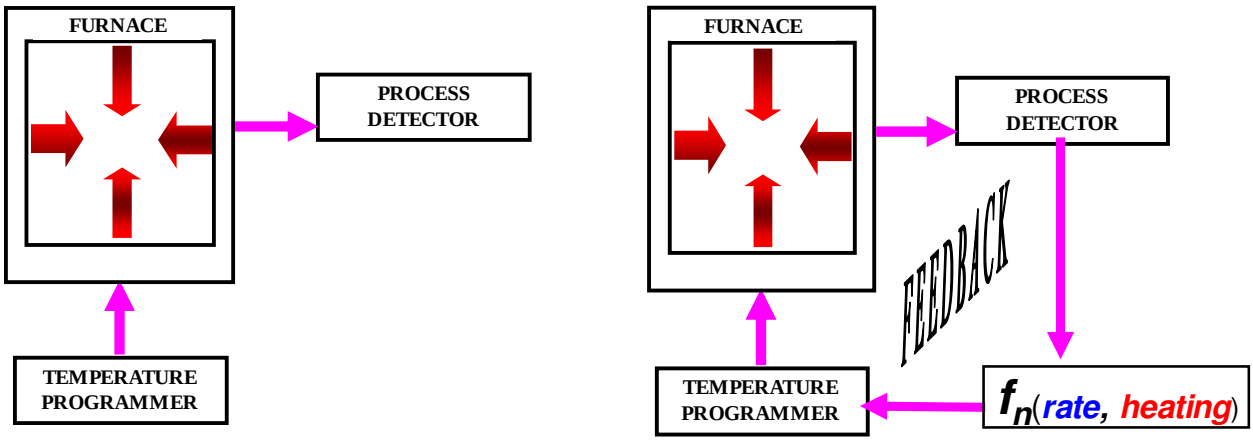

Fig. 1.4 Schematic comparison of the approaches of conventional thermal analysis and sample controlled thermal analysis.

The technique was pioneered independently in the 1960's by the Pauliks in Hungary who patented an approach called Quasi-Isothermal Quasi-Isobaric Thermal Analysis [9,10] and by Rouquerol in France who developed a technique for use at reduced pressures called Constant Rate Thermal Analysis [11,12]. A range of sample controlled techniques based on evolved gas analysis [13], thermogravimetry (TG) [14], thermomicroscopy [15] have also been developed which include a technique where the concentration of the reactive gas is used to control the reaction [16].

The enhanced resolution which can be obtained using the sample controlled technique is illustrated in Fig. 1.5 where TG and SC-TG curves for the dehydration of strontium hydroxide octahydrate are compared [17]. The techniques have been applied to a wide renge of materials including: adsorbents [18], carbons [19,20], catalysts [21,22], cements [23], ceramics [24,25], diesel fuels [26], inorganics [27,28], materials sythesis [29], minerals [30,31], polymers [32] and pyrotechnic components [17]. In addition, Constant Rate Thermal Analysis has proved of particular value in deriving reliable kinetic data [33,34].

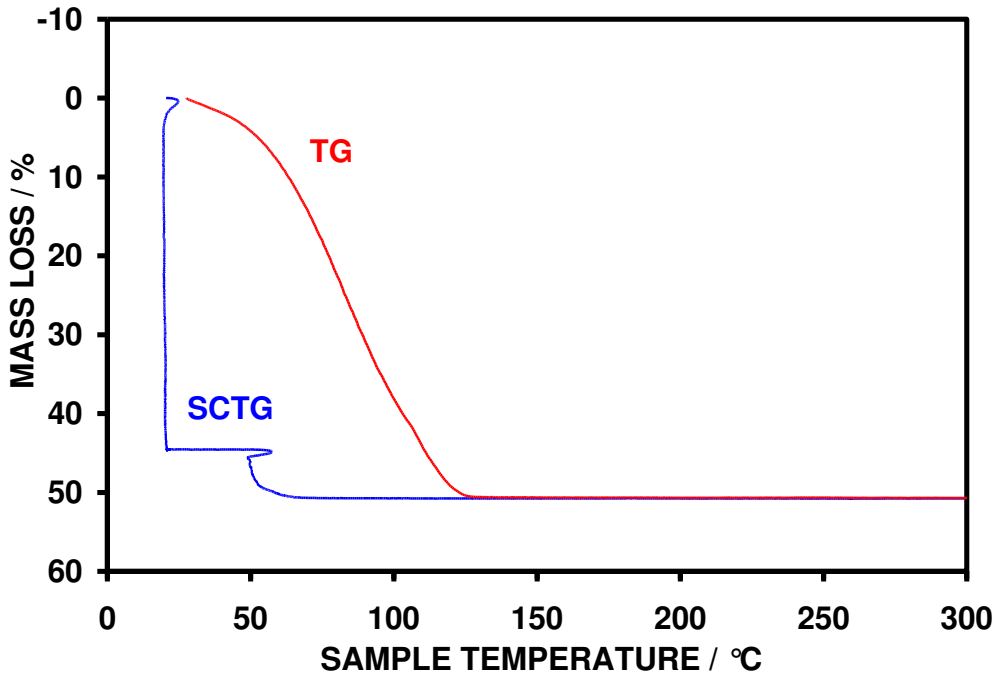

Fig. 1.5 TG and SC-TG curves for the dehydration of strontium hydroxide octahydrate [17] (sample mass, 20 mg; atmosphere, argon)

1.4 Aim of the Project

To date the SC-TA techniques have largely been based on the measurement of changes in gas concentration or mass. The aim of this project is to develop an apparatus which will enable the SC-TA technique to be applied to DSC which is the most powerful and widely used thermal analysis method.

Chapter 2 Instrumentation

2.1 Instrumentation

The heat flux DSC system used was that of a commercial Du Pont DSC 910 cell base unit (Fig. 2.1).

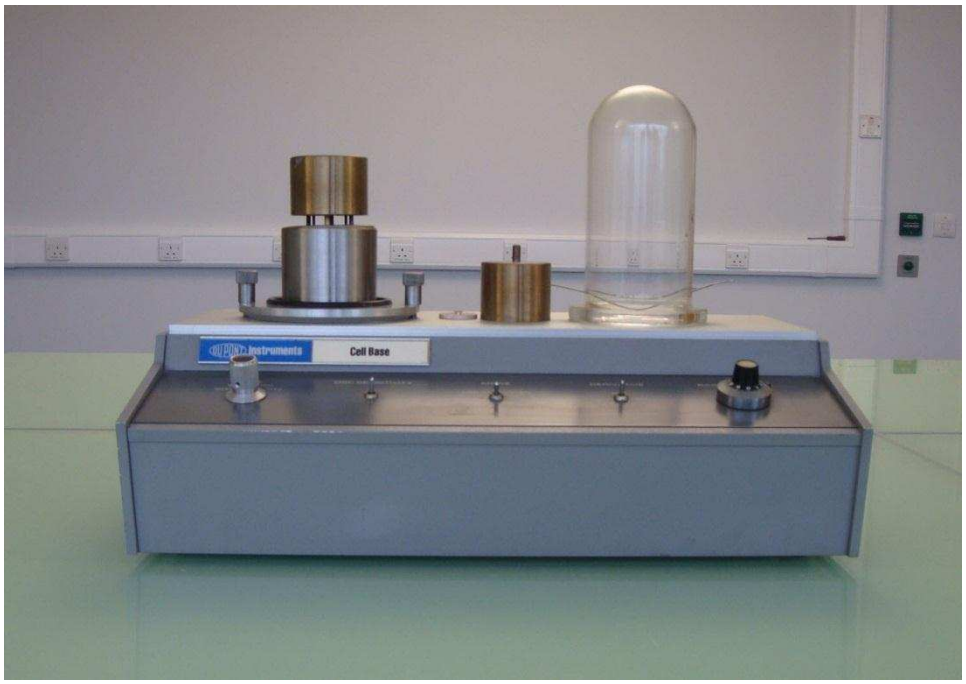

Fig. 2.1 Du Pont Heat Flux DSC 910 Cell Base

The DSC cell comprised of a constantan disc as the primary heat transfer element which is enclosed in a silver heating block with a silver lid (Fig. 2.2). The sample and reference sit on raised platforms on the disc and the heat flow is transferred through the disc into the sample and reference. The differential heat flow to the sample and reference is monitored using chromel-constantan thermocouples formed by the junction of the constantan disc and a chromel wafer covering the underside of each platform. Chromel and alumel wires are connected to the chromel wafers and the junction beneath the sample platform monitors the sample temperature. The heating of the sample chamber is achieved using a resistively wound heater within the silver heating block arrangement and is controlled using a Platinel II control thermocouple.

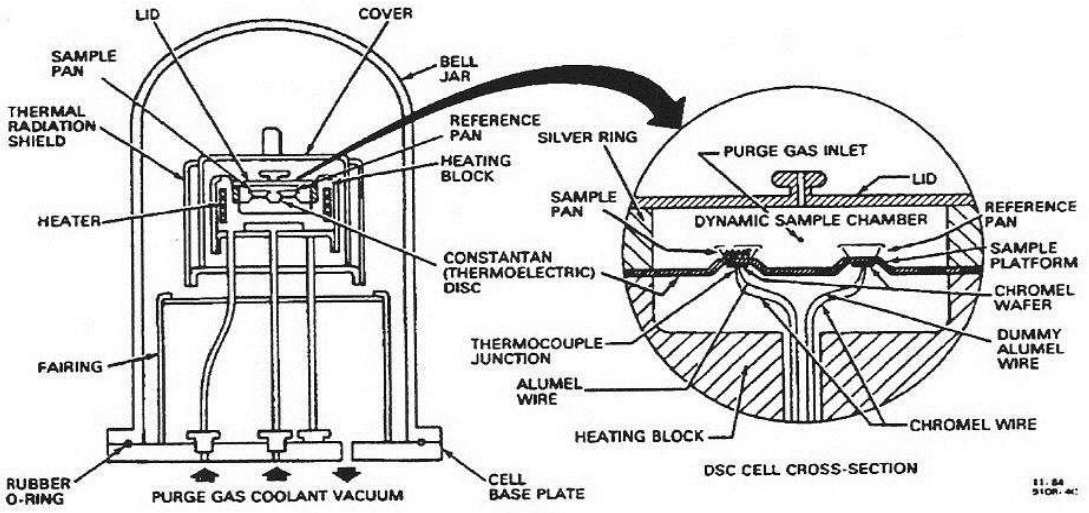

Fig. 2.2 DSC Head and Furnace Arrangement in Du Pont DSC 910 Cell [35]

This cell was particularly favourable for SC-TA studies as it has a small volume and the constantan disc is in contact with the heating block enabling fast response from the heating block to the sample and good control in following the temperature programme. This cell was chosen not only for its sensitivity and baseline stability but also for its ease of interfacing to the in-house control and data processing system (see section 2.3).

2.2 Modification of the Du Pont DSC 910 Base Unit

Modifications included removal of the integral power supply, amplifier and linearization components. An external power supply, programmer and amplifier were attached so as to provide a means of heating and monitoring the thermocouple system. Fig. 2.3 shows the pin positions of the wiring arrangement that was used as a guide to modify the instrument with the schematic of the additional components shown in Fig. 2.4.

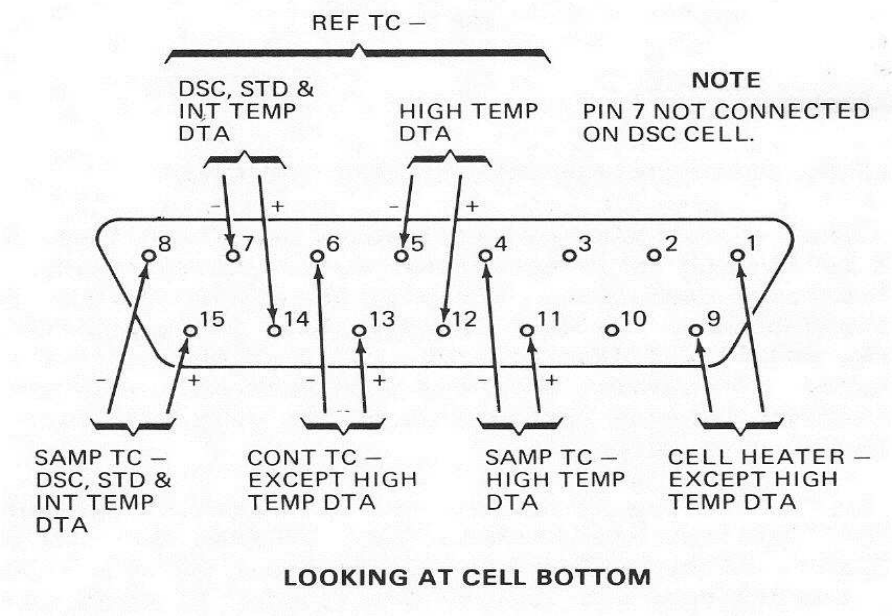

Fig. 2.3 Wiring arrangement for controlling the Du Pont DSC 910

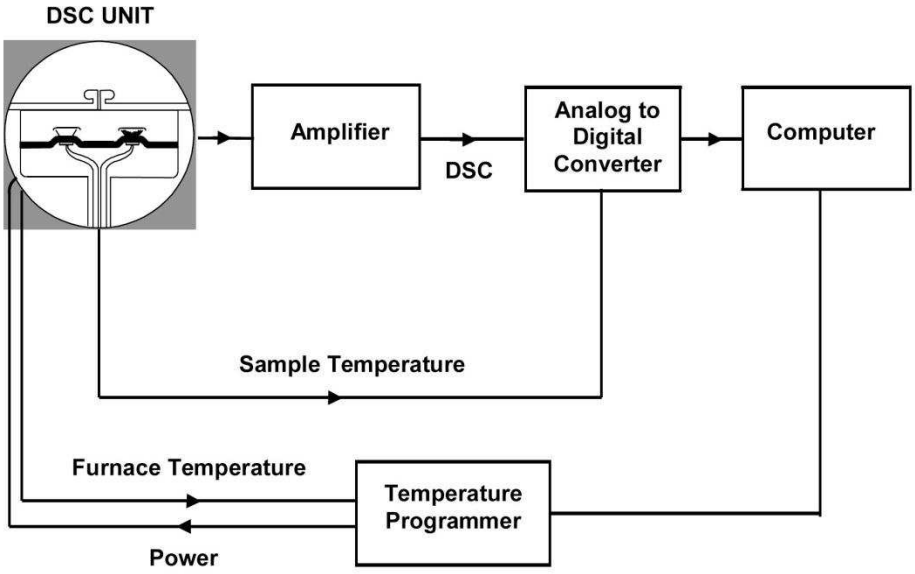

Fig. 2.4. Schematic of the components of the SC-DSC

The additional components required to modify the DSC 910 are described below.

2.2.1 Power Supply

The heating block required a maximum of 140 W. As the resistance of the heating element was found to be 80 Ω, then the voltage rating required was to be an absolute maximum of 106 V. A power supply was built using a variable transformer (variac) connected in series to a step down transformer (240 V to 70 V secondary voltage). This arrangement allowed the supply to be varied between 0 and 70 V (AC) as required (i.e. almost 70% of the heating block's maximum capacity). Wires from pins 1 and 9 were attached to the power supply.

2.2.2 Temperature programmer

A Eurotherm 818P temperature programmer was used to control the DSC furnace. It has an accuracy of 0.1 ℃ and the terms of the internal PID (Proportional, Integral and Derivative) function can be automatically tuned to optimise control of the furnace temperature. The output from the 818P is a digital signal used to switch a solid state relay (SSR) which in turns switches the power supply connected to the DSC furnace.

The 818P can be fully controlled from a computer via a RS232C serial interface. In operation, the SC-DSC control software (see section 2.3) periodically updates a value in the 818P called the *setpoint*, which is the furnace temperature the 818P is continuously trying to maintain. In effect, the SC-DSC software selects the desired furnace temperature at any given time while the 818P controls the power to actually achieve that temperature.

The thermocouple input of the 818P was connected to the DSC furnace control thermocouple (Platinel II) using the appropriate thermocouple compensation cable. The use of type K thermocouple cable was used to determine the temperatures as it was found to have similar temperature sensitivity to Platinel II.

2.2.3 Amplifier

The thermocouple output leads from the base of the DSC cell were led to a Stanton Redcroft DC Amplifier which has various range settings to accommodate a thermocouple output from 20 µV to 200 µV and a maximum of 10 mV output. Therefore with a setting of 20 µV on the amplifier, a 20 µV differential signal would register 10 mV on the amplifier output.

2.2.4 Analogue-to-digital convertor

After trials using several data acquisition systems, the data collection system that was chosen for this study was a DataShuttle USB/54 (Adept Scientific). This unit is able to take in five differential input channels (although only two required) and has a high resolution 22-bit A/D converter. It can operate in ranges from ±31 mV to ±20 V full scale and can autorange to give the maximum resolution for a given input. Theoretically, on the most sensitive range, a resolution of 7.4 e^{-9} V or 0.0074 µV is achievable.

The DataShuttle has an inbuilt cold junction that has a quoted accuracy of ±0.7 ℃ (15 – 35 ℃). In normal operation, the DataShuttle updates the cold junction compensation value periodically and thus corrects for temperature drifts that may occur. However, it was found that the use of this feature had an adverse effect on the timing related to data collection and was disabled. Experiments carried out to view the temperature drift showed that there was a slight drift over a period of several hours but or shorter runs of less than 3-4 hours then this temperature drift was negligible.

2.3 Software

The data acquisition and control software was developed by G. Parkes using Visual Basic (Microsoft) running under the Windows XP environment [13]. In addition to conventional Linear Heating, it provides a range of Sample Controlled methods including Proportional Heating, Constant Rate and Stepwise Isothermal Analysis. A novel method called 'Run Replay', where the temperature-time profile of a previous experiment could be replayed with either a previously run sample or a new one, was also implemented.

The software used an overall control/acquisition cycle of 800 ms. During each cycle, the following occurs:

1. The sample temperature and the μV signal from the DSC head are read from via a DataShuttle USB54 analogue to digital converter (ADC).
2. The data is processed to allow for real-time temperature calibration, baseline correction and to convert the μV signal into mW.
3. The mW signal is further processed by a control algorithm (specific to the experiment mode) and a new furnace temperature setpoint is calculated and sent to a Eurotherm 818P temperature programmer which actually controls the SC-DSC furnace.
4. The real-time display is updated and data is saved to hard disc in the CSV (comma separated variable) format to facilitate ease of subsequent processing / plotting in programmes such as Microsoft Excel.

2.4 Evaluation of the SC-DSC components

After the various modifications to the Du Pont DSC 910 to produce the SC-DSC were completed, the components of the system were evaluated and, where possible, optimised.

2.4.1 Evaluation of the ADC

A series of experiments were performed to evaluate the accuracy and noise level of the DataShuttle USB54 ADC on its most sensitive range using a potentiometer set from 0 to 30 mV in 1 mV increments. For each experiment, one hundred data points were measured. The performance of the ADC was very consistent over the entire range with an average accuracy of +/- 0.01% and an average noise level of +/- 0.7 μV.

2.4.2 Evaluation of the amplifier

The noise level of the Stanton Redcroft DC Amplifier was assessed by comparing the achieved signal with and without the DSC apparatus in place. Using the potentiometer input signals with the amplifier in circuit but switched off the average noise level was found to be +/- 0.9 nV. Switching the amplifier on and the input of similar potentiometer signals was seen to increase the noise level to +/- 11.5 nV. Replacing the potentiometer with signals from the DSC cell achieved the same noise level seen for the potentiometer. Removing the programmer and power supply did not reduce the level of noise and thus the majority of the noise produced was attributed to the amplifier.

2.4.3 Power settings

The power to the instrument cell is provided by an inline variable power supply (variac) that operates by taking in the power from the mains (at 240 V) and uses a step down transformer to reduce the user voltage to 70 V. The user can then change the power setting on the variac dial to provide the power required for the experiment. An experiment was carried to monitor the maximum temperature achievable at a chosen power setting (Fig. 2.5). It can be seen that there is a linear relationship between voltage and maximum achievable temperature.

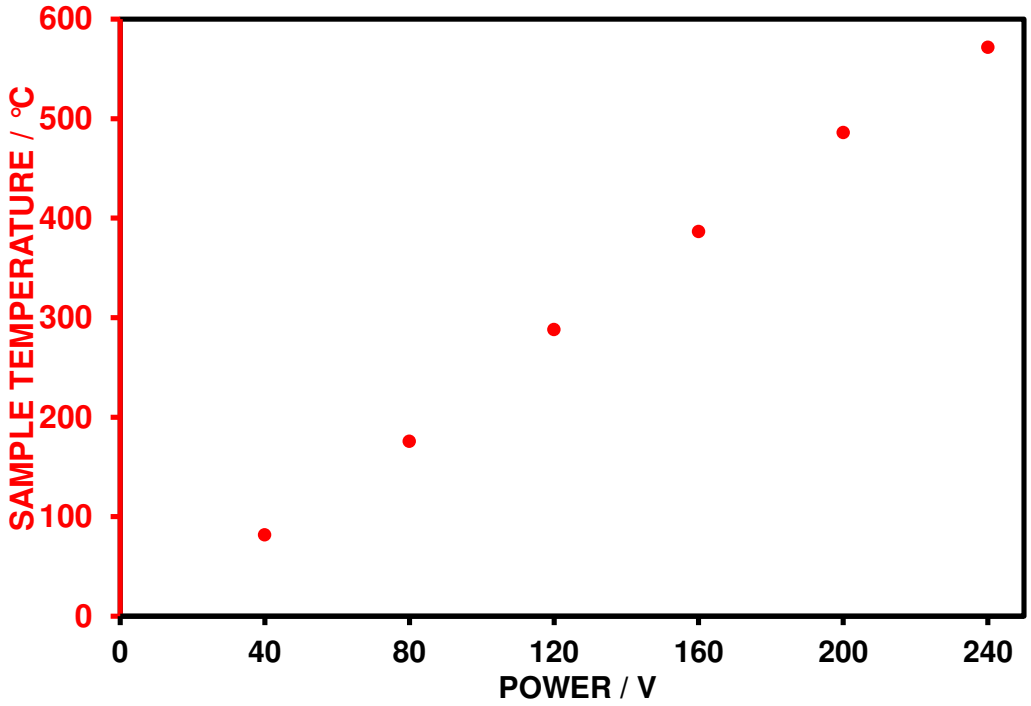

Fig. 2.5 Plot of maximum temperature achieved in DSC cell using different voltage settings from the power supply

2.4.4 Heating performance of the SC-DSC

It was found that optimum temperature control was achieved by adjusting the variac so that the power supply provided a voltage just sufficient to achieve a temperature approximately 10% higher than that required for a particular experiment and then using the 818P's automatic retune facility.

The performance of the power supply and the programmer to heat the DSC cell was observed by heating the empty DSC at 5 ℃ min^{-1} from 30 ℃ to 100 ℃ and holding isothermally at 100 ℃ for a period of 20 minutes. The heating was then resumed at the same heating rate to 200 ℃ followed by the same isothermal period and so on at 100 ℃ intervals to 400 ℃. It can be seen from Fig. 2.6 that the instrument showed good control in achieving and maintaining the set temperatures. The importance of having the good control is so that it would be able to respond quickly and precisely to any changes required.

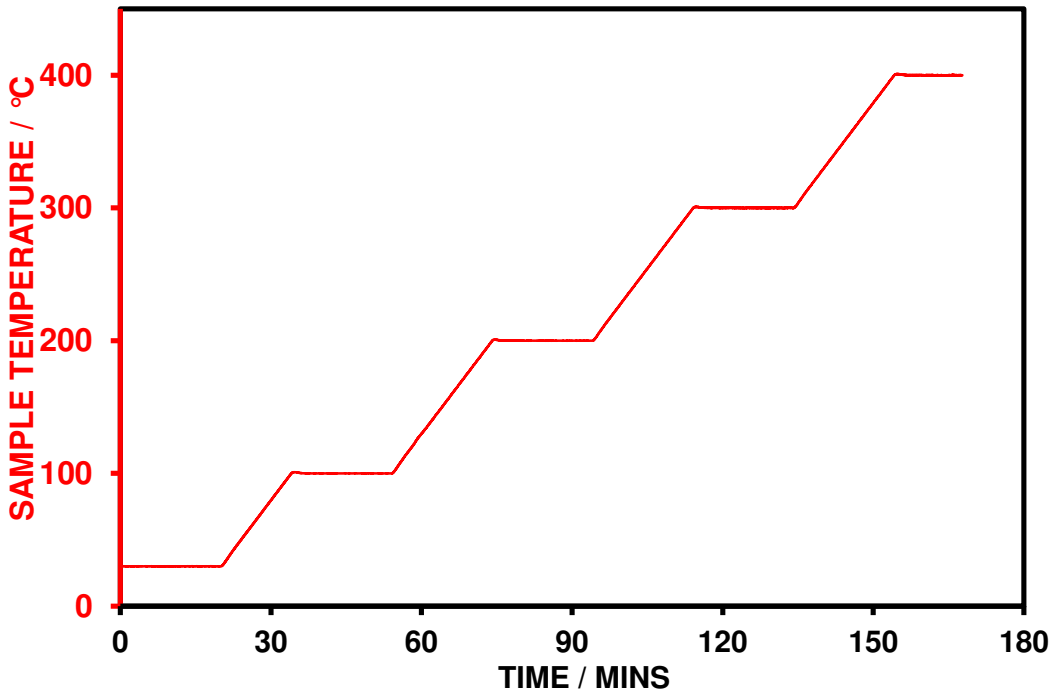

Fig. 2.6 SC-DSC sample temperature profile to illustrate the performance of the power supply and temperature programmer

2.4.5 Cooling rate of the SC-DSC

Using sample controlled techniques it may be necessary to invoke cooling of some types of reactions, in particular those that are exothermic or are autocatalytic. In these instances the ability to control the reaction is lost without the ability to cool sufficiently rapidly.

The rate of cooling was investigated experimentally by monitoring the natural cooling of the DSC cell from 500℃. The natural cooling of the DSC cell is shown in Fig. 2.7. The temperature follows the expected exponential decay. Below 150 ℃, initial cooling rates were less than -5 ℃/min, a rate that could mean a reaction could not be cooled sufficiently rapidly to maintain sample controlled conditions.

In cases where the reactions dictate a faster cooling at lower temperatures, a mechanical cooling attachment (TA Instruments) was fitted. The attachment can reduce the cell environment to -70 ℃. With the attachment in place cooling rates of -5 ℃ min^{-1} or better were achievable down to room temperature.

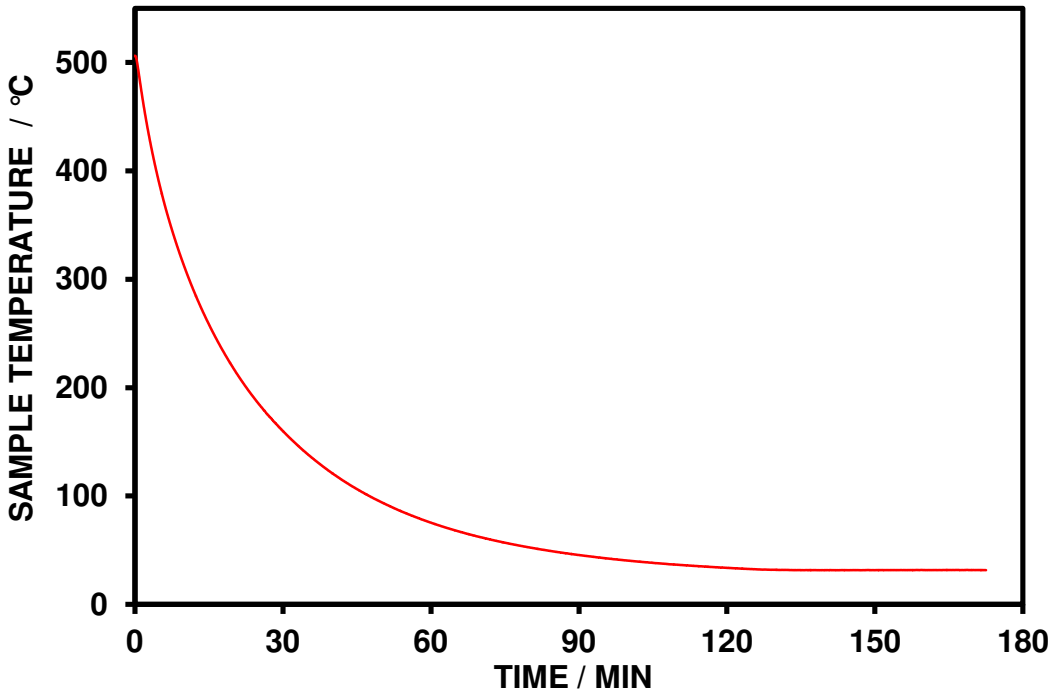

Fig. 2.7 Sample temperature curve for the natural cooling of the empty DSC cell from 500℃ in nitrogen

2.5 Baseline evaluation and correction

The baselines of a DSC can be influenced in many ways. The mismatch and positioning of the sample and reference pans represents possibly the worst effect whereby offsets are created which are then exaggerated by a change of heating rate. Also the DSC itself may have an intrinsic imbalance or a drift which can be detrimental to sample controlled studies. A series of baselines for the DSC using empty pans is shown in Fig. 2.8 and it can be seen that the baselines appeared reproducible with an endothermic drift from above 250 ℃. The magnitude of this drift was less than 0.5 µV. The signals were taken directly from the amplified thermocouple signal as µV.

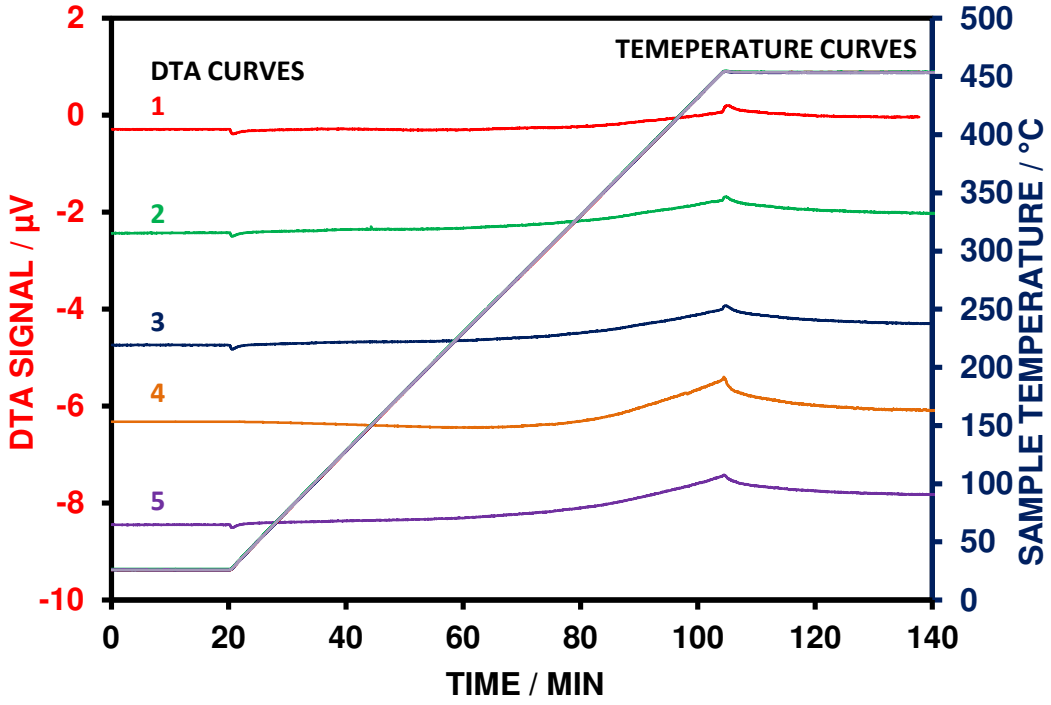

Fig. 2.8 Overlay of DSC baselines at 5 ℃ min^{-1} with empty crucibles in a nitrogen atmosphere

It is of utmost importance that the baseline is flat, reproducible and contains a minimal offset with change in heating rate. This is because in SC-TA studies, a 'target' is set which is equal to the DSC signal above the baseline. Should the baseline change or drift with temperature, then in effect, the target is changed.

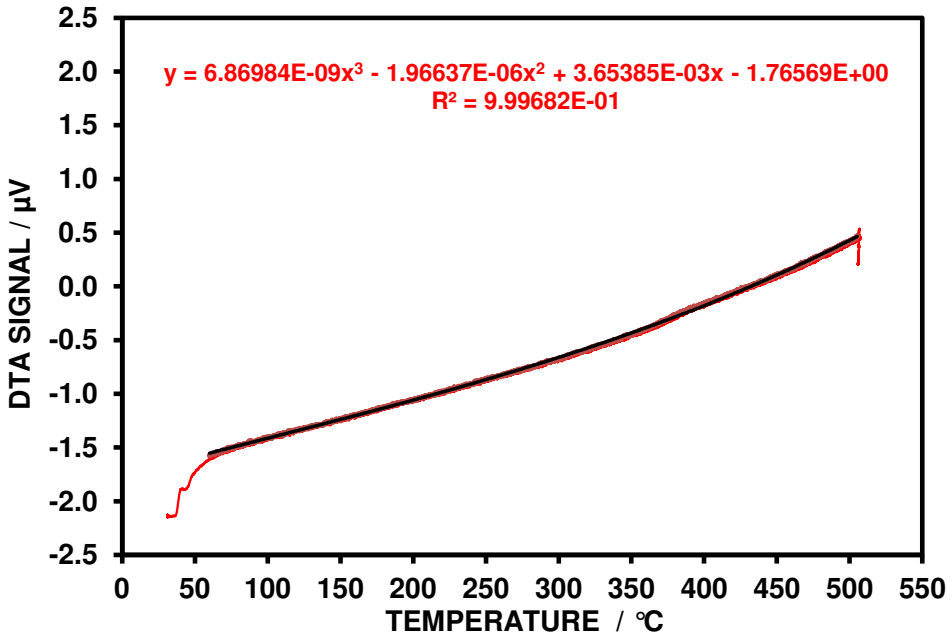

Fig. 2.9 Empty plate baseline for the SC-DSC apparatus
(Heating rate, 5℃ min^{-1}, no baseline correction)

The software incorporates a 3rd order polynomial function that allows an instanteous correction of the baseline as a function of temperature. The parameters for the polynomial are stored on disc as a file that can be edited as required. The parameters are obtained by doing repeat baseline experiments over the temperature range of interest. Fig. 2.9 shows a typical result for a polynomial fitted curve to a baseline for an empty pan experiment between 50 ℃ and 500 ℃ and a heating rate of 5 ℃. Fig. 2.10 shows a typical baseline with the baseline correction.

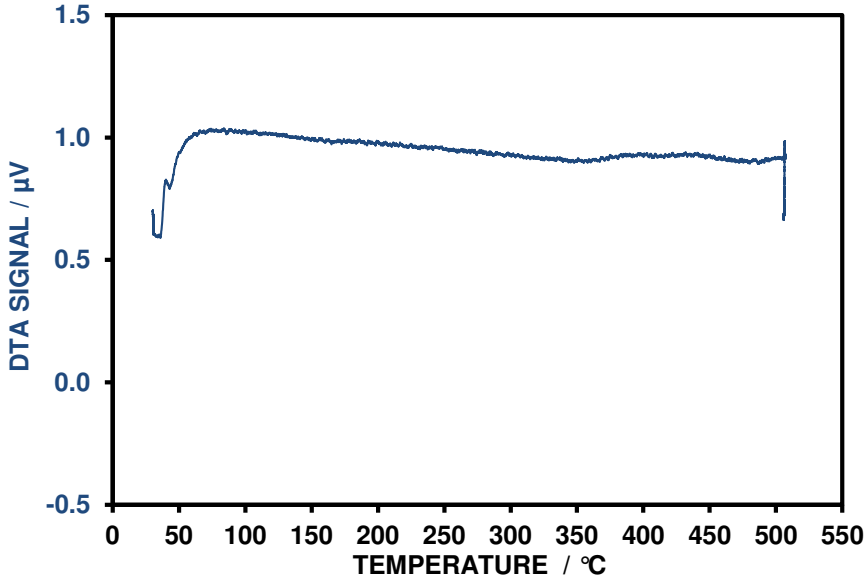

Fig. 2.10 Empty plate baseline for the SC-DSC apparatus
(Heating rate, 5℃ min^{-1}, with baseline correction)

2.6 Calibration

In DTA the ΔT signal is measured in microvolts (μV) and not in calorimetric units of milliwatts (mW), therefore a direct energy reading is not obtained by determining the peak area. Also the performance of the thermocouple sensitivity with increasing temperature becomes less (Fig. 2.11). This means that two separate peaks at different temperatures that may have the same energy of transition may not be produce peaks of the same size.

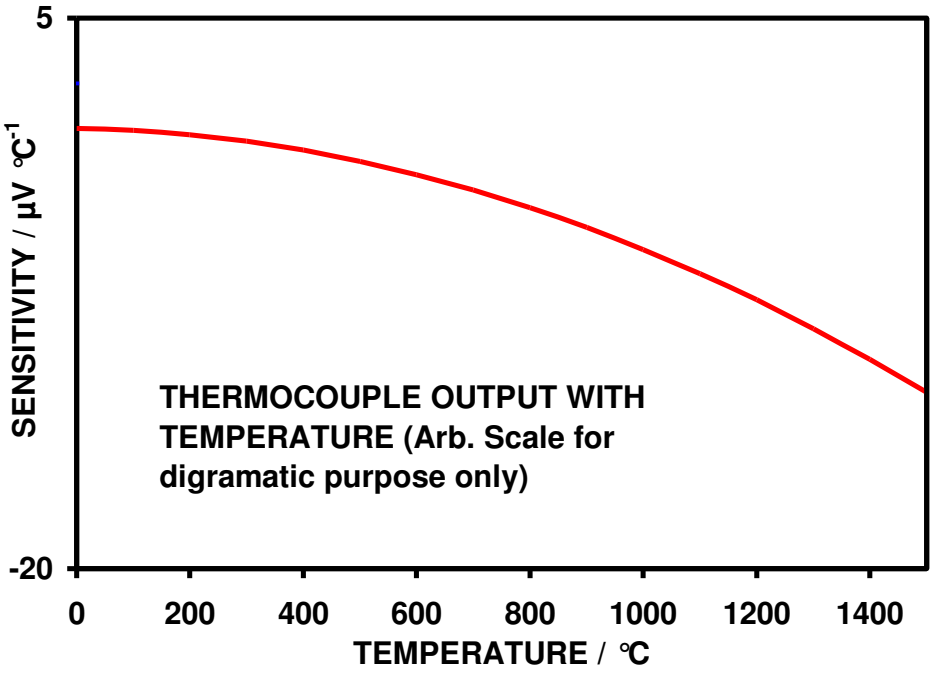

Fig. 2.11 Example of the change in thermocouple sensitivity as a function of temperature

The software incorporates a further polynomial function to allow an instant conversion of the unlinearised DSC signal (μV) to a produce a DSC signal (mW). Again, the parameters for the polynomial are stored on disc as a file that can be edited as required.

At lower temperatures (<800°C), calibration materials with well-studied transition temperatures and known enthalpy changes are available. Above 800°C calibration for enthalpy is more difficult. Silver and gold are available for temperature calibration but not suitable for enthalpy.

The calibration of the DTA signal using known enthalpy calibration materials converts the obtained DTA signal in µV into the real DSC enthalpy units of mW.

The parameters for this polynomial were obtained from the melting enthalpies of high purity metals (99.99% LGC or Goodfellow's) to cover the temperature range 156 ℃ to 419 ℃. High purity organic standards (99.99% LGC) were used to cover the temperature range below 156 ℃.

The metal standards used were:

- Indium; 99.99% (LGC2601)
- Tin; 99.99% (LGC2609)
- Lead; 99.99% (LGC2608)
- Zinc; 99.99% (Goodfellow's)

The Organic Standards used were:

- Phenyl Salicylate; 99.99% (LGC2607)
- Benzil; 99.99% (LGC2604)

The calibration experiments were carried out in duplicate and used 5 mg sample masses of metal standards and 2.5mg of the organic standards heated at 5 ℃ min^{-1}. An overlay of example experiments on the calibration materials is shown in Fig. 2.12.

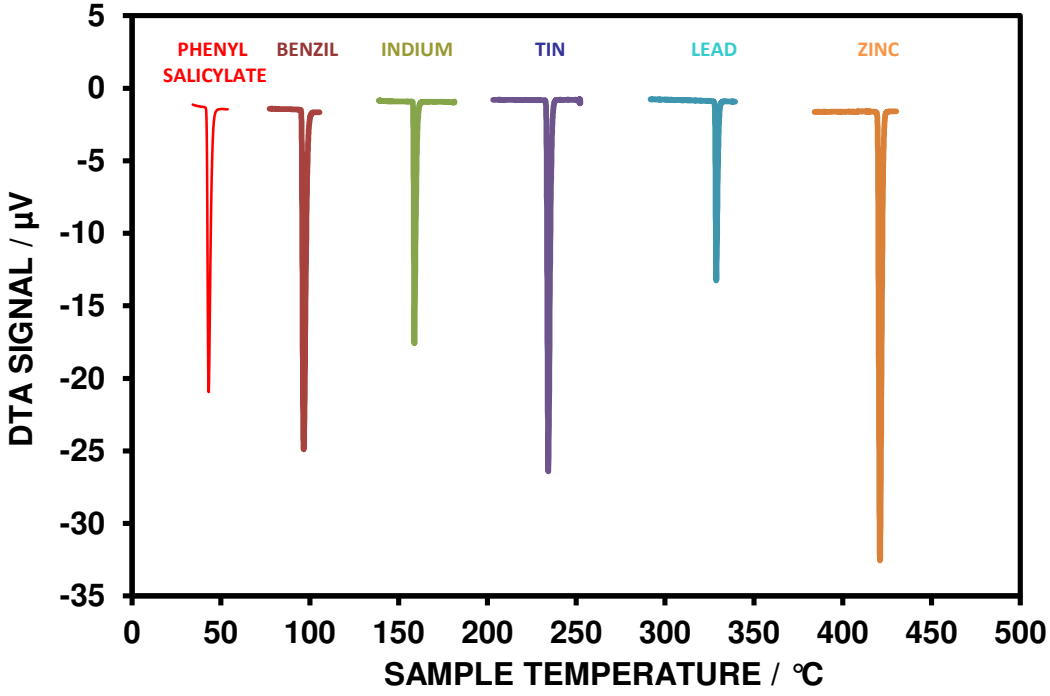

Fig 2.12 Plot of the unprocessed µV signal produced by the melting of various materials used to calibrate the SC-DSC in a nitrogen atmosphere

It was found that the μV to mW conversion had no impact on the baseline correction. Table 2.1 shows the temperature and enthalpy values for four metals with the temperature and enthalpy calibration corrections incorporated. These were based on single evaluations post calibration.

Table 2.1

Temperature and enthalpy values (measured and literature) for a series of calibration materials using the SC-DSC

Calibrant	Lit Temp ℃	Measured Temp ℃	Error ℃	Enthalpy / J g^{-1}	Measured Enthalpy / J g^{-1}	Deviation %
Indium	156.6	157.2	+0.6	28.7	28.8	+0.3
Tin	231.9	232.8	+0.9	60.6	59.0	-2.7
Lead	327.5	327.7	+0.2	23.0	23.4	+1.8
Zinc	419.5	419.0	-0.5	108.6	106.9	-1.6

2.7 Sample Control methods

The SC-DSC software supported a variety of Sample Control methods (in addition to conventional linear heating). Most of these methods involved the setting of following parameters:

Experiment mode — Selects the Sample Control function which dictates the nature of feedback from the reaction of the sample to the furnace temperature.

Target — A set rate of reaction (equivalent to a mW signal from the DSC). It is the difference between the target and the actual DSC signal that is fed to the feedback function.

Lower target — A set rate of reaction (equivalent to a mW signal from the DSC) which is always smaller than the Target. Only used for Stepwise Isothermal experiments.

Threshold — A level (equivalent to a mW signal from the DSC) below which the sample control function is disabled and the furnace is heated at the maximum set heating rate.

Maximum heating rate — The maximum rate at which the furnace will be heated.

Minimum heating rate — The minimum rate at which the furnace will be heated.

2.7.1 Constant Rate

In Constant Rate the furnace temperature is adjusted (between the maximum and minimum heating rates) so as to maintain the DSC signal exactly at the set *Target*. Usually, symmetrical heating rates are used (i.e. *Maximum heating rate* = +5 °C/min, *Minimum heating rate* = -5 °C/min). The SC-DSC software incorporates a PID control algorithm as part of the Constant Rate function. This allows the best control to be achieved but the optimising of the PID parameters has to be done by inspection and can require several experiments.

2.7.2 Stepwise Isothermal

In Stepwise Isothermal Analysis, the *Minimum heating rate* is usually set to 0 °C min^{-1} (i.e. isothermal). In operation, if the DSC signal exceeds the *Target* the furnace is held isothermally. Eventually, the DSC signal will fall below the *Lower target* and the furnace will be heated at the *Maximum heating rate* until (or if) the *Target* is exceeded again. Thus a process proceeds stepwise in a series of temperature steps and isothermal holds.
Stepwise Isothermal was initially developed by Sorensen for dilatometry studies.

2.7.3 Proportional Heating

In Proportional Heating [13], the heating rate is linearly proportional to the difference between the *Target* and the actual DSC signal. If the DSC signal exceeds the Target, then the furnace is set to the *Minimum heating rate* while if it is less 0 then the furnace is set to the *Maximum heating rate*. If the DSC signal is between 0 and the *Target*, the heating rate is set proportionally between the two.

The setting of the *Minimum heating rate* can have a significant effect on the experiment. If it is set to zero ('unsymmetrical heating') then cooling is not possible. As the DSC signal approaches the *Target* then the heating rate proportionally falls to zero. This is similar in some ways to Constant Rate but if the DSC signal should exceed the target even when the heating rate is zero (as may occur in processes that are autocatalytic or have a significant induction stage) then no further control is

possible. However, it was found that 'unsymmetrical heating' was occasionally useful when studying sharp thermal events (such as fusions) as it can prevent temperature oscillations that may otherwise occur.

If the *Minimum heating rate* is set to be the opposite of the *Maximum heating rate* ('symmetrical heating') then Proportional Heating more closely emulates Constant Rate with isothermal conditions being achieved when the DSC signal is at 50% of the target. Although, lacking the additional PID algorithm that can provide the Constant Rate with theoretically better control, symmetrical Proportional Heating with a low *Target* can produce results that are nearly as good and is simpler to set up.

2.7.4 Temperature Replay

Temperature Replay allows the user to load a previous data file from a previous experiment and to exactly repeat the furnace temperature-time profile. It can provide a useful method of investigating the effect of temperature on the DSC baseline either with empty pans or with just the product material of the earlier experiment.

2.8 Requirements for successful Sample Control experiments

2.8.1 Choice of Heating Rate

The choice of heating rates in the study was centred on 5°C min^{-1}. This heating rate was found to be the best compromise between the length of time taken for the experiment and the level of noise and lack of control that may be produced. For example, heating at a faster rate, say 10°C min^{-1} would exaggerate the deflection at the start of the experiment due to the imbalance produced by heat capacity differences. The faster heating would also exaggerate the noise in the system for the same reason. Faster heating would produce a longer lag time from power input to the response of the furnace. Slower heating rates may act to reduce the level of noise observed and reduce the lag time of response but the length of time to carry out the study will be extended somewhat. Another aspect of slower heating is that the DSC signals produced would be reduced in size and the effect of noise and/or

drift would have a greater effect on the feedback using Sample Controlled techniques.

For the majority of the studies reported here, linear heating mode used a heating rate of 5 °C min^{-1}. Proportional Heating experiments used heating rates between ±5 °C min^{-1} (symmetrical mode) or at +5 and 0 °C min^{-1} (unsymmetrical mode).

2.8.2 Types of Crucibles used in the experiments

The majority of the experiments were performed in aluminium T Zero Crucibles (TA Instruments). These crucibles were machined by the manufacturer to have a perfectly flat base and be of 30µl volume and can have an aluminium lid fitted if required. These crucibles were ideally suited for this study as the flat base allowed for the best contact with the raised platform in the DSC head. Aluminium is also a light material with very good thermal conductivity (237 W m^{-1} K^{-1}) [36] therefore there is a low thermal mass and a quick response from the sample through the base of the crucible to the measuring circuit.

2.8.3 Balancing for sample heat capacity component

The specific heat capacity of the sample has an intrinsic effect on the DSC signal achieved. The deflection in the DSC curve caused by any imbalance between the sample and reference in the DSC head is more exaggerated at increase heating rates. An example of the imbalance is shown in Fig. 2.13 for the heating of a 20 mg sample of sodium hydrogen carbonate. In this case, a deflection of 2.0 mW was observed on going from the isothermal state to 5 °C min^{-1} heating rate.

The main reason for an offset on start of heating is due to the mismatch in heat capacity between the sample and reference sides of the DSC plate. If a mismatch exists then on changing heating rate, the heat capacity component would exaggerate the measured DSC signal. Such a mismatch could result in anomalous peaks being observed.

The heat flow per unit mass obtained by DSC is governed by the following equation: (Eq. 1)

$$\Phi = \beta \times C_p \qquad \text{(Eq. 1)}$$

Where:

Φ = Heat flow (mW)

β = Heating rate (°C s^{-1})

C_p = Specific heat capacity (J g^{-1} °C^{-1})

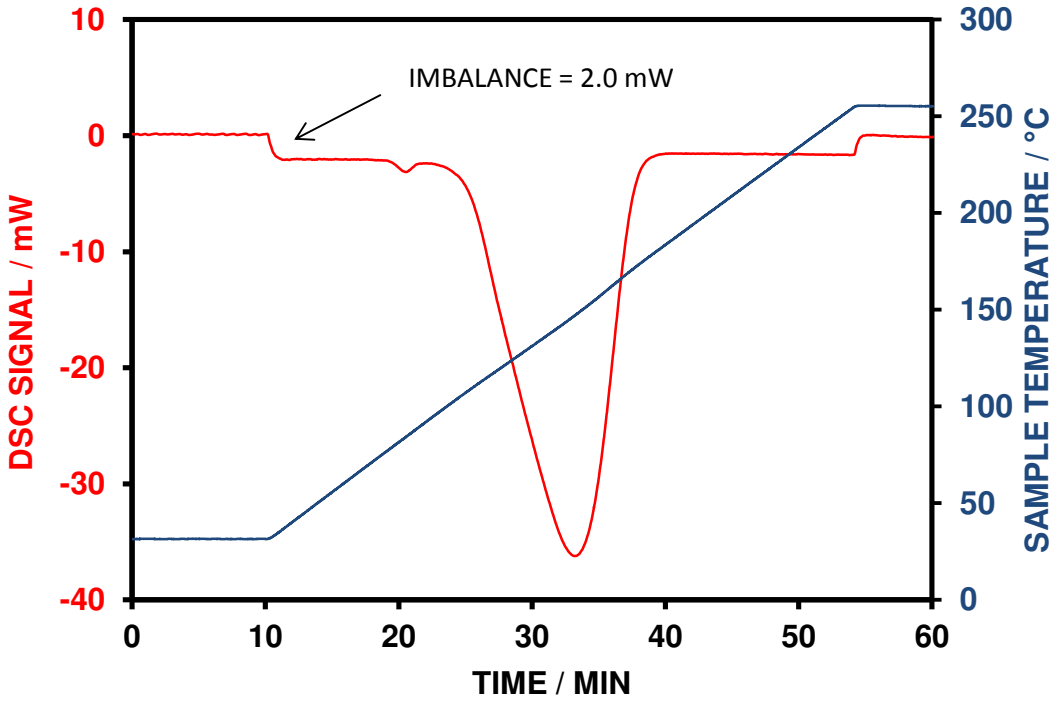

Fig. 2.13 Linear heating of sodium bicarbonate showing the imbalance between sample and reference
(sample mass, 20mg; heating rate, 5°C min^{-1}; atmosphere, nitrogen)

The C_p differences can be corrected for by the loading of the reference with amounts of an inert material at the start of the experiment to minimise the offset at the start of the experiment. However this may be different at the end of the experiment when it is possible that the sample may change its apparent heat capacity during its reaction due to a change in sample mass.

Several experiments were carried out by loading various levels of alumina powder in the reference crucible compared to an empty sample crucible. The system was then held isothermally for 5 minutes before heating at 5 °C min^{-1} until a steady signal was

achieved. The deflection in DSC signal observed with different masses of alumina produced a good linear relation with an R^2 value at 0.9914. The magnitude of the deflections are tabulated in Table 2.2 and plotted in Fig. 3.2 as deflection in mW against mass of alumina in the reference crucible.

Using the linearity equation produced, it is possible to estimate the level of alumina required to balance for the heat capacity component of the sample. The balancing of the system before each sample controlled experiment is of the utmost importance as any deflection will affect at which point the target is and when the sample control becomes effective.

Table 2.2

Deflection on Heating at 5°C min^{-1} of the DSC Signal from an Isothermal Temperature with Varying Mass of Alumina in Reference Crucible

Mass Alumina in Reference / mg	Deflection in DSC Signal on Heating / mW	Normalised Nett Deflection / mW mg^{-1}
0.000	-0.176	0.000
2.538	0.1263	0.119
5.017	0.3772	0.110
10.024	1.070	0.124
15.130	1.649	0.121
20.123	2.463	0.131
25.094	3.180	0.134
30.007	4.011	0.140
35.041	4.118	0.123

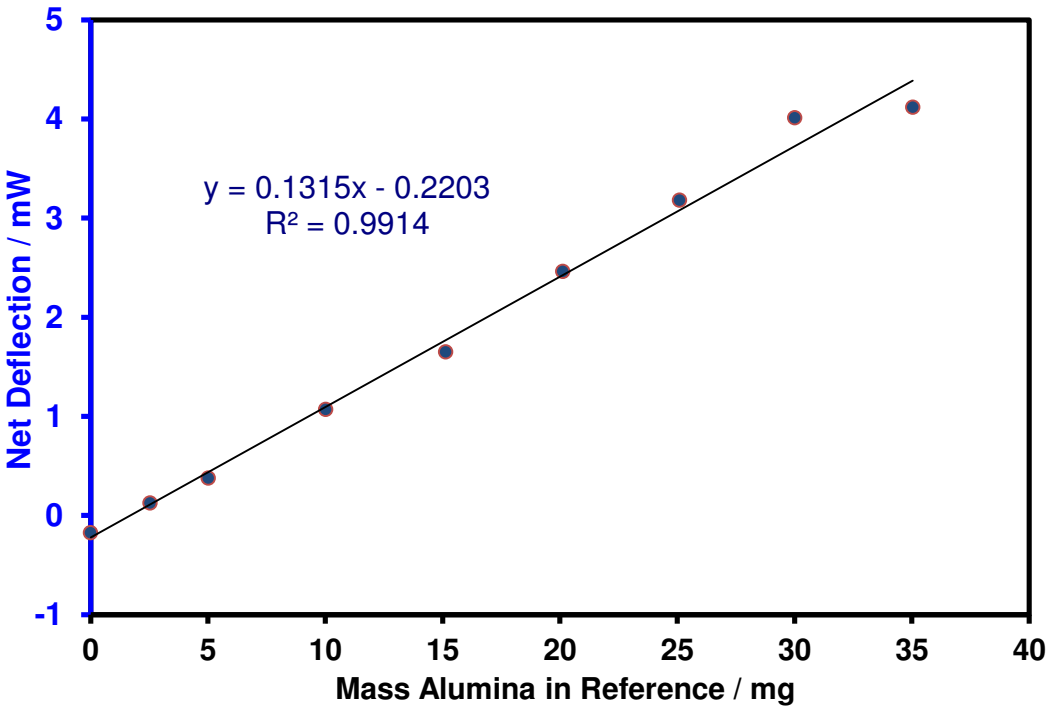

Fig. 2.14 Plot of mass of alumina in reference required to balance for heat capacity component of a sample for SC-DSC experiments

Therefore for each of the applications described in Chapters 3 and 4, experiments were carried out initially with empty reference crucibles to assess the offset produced by the sample. Using the trend equation from Fig 2.14 the mass of alumina required in the reference to balance out for the sample heat capacity can be accurately estimated.

Chapter 3 Applications: Reactions that take place with a Change in Mass

3.1 Aim and applications of SC-DSC to reactions with a mass change

The aim of this chapter is to evaluate the applicability of the sample controlled DSC technique to a wide range of reaction types. Discussed in this chapter will be reactions that occur with a change in sample mass such as decomposition reactions and dehydration reactions.

3.2 Endothermic Decomposition of Sodium Hydrogen Carbonate

On heating, sodium hydrogen carbonate undergoes decomposition to yield water and carbon dioxide according to the following equation (Eq. 2):

$$2NaHCO_3\,(s) \rightarrow Na_2CO_3\,(s) + H_2O\,(g) + CO_2\,(g) \qquad \text{(Eq. 2)}$$

In a kinetic analysis of the decomposition of sodium hydrogen carbonate, studies by Tanaka and Takemoto [37] showed the decomposition by thermogravimetric analysis to occur as a single mechanistic event. Their work involved evaluating the decomposition reaction at various isothermal temperatures within the temperature range of the decomposition followed by experiments at heating rates of 0.1K min^{-1} - 0.5K min^{-1} and using the Ozawa method [38] to determine the Arrhenius parameters and hence the kinetics. A study of the decomposition reaction in the solid state was carried out by Tiernan, Barnes and Parkes [39] whereby a solid insertion probe mass spectrometry was used in conjunction with Constant Rate Thermal Analysis. During this study, the rate of reaction was controlled via the evolved gases during decomposition and the activation energies were estimated using the previously mentioned Ozawa method.

TG-Mass spectrometry curves are shown in Fig. 3.1. It can be seen that a mass loss of 36.4% was observed which is in agreement with the decomposition stoichiometry. Also shown are the evolved gas analysis curves for the decomposition which confirm the simultaneous production of gaseous water and carbon dioxide. Although the decomposition was expected to occur as a single step, there was a small mass loss in the region of 80 ℃ preceding the main decomposition reaction. This was also observed using DSC by Dei and Guarini [40] who also investigated the evolved gas analysis of this event and found that water and carbon dioxide was also produced at this minor endothermic peak.

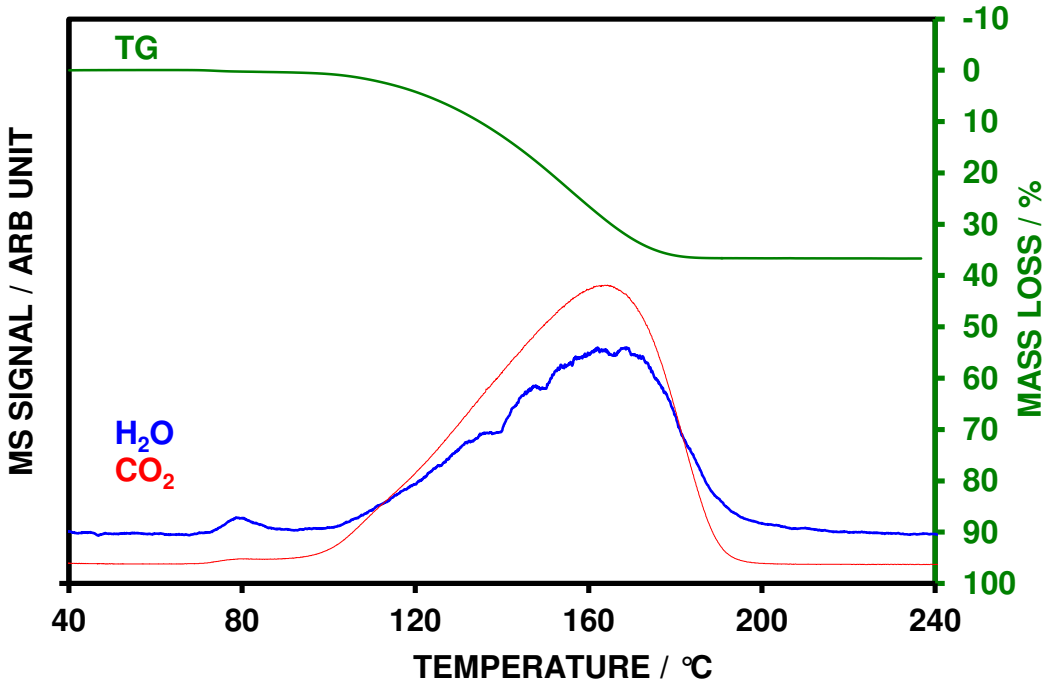

Fig. 3.1 TG and mass spectrometry curves for sodium hydrogen carbonate (sample mass, 20mg; heating rate, 10℃ min^{-1}; atmosphere, nitrogen)

A linear heating DSC curve for sodium hydrogen carbonate is presented in Fig. 3.2 and showed that the thermal decomposition produces two endothermic events in agreement to that seen in the TG-MS experiment. The first of these peaks appeared in the region of 80 ℃ and was seen to be relatively small compared to the large endothermic peak starting at around 100 ℃ and ending at around 180 ℃.

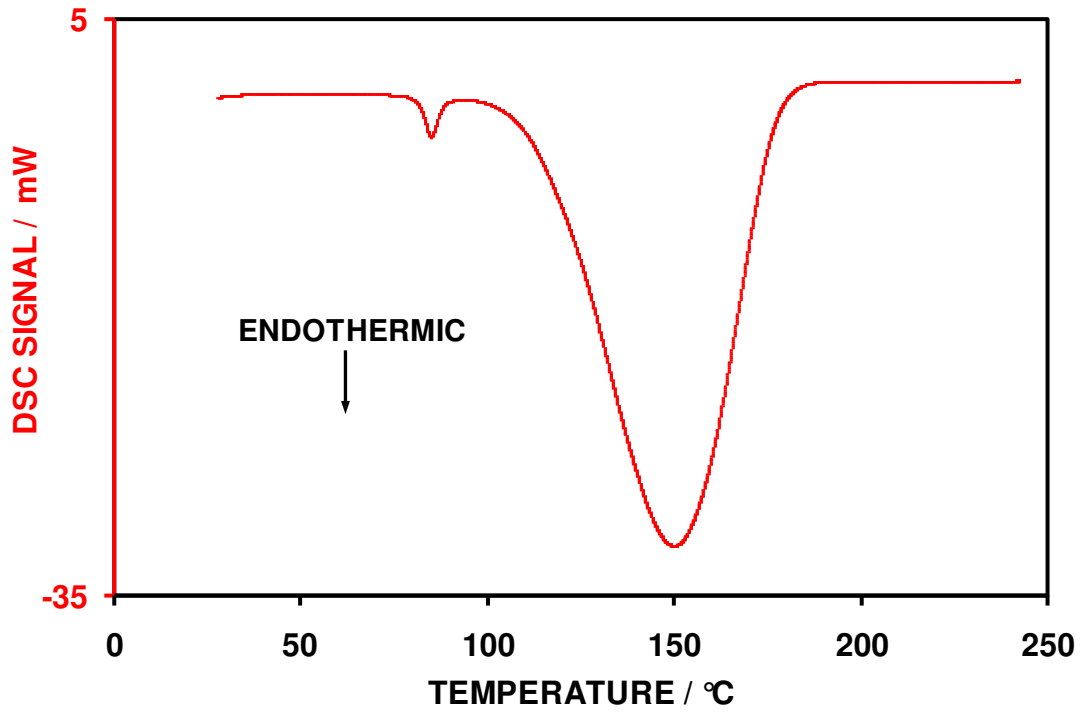

Fig. 3.2 DSC curve for the linear heating of sodium hydrogen carbonate (sample mass, 20mg; heating rate, 5℃ min^{-1}; atmosphere, nitrogen)

As the strategy to be used for the sample controlled DSC experiments was to be proportional heating, then as the sample undergoes decomposition, it will give rise to varying heating rates. A study was undertaken to establish the effect of heating rate on the decomposition reaction of sodium hydrogen carbonate. Heating rates between 1℃ min^{-1} and 10℃ min^{-1} were used on 20 mg sample masses and it can be seen from Fig. 3.3 that as the heating rate increased then so did the magnitude of the DSC peak. The temperature at which the decomposition events occurred was also increased along with the temperature range of the decomposition reaction. This is shown more clearly in the extent of reaction plot in Fig. 3.4 where it can be seen that the decomposition reaction at 10℃ min^{-1} occurs over around 110℃ temperature range (86℃ – 190℃) compared with a narrower temperature range at the 1℃ min^{-1} heating rate (63℃ – 152℃). The start and end temperatures of the entire decomposition reaction at each heating rate is shown in Table 3.1 and shows that the decomposition reaction is heating rate dependent. It can also be seen that as the heating rate is increased, then the peak temperatures and the width at half height also increases. In general, lowering the heating rates will promote the onset of

decomposition to a lower temperature with the completion of the reaction also at a lower temperature.

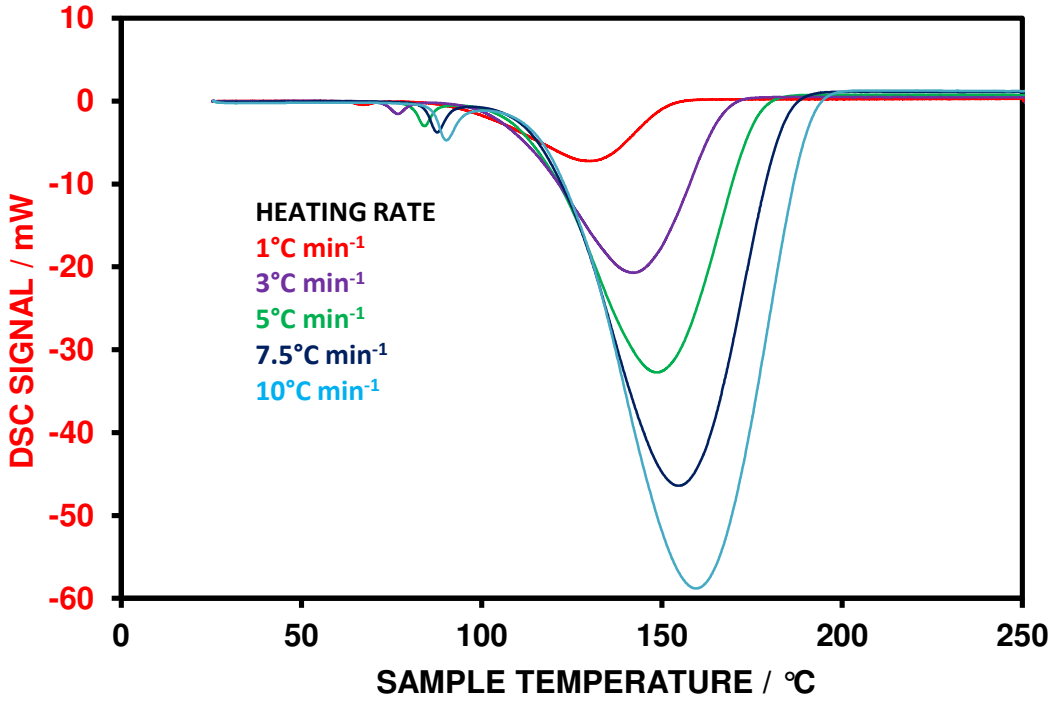

Fig. 3.3 Heating rate dependence of the decomposition of sodium hydrogen carbonate
(sample mass, 20mg; heating rates, 1 – 10 °C min^{-1}; atmosphere, nitrogen)

Table 3.1

Extrapolated Onset and Offset Temperatures for the Decomposition of Sodium Hydrogen Carbonate at Different Heating Rates
(sample mass, 20mg; atmosphere, nitrogen)

	Temperatures / °C			
Heating Rate / °C min^{-1}	Onset	Peak	Offset	Peak width at half height / °C
1	63	130	152	33
3	73	142	168	36
5	81	149	176	38
7.5	84	155	184	40
10	86	160	190	42

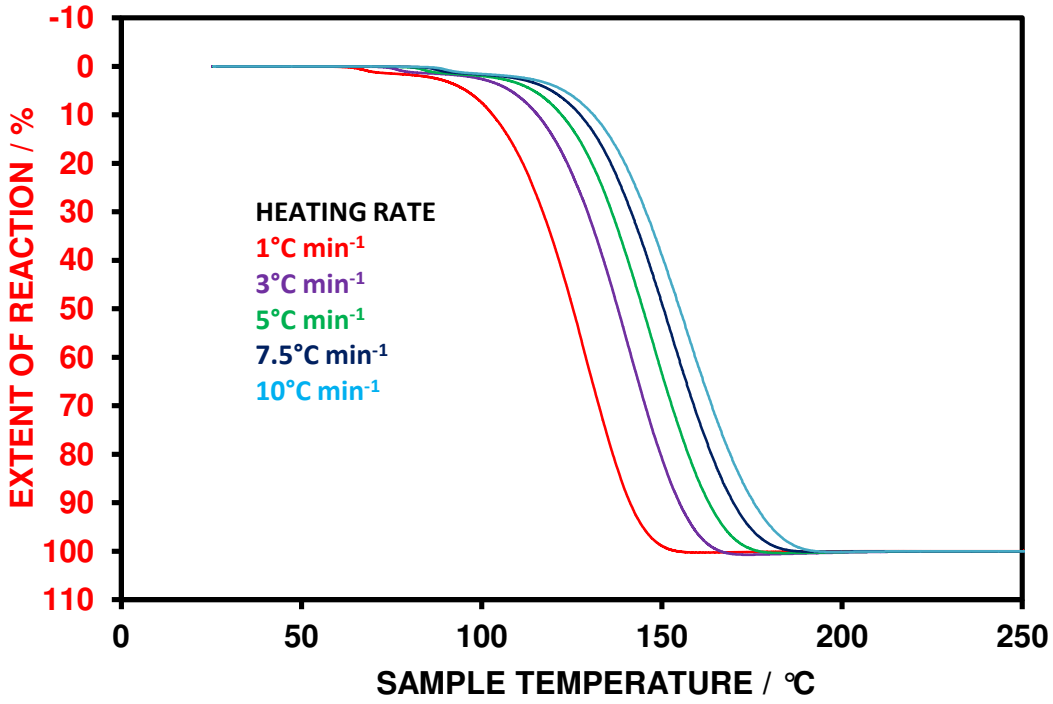

Fig. 3.4 Extent of reaction with respect to temperature for heating rate dependence of the decomposition of sodium hydrogen carbonate (sample mass, 20mg; heating rates, 1 – 10 °C min^{-1}; atmosphere, nitrogen)

Fig. 3.5 shows an SC-TG experiment on sodium bicarbonate it can be seen that after the onset of the main reaction, the sample initially had to be cooled to avoid exceeding the set reaction rate. This behaviour in sample controlled studies of decomposition reactions is considered to be typical of a nucleation and growth mechanism [41] in agreement with the kinetic studies by Tanaka [42]. The amount cooling required was 10 °C before control was regained with the remainder of the decomposition following the linear target rate to completion. A comparison of the linear heating and proportional heating TG experiments is shown in Fig. 3.6 and it can be seen that there is a large reduction in temperature of the decomposition using the sample controlled method with a 23 °C difference in temperatures at 50% decomposition.

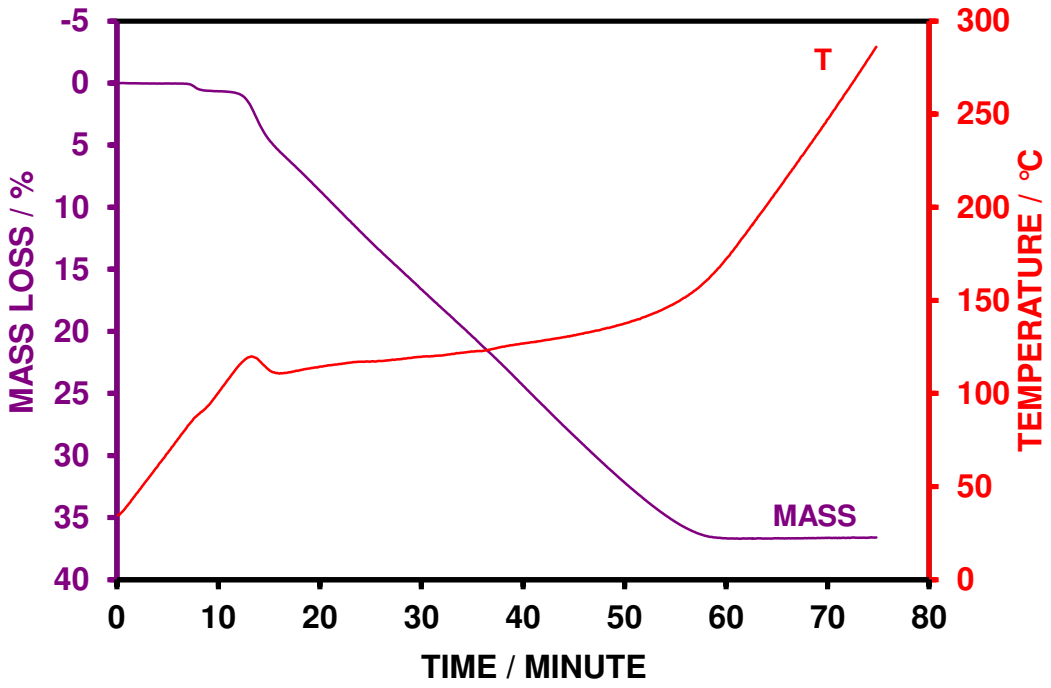

Fig. 3.5 Sample mass and temperature curves for the SC-TG experiment using proportional heating for sodium hydrogen carbonate
(sample mass, 10mg; heating rate, ±10 ℃ min^{-1}; atmosphere, nitrogen)

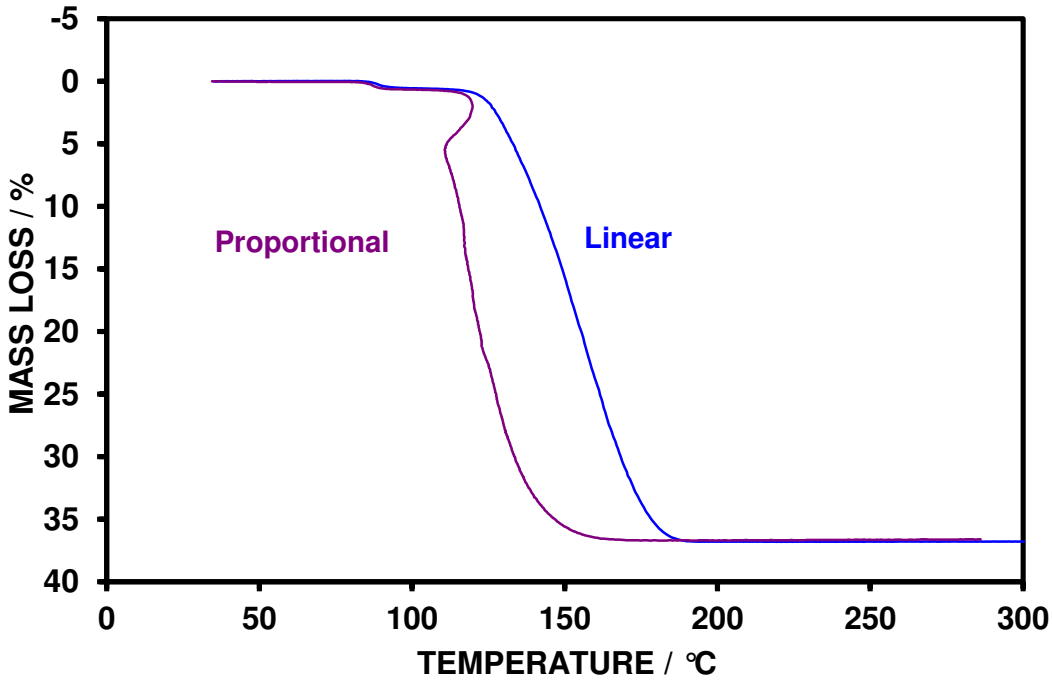

Fig. 3.6 Comparison mass loss curves for sodium hydrogen carbonate using linear heating and proportional heating

A series of sample controlled DSC experiments were carried out on sodium hydrogen carbonate in the proportional heating mode using the symmetrical heating and target levels of 10, 5 and 2mW with Fig. 3.7 showing the overlay of the linear heating experiment with a proportional heating experiment carried out with a target of 5 mW. It can clearly be seen that by using the sample controlled method that the decomposition reaction has been prolonged.

An extent of reaction plot with respect to temperature is given in Fig. 3.8 where an interesting aspect of the decomposition reaction can be seen. In order to attain a level of control, it can be seen at the lower target level that the sample had to be cooled significantly by approximately 15℃ from the onset of decomposition. Using a target level of 2mW provided oscillations and this was observed towards the end of the decomposition reaction where the influence of the change in heat capacity will in effect move the target level relative to where it was the start. This means that there would be a rapid change between the heating and cooling as the DSC signal is around the target level.

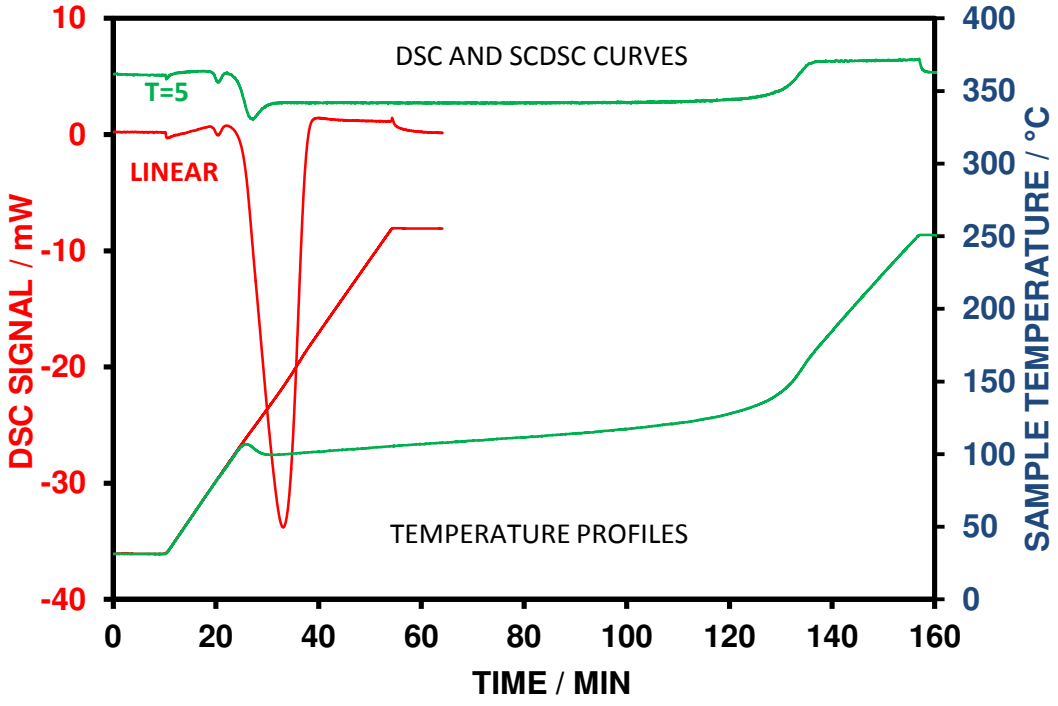

Fig. 3.7 Overlay of DSC and temperature curves for the linear heating and proportional heating at target level of 5mW for sodium hydrogen carbonate (sample mass, 20mg; heating rates, 5℃ min^{-1} and ±5℃ min^{-1}; atmosphere, nitrogen)

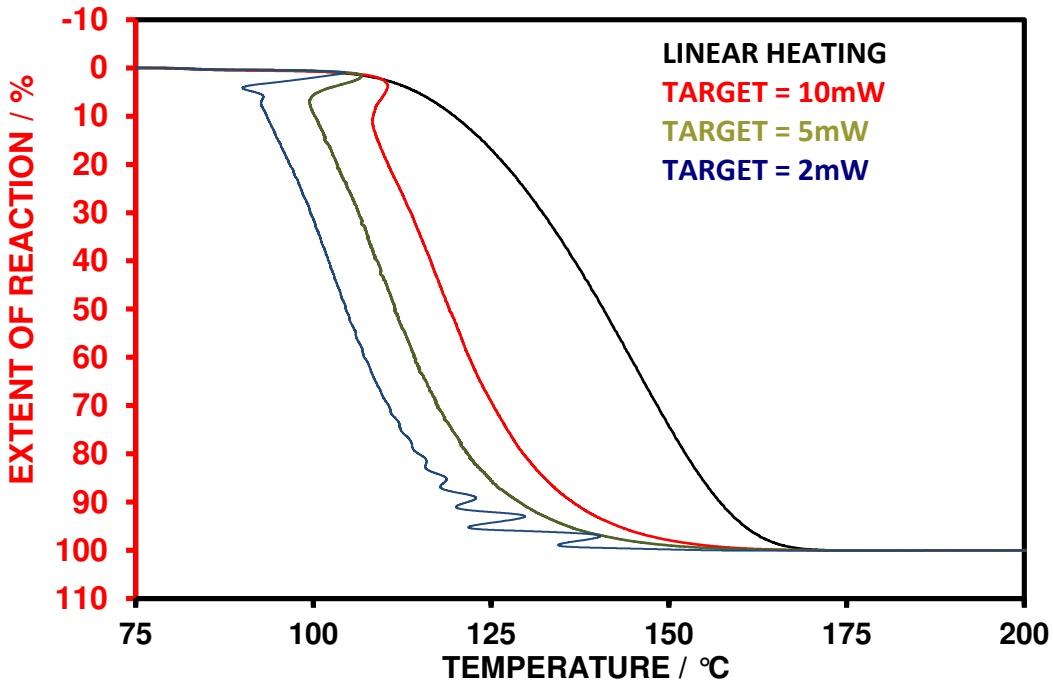

Fig. 3.8 Extent of reaction for the linear heating and symmetrical proportional heating at several target levels for sodium hydrogen carbonate with respect to temperature

Similar experiments were performed using proportional heating method in the unsymmetrical heating mode. It was found that when using a target level of 5mW that the decomposition reaction can be extended over a 50 minute period. Fig. 3.9 shows the extent of reaction with respect to temperature and it can be seen that the lacking of cooling available is evident at the 5mW target level with there being approximately 30% decomposition occurring while being held at an isothermal temperature before heating was resumed.

To conclude, this suggests that once the temperature at the onset of reaction has been reached then it would be difficult to bring under control in the early stages of the decomposition.

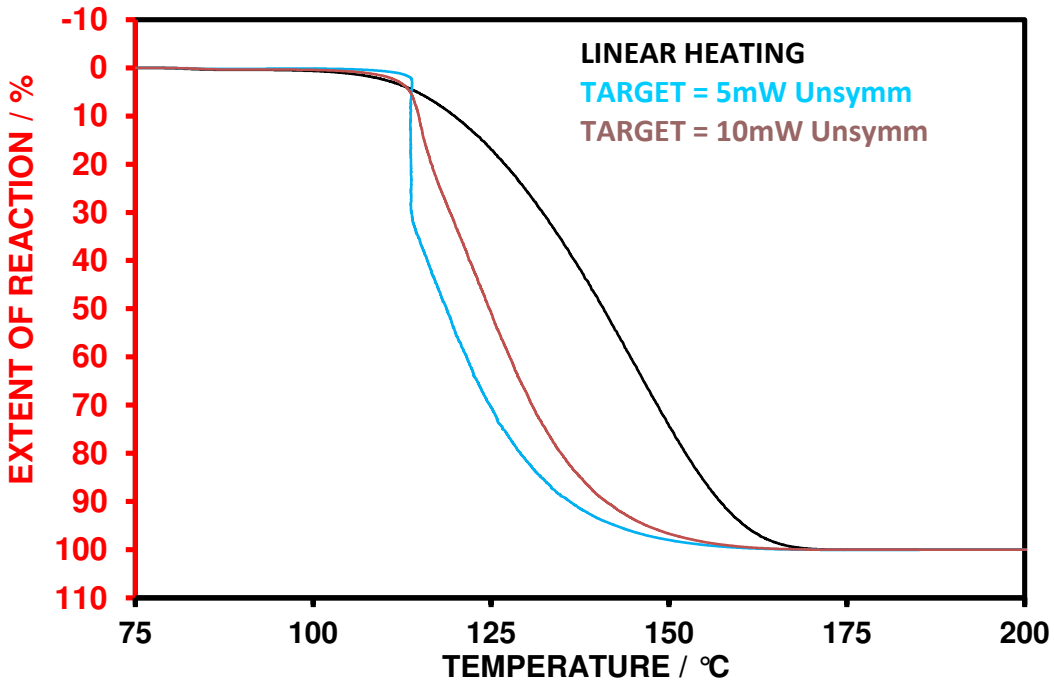

Fig. 3.9 Extent of reaction for the linear heating and unsymmetrical proportional heating at two target levels of sodium hydrogen carbonate with respect to temperature

3.3 Endothermic Dehydration of Calcium Oxalate Monohydrate

When calcium oxalate monohydrate is subjected to an increasing linear heating programme it firstly becomes anhydrous before undergoing its decarboxylation stages according to steps (Eq. 3a, 3b and 3c below).

$CaC_2O_4.H_2O \rightarrow CaC_2O_4 + H_2O$ (Eq. 3a)

$CaC_2O_4 \rightarrow CaCO_3 + CO \quad (2CO \rightarrow C + CO_2)$ (Eq. 3b)

$CaCO_3 \rightarrow CaO + CO_2$ (Eq. 3c)

The decomposition reactions for calcium oxalate have been studied using Constant Rate Thermal Analysis by Paulik [43]. They found that the rate of mass loss was virtually linear with the temperature profile showing some degree of cooling involved.

For the purpose of this study, the dehydration reaction (step a) will be examined in detail. The dehydration stage involves a theoretical mass loss of 12.3% and this is

illustrated in Fig. 3.10 where 20mg sample of calcium oxalate monohydrate has been heated using a thermogravimetry at a linear heating rate of 10 ℃ min^{-1}.

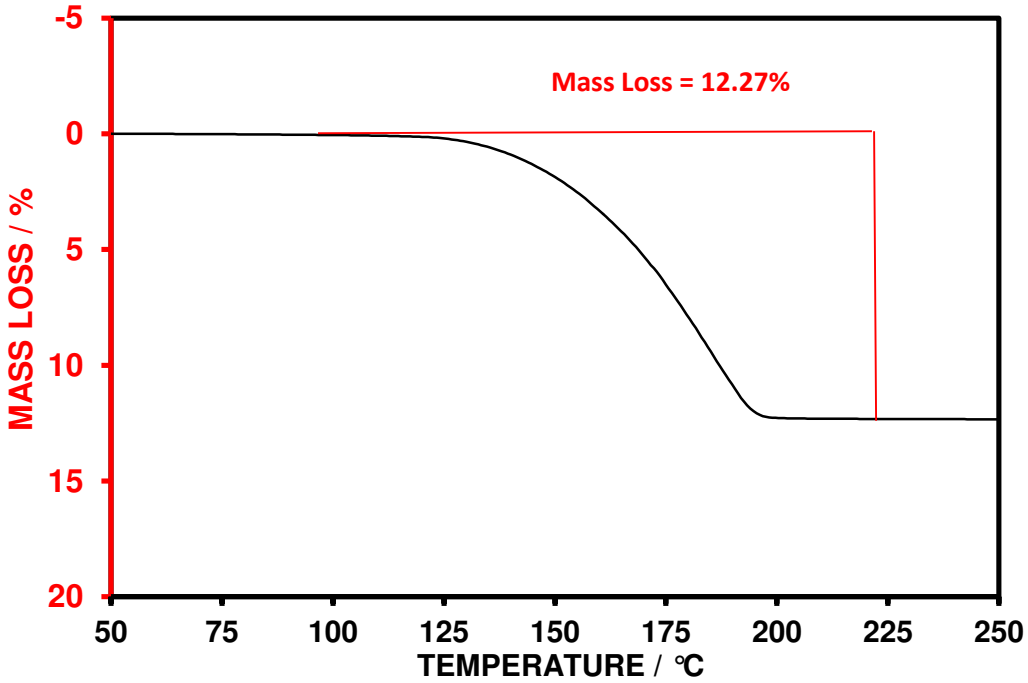

Fig. 3.10 TG curve for the dehydration of calcium oxalate monohydrate (sample mass, 20mg; heating rate, 10℃ min^{-1}; atmosphere, nitrogen)

A DSC experiment was carried out using linear heating on a 20 mg sample in a nitrogen atmosphere to cover the dehydration event with isothermal holding temperatures at 30 ℃ and 200 ℃. It can be seen from Fig. 3.11 that there was a large endothermic peak to accompany the dehydration reaction. There was also a very small endothermic peak preceding the main reaction which is due to a phase change of the monohydrate from the low temperature phase to the high temperature phase [44]. The temperature at the start of the dehydration reaction from after the minor endothermic event was 88 ℃ and appeared to complete at 183 ℃ with the time taken over the reaction being 19 minutes. The peak height was seen to be around 23 mW in magnitude which provides enough scope to allow sample controlled studies on this reaction.

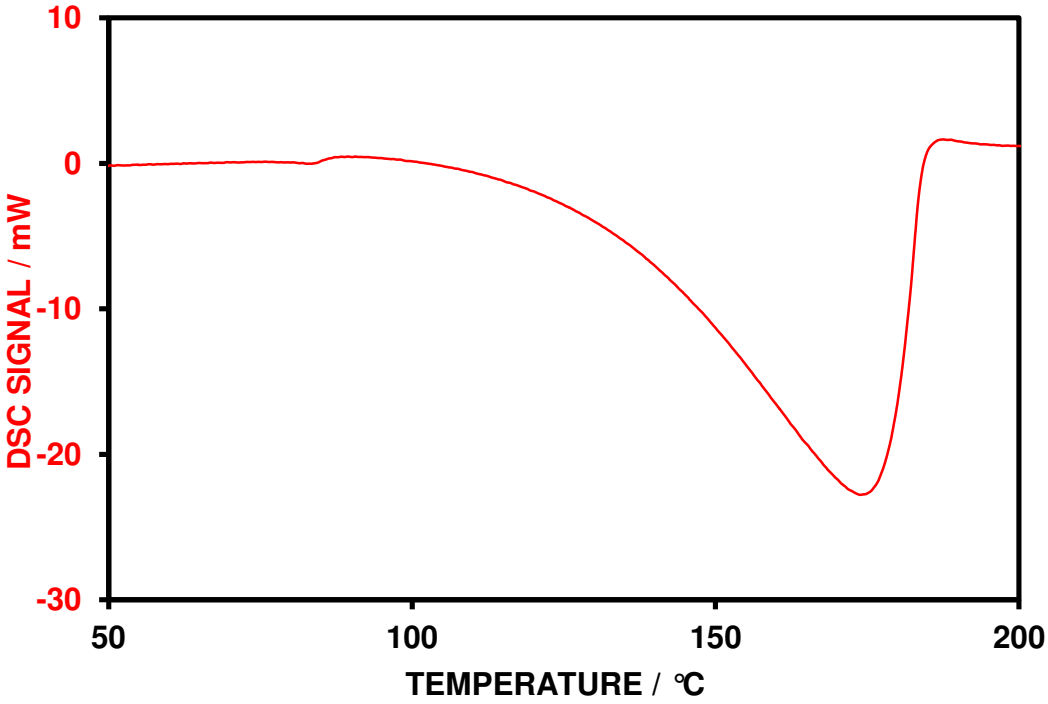

Fig. 3.11 Linear heating DSC curve for the dehydration reaction of calcium oxalate monohydrate (sample mass, 20mg; heating rate, 5℃ min^{-1}; atmosphere, nitrogen)

Several SC-DSC experiments were carried out using the proportional heating strategy. Symmetrical heating was used with the target levels examined being 10mW, 5mW and finally at 2mW in an attempt to lengthen the time of the dehydration reaction. Fig. 3.12 shows the DSC and temperature curves for the dehydration of calcium oxalate monohydrate using a target of 5mW where good control can be seen with the reaction taking place within a narrow temperature range. An overlay of the DSC and temperature curves of the linear and proportional heating experiments is shown in Fig. 3.13 when the target level was set to 2mW and it can be seen that there is good control of the dehydration step.

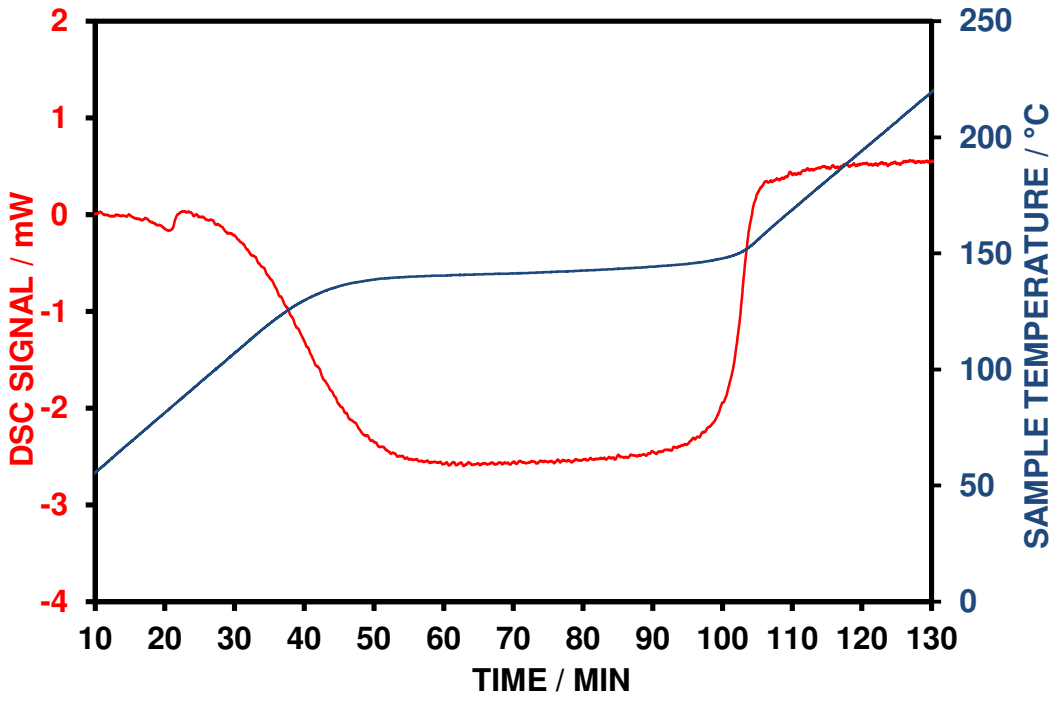

Fig. 3.12 DSC and temperature curves for the dehydration of calcium oxalate monohydrate in proportional heating mode
(sample mass, 20mg; heating rates, ±5℃ min^{-1}; target, 5mW; atmosphere, nitrogen)

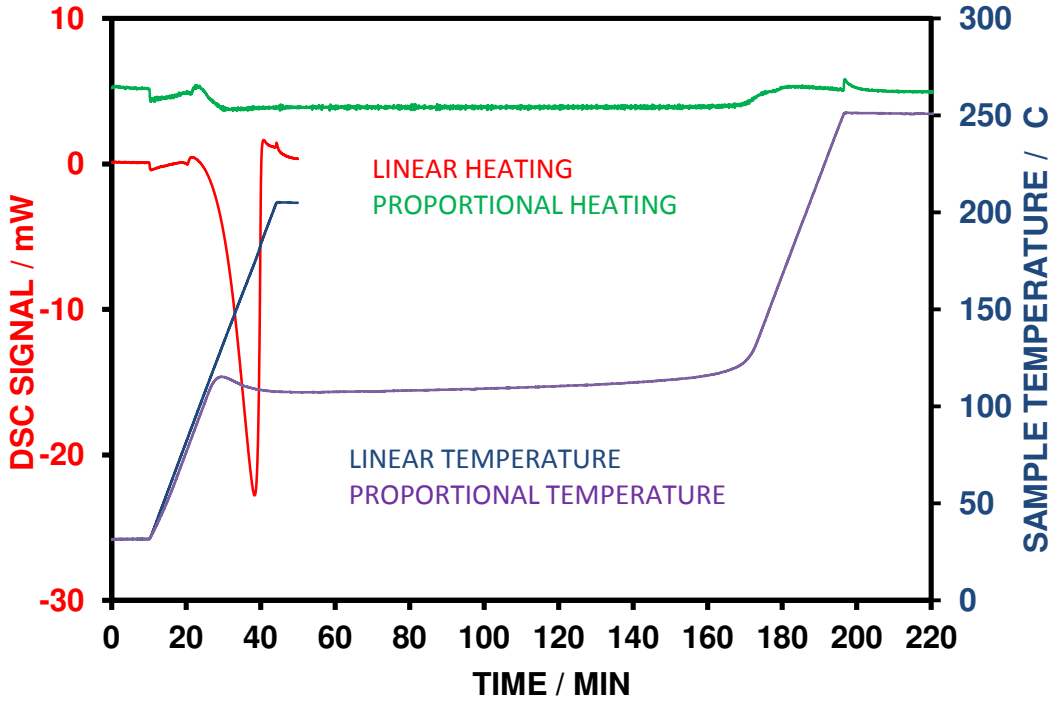

Fig. 3.13 Overlay of DSC and temperature curves for the linear heating and proportional heating (target, 2mW) experiments with respect to time

A plot of extent of reaction against temperature given in Fig. 3.14 showed that the dehydration reaction in the linear experiment covered a temperature range from 91 ℃ to 179 ℃. Reducing the target level caused the reaction to be completed over a narrower temperature range with the experiment carried out with a target of 2 completing at 130 ℃, a reduction in nearly 50 ℃ to complete the dehydration reaction compared with the linear heating experiment. It can also be seen that at the lower the target level used that there is an element of cooling induced which indicates that the start of the dehydration step once initiated caused the reaction to proceed at a lower temperature than the starting temperature, a reason which suggested by Tanaka et al as a random nucleation and subsequent growth mechanism [45]. It can be seen that by using lower target levels the reaction can be promoted to occur over a tighter temperature range.

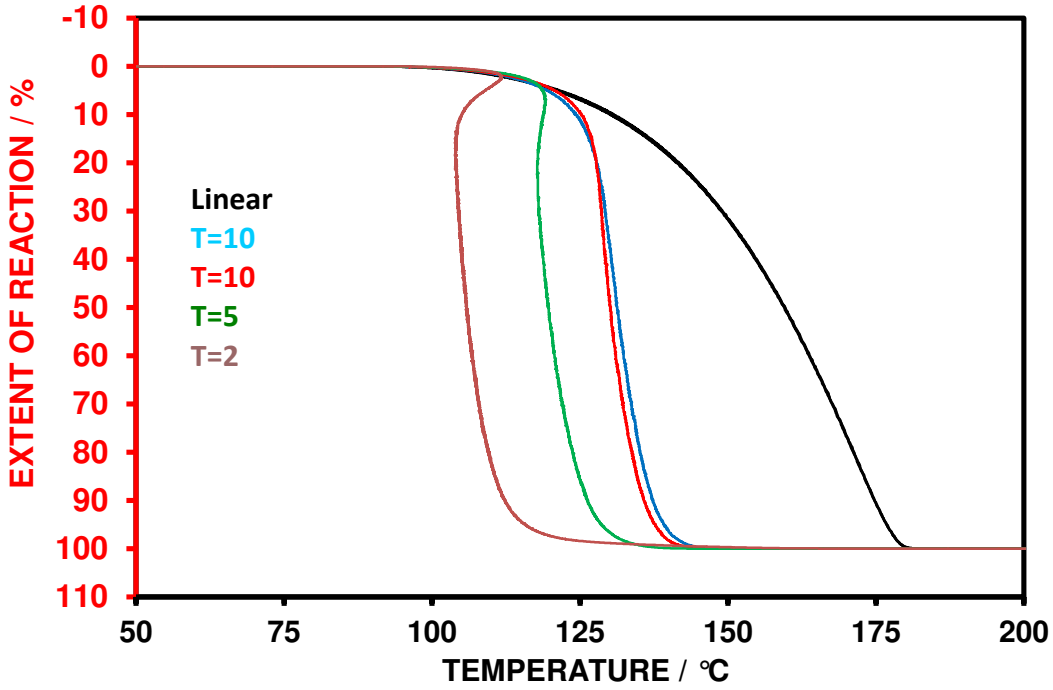

Fig. 3.14 Plot of extent of reaction by peak area against temperature for a series of proportional heating experiments using several target rates for the dehydration of calcium oxalate monohydrate

3.4 Endothermic Dehydration of Strontium Nitrite Monohydrate

In a study using microcalorimentry and thermal analysis techniques, strontium nitrite was found to be formed during the ageing process of the pyrotechnic composition of magnesium with strontium nitrate [46]. The ageing process was carried out using a microcalorimeter at elevated humidities. It was found that the formation of strontium nitrite eliminated the induction reaction of magnesium and strontium nitrate. The nitrite hydrates to form its stable monohydrate. On heating strontium nitrite monohydrate, the dehydration reaction was seen to take place at around 150 ℃. Gallagher carried out a study on the monohydrate using TGA and mass spectrometry which determined a mass loss of 9.1% and confirmed that the dehydration took place with the sole evolution of water [47]. The theoretical mass loss for the dehydration is 9.1% according to the following equation (Eq. 4):

$$Sr(NO_2)_2.H_2O \rightarrow Sr(NO_2)_2 + H_2O \qquad \text{(Eq. 4)}$$

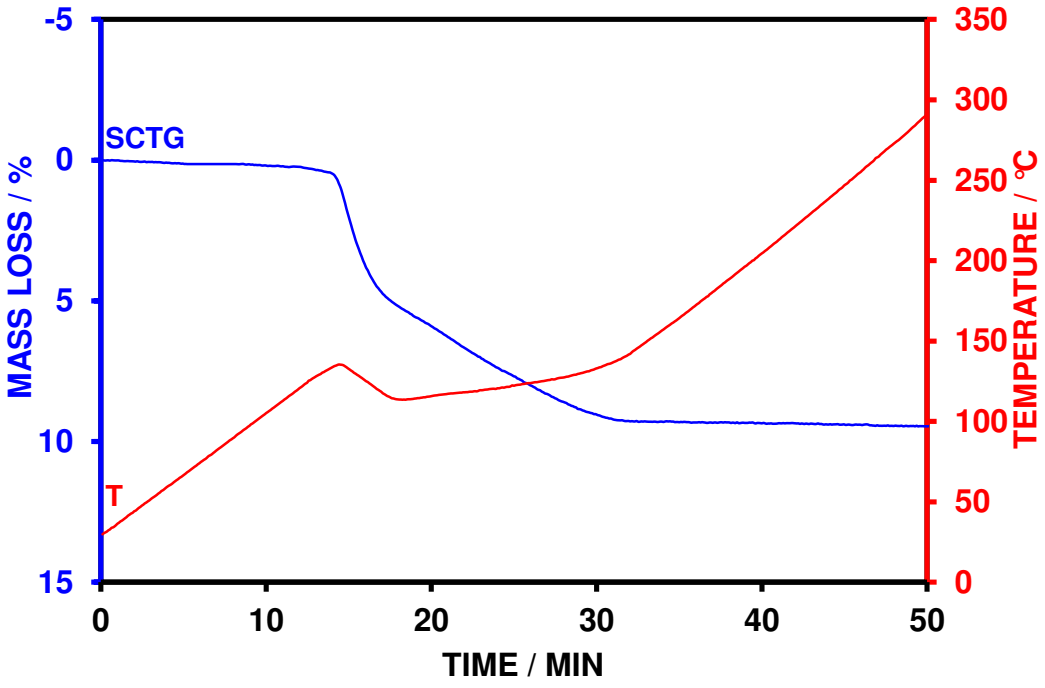

Fig. 3.15 SC-TG and temperature curves for the dehydration reaction of strontium nitrite monohydrate [46]
(sample mass, 10mg; heating rate, ±10 ℃ min^{-1}; atmosphere, nitrogen)

A SC-TG experiment was carried out on the monohydrate sample and it can be seen in Fig. 3.15 that once the mass loss begins that cooling was required to regain control. Almost 50% of the mass loss had occurred before the target rate of mass loss was adequately under control. The temperature at the end of the decomposition was seen to be less than 10 ℃ greater than that of the onset of dehydration showing the effect created by the nucleation and growth of the anhydrous material.

A linear heating DSC experiment for the dehydration reaction of strontium nitrate monohydrate is presented in Fig. 3.16 and it can be seen that the reaction occurred as a single endothermic event in agreement with the TG studies by Gallagher.

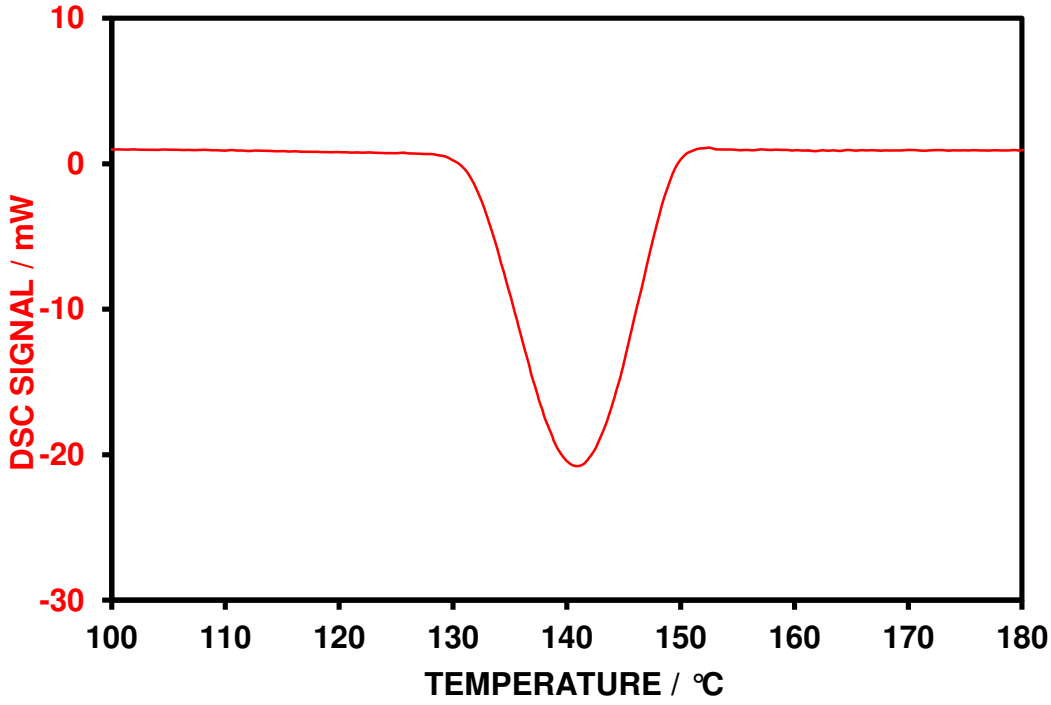

Fig. 3.16 Linear heating of strontium nitrite monohydrate
(sample mass, 10mg; heating rate, 5℃ min^{-1}; atmosphere, nitrogen)

A series of proportional heating experiments were performed on fresh samples at target levels of 10, 5 and 2mW using symmetrical heating.

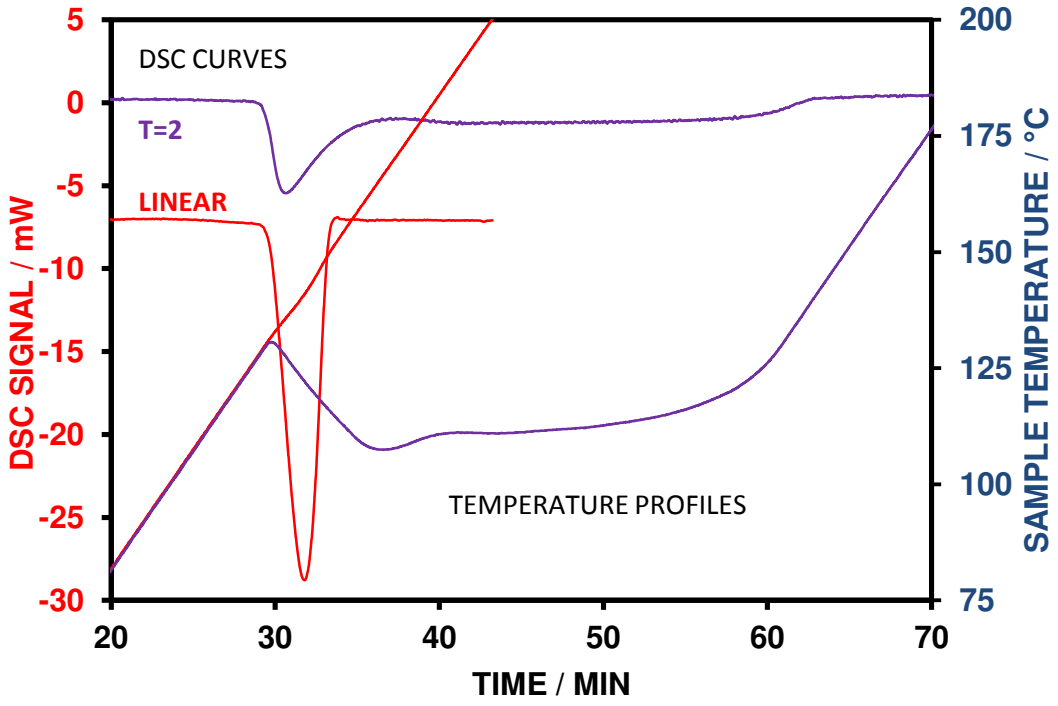

Fig. 3.17 Overlay of DSC and temperature curves for the linear heating and proportional heating at a target level of 2mW of strontium nitrite monohydrate (sample mass, 10mg; heating rates, 5°C min^{-1} and ±5°C min^{-1}; atmosphere, nitrogen)

A comparison of the linear heating and a proportional heating experiment is presented in Fig. 3.17 where it can be seen that the time of the dehydration event had been lengthened to around 35 minutes at the 2mW target level compared to 4 minutes for the linear heating experiment.

In the sample controlled experiments it can be seen that as the dehydration reaction is initiated the DSC signal exceeded the target level so that cooling was required. In the case of the 2mW target level, cooling of around 25°C was achieved before heating was resumed.

When the extent of reaction was plotted with respect to sample temperature, shown in Fig. 3.18 it can be seen clearly the level of cooling that was required. Although it appears that the end of the dehydration reaction is at a similar temperature in the linear and proportional heating experiments, the effect of cooling in the proportional heating experiments has meant that over 95% of the reaction has occurred at a temperature that is lower than the temperature at which the dehydration began. This

implies that the dehydration reaction was catalysed by nucleation and growth of the dehydrated product once the reaction was initiated. Comparing the sample controlled experiments using TG and DSC it can be seen that the temperature profiles appear to have a similar profile for the decomposition with both showing an initial cooling before proceeding at a slow temperature rise through the remainder of the decomposition. The change in rates seen by TG and DSC imply that the dehydration reaction is a multi-mechanism event. In addition, the lowering of the target level to 2 mW produced an exaggerated cooling until around 40% through the reaction. This unusual shape would require further investigation.

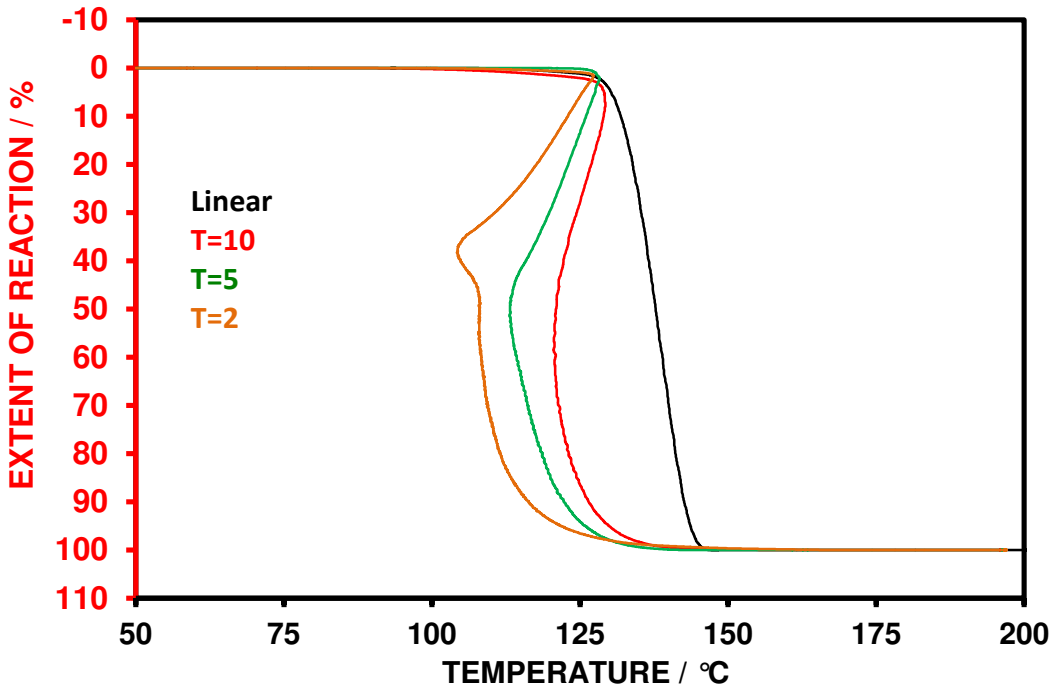

Fig. 3.18 Extent of reaction by peak area against temperature for a series of proportional heating experiments using several target rates for the dehydration of strontium nitrite monohydrate

3.5 Exothermic Decomposition of Potassium Dinitramide

Dinitramide based compounds, ($xN(NO_2)_2$ where x = cation) have the potential to replace many of the energetic compounds with the suggestions that they may be used in applications such as lead free detonators, insensitive ammunition, primary and secondary explosives, pyrotechnics and also as oxidisers in liquid and solid rocket propellants [48]. As potassium dinitramide is a potent oxidiser and chlorine free it provides a more environmentally friendly option to that of perchlorate based oxidisers that are more commonly employed.

Potassium dinitramide (KDN) decomposes in the solid state to form potassium nitrate with the evolution of nitrogen oxides. The thermal decomposition is different however as when the decomposition occurs in the liquid state then there is the formation of potassium nitrite to compete with potassium nitrate formation.

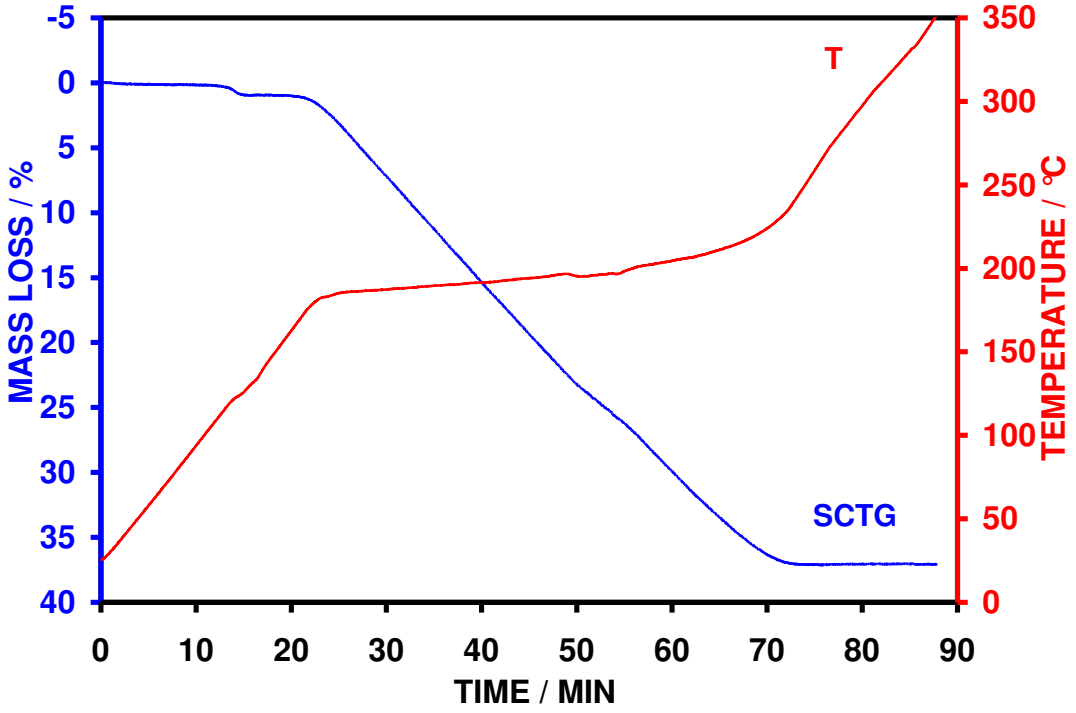

Fig. 3.19 SC-TG and temperature curves for the proportional heating of potassium dinitramide
(sample mass, 5mg; heating rate, ±10 °C min^{-1}; atmosphere, nitrogen)

Fig. 3.19 shows a sample controlled TG experiment on potassium dinitramide and it can be seen that there is a small step of 0.9% in the region of 125 °C due to

decomposition in the solid state prior to the fusion reaction. Following the fusion reaction, a steady rate of mass loss was seen from around 175 ℃ and continued linearly to around 195 ℃ after which there is a noticeable inflection in the SC-TG and temperature curves. The slight inflection is seen to create a slight delay in the decomposition before resuming a steady rate of mass loss.

Fig. 3.20 shows a linear heating DSC experiment for a 5mg sample of KDN (Bofors 503) at 5℃ min^{-1}. It can be seen that the sample undergoes a fusion reaction at around 130 ℃. The fusion endothermic reaction was seen to have a small event at 108℃ which is due to the eutectic formation of KDN and KNO_3 [49] which was followed by the sharp endothermic event of the bulk fusion. A small overlapping peak was seen on the preceding edge of the fusion peak and this may be due to a small level of solid state decomposition prior to the fusion. At around 160 ℃, the DSC curve developed an exothermic event due to a vigorous bubbling decomposition of the sample. Superimposed on the exothermic decomposition peak is an increase in the heat output and this is due to the exothermic recrystallization of the potassium salts formed during decomposition.

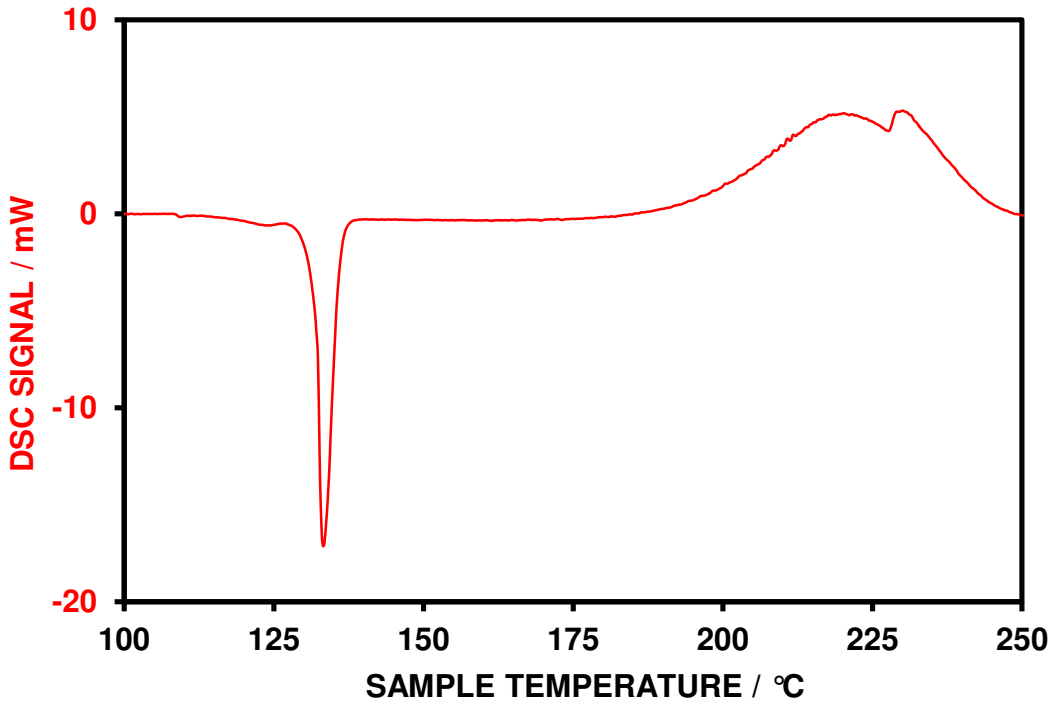

Fig. 3.20 DSC curve for the linear heating of potassium dinitramide (Bofors 503)
(sample mass, 4.96mg; heating rate, 5℃ min^{-1}; atmosphere, nitrogen)

A series of sample controlled experiments were carried out using the proportional heating method in both symmetrical and unsymmetrical heating modes. Fig. 3.21 shows a comparison of a linear heating experiment with a proportional heating experiment where sample was heated symmetrically with a target of 5mW.

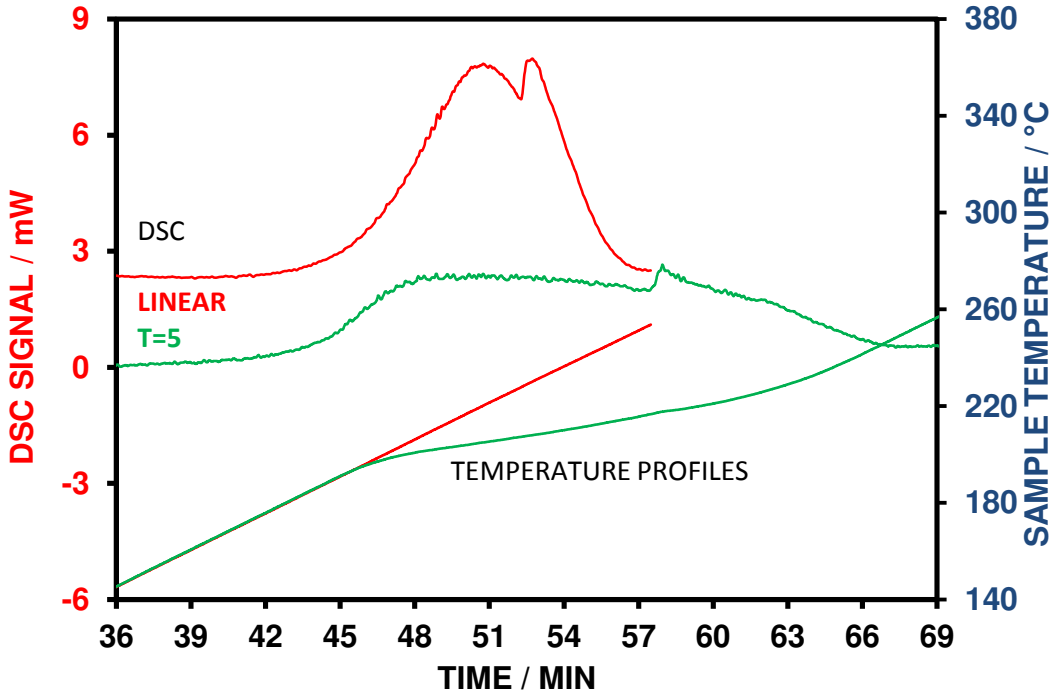

Fig. 3.21 Overlay of DSC and temperature curves for the linear heating and proportional heating of potassium dinitramide (Bofors 503)
(sample mass, 5mg; heating rates, 5 °C min^{-1} and ±5 °C min^{-1}; atmosphere, nitrogen)

There appeared to be good control of the exothermic decomposition reaction. Plotting the DSC curves with respect to temperature (Fig. 3.22) showed that the recrystallization temperature during the exothermic reaction had been promoted to an earlier temperature. The heating rate observed at the point of recrystallisation was seen to have a reduction in temperature and is assumed to reflect the heating rate dependence of the recrystallization peak as shown in Fig. 4.23 [48] on this material.

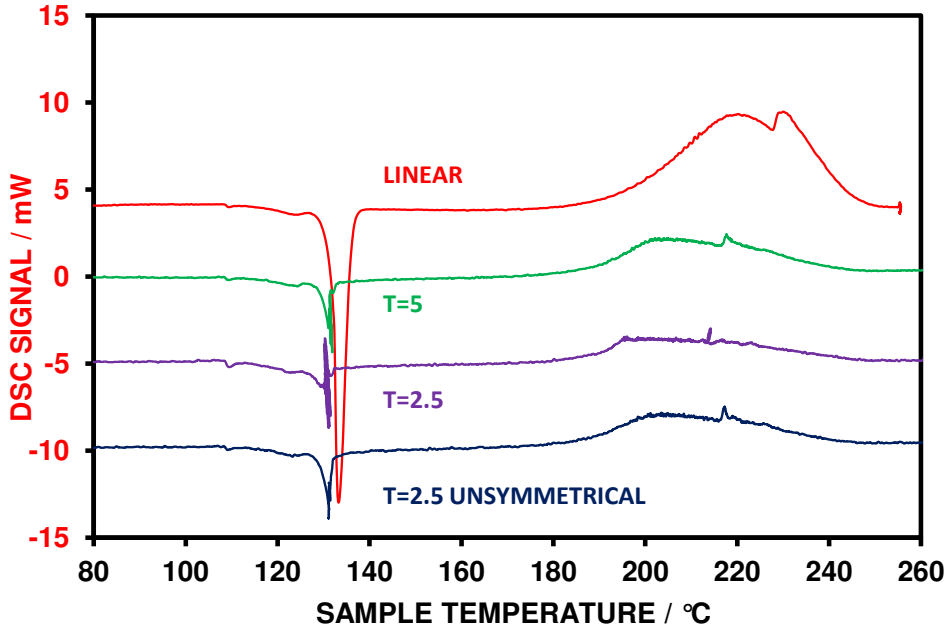

Fig. 3.22 Overlay of DSC and temperature curves for the linear heating and proportional heating at several target levels of potassium dinitramide (sample mass, 5mg; heating rates, 5℃ min^{-1} (linear), ±5℃ min^{-1} (symmetrical) and 5 & 0℃ min^{-1} (unsymmetrical); atmosphere, nitrogen)

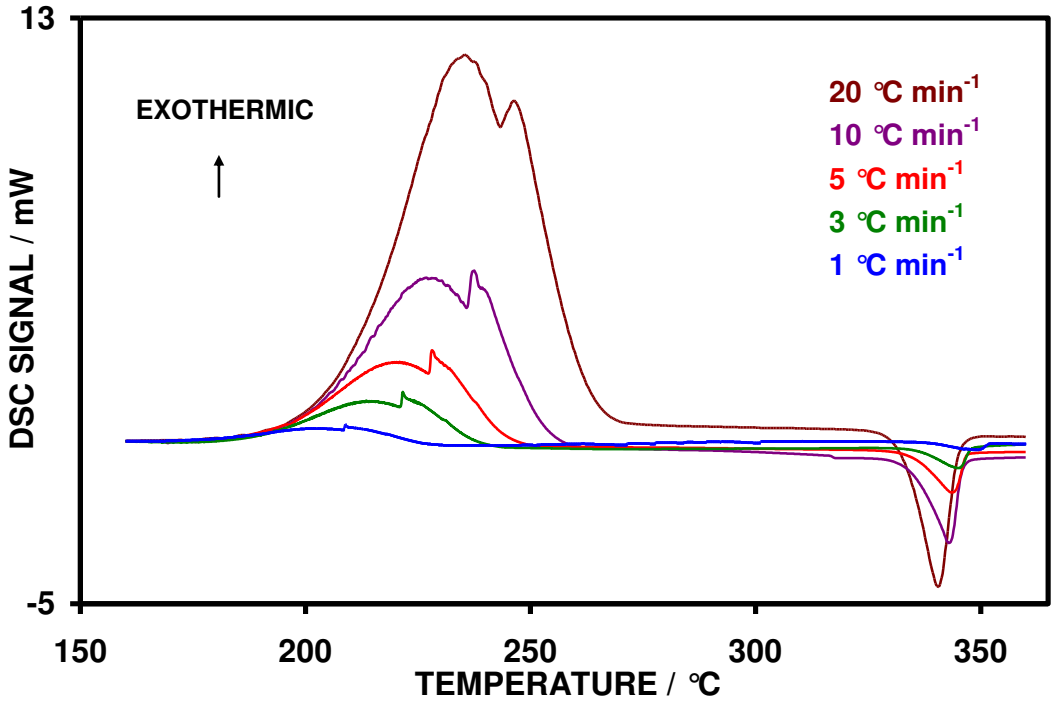

Fig. 3.23 DSC curves for the heating rate dependence of potassium dinitramide (sample mass, 2.5mg; heating rates, 1 – 20 ℃ min^{-1}; atmosphere, nitrogen)

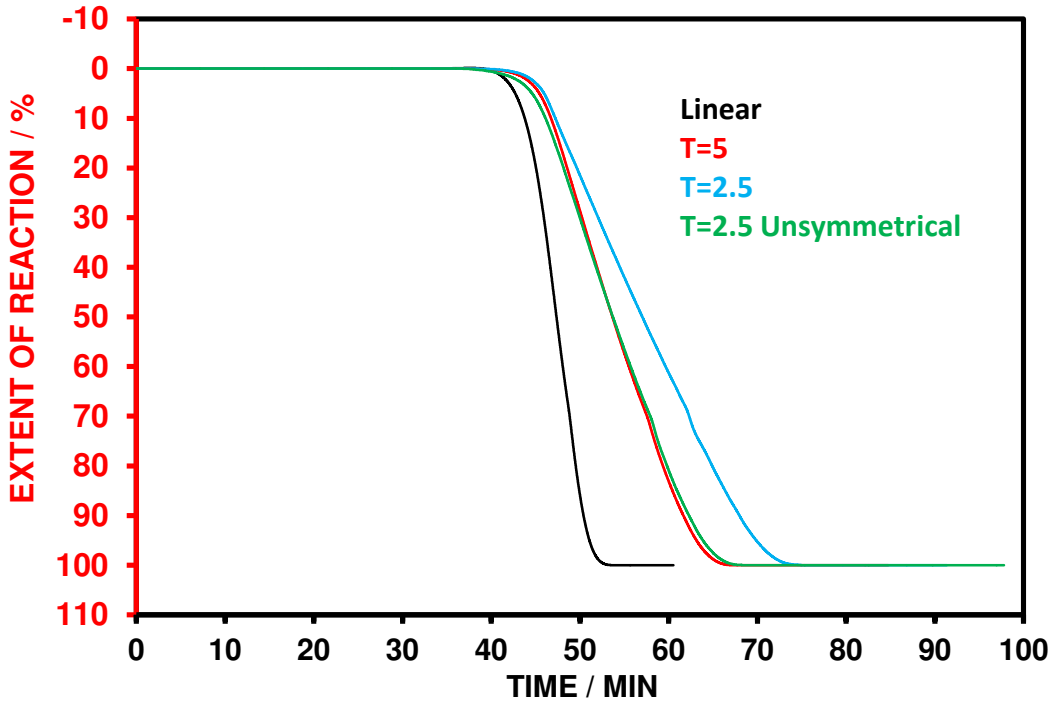

Fig. 3.24 Extent of Reaction for the linear heating and proportional heating at several target levels of potassium dinitramide with respect to time

Fig. 3.24 shows the extent of exothermic decomposition reaction with respect to time and it can be seen that there is a reasonably good control of the decomposition reaction. From Fig. 3.25 it can also be seen that where there has been some form of sample control, that there is an inflection at around the 70% reaction level. The inflection in the curve confirms the arrest in the temperature curve observed in the SC-TG experiment (Fig. 3.19).

A similarity that arose from this series of experiments is that the symmetrically heated proportional experiment carried out with a target of 5mW appeared to be almost identical to the unsymmetrically heated sample at a target of 2.5mW and can be seen in Fig. 3.25. The explanation to this occurrence is that although a low target was employed, the signal did not exceed the target level to initiate the cooling portion of the symmetrical heating and continual heating was seen. This effectively means that the target of 5mW for the symmetrical heating was being controlled over a 10℃ range whereas in the 2.5mW unsymmetrical it was 5℃. The ratio of target to heating rate was the same and therefore similar DSC and temperature curves were produced. The extent of reaction plotted with respect to temperature is shown in Fig. 3.26 that illustrates the close similarity of these experiments.

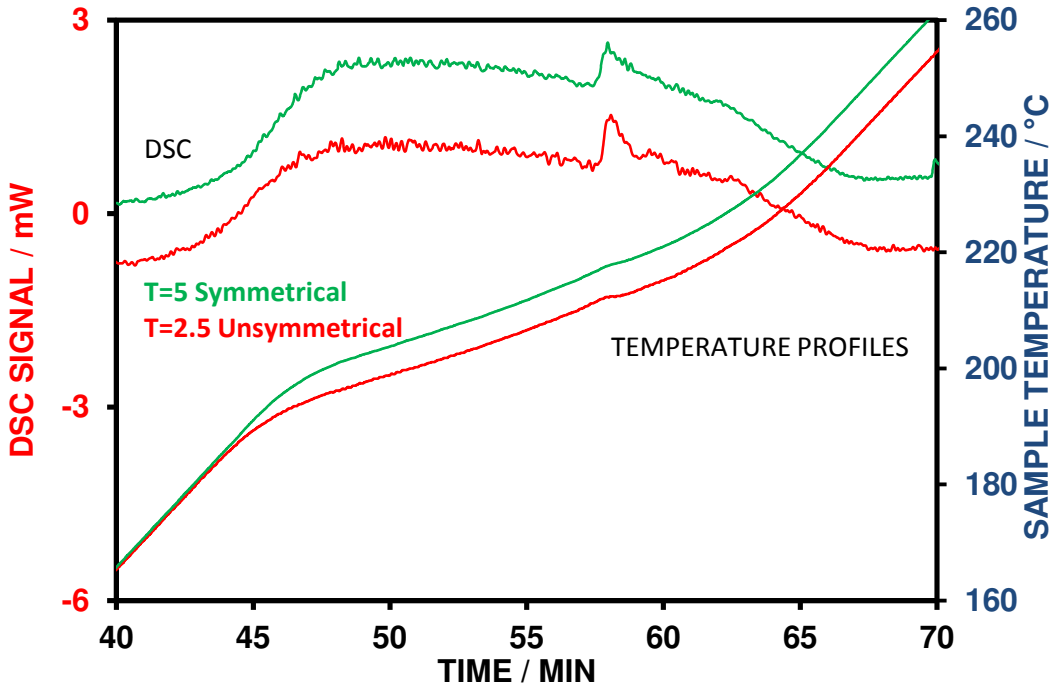

Fig. 3.25 Overlay DSC and temperature curves for the symmetrical and unsymmetrical proportional heating experiments for potassium dinitramide

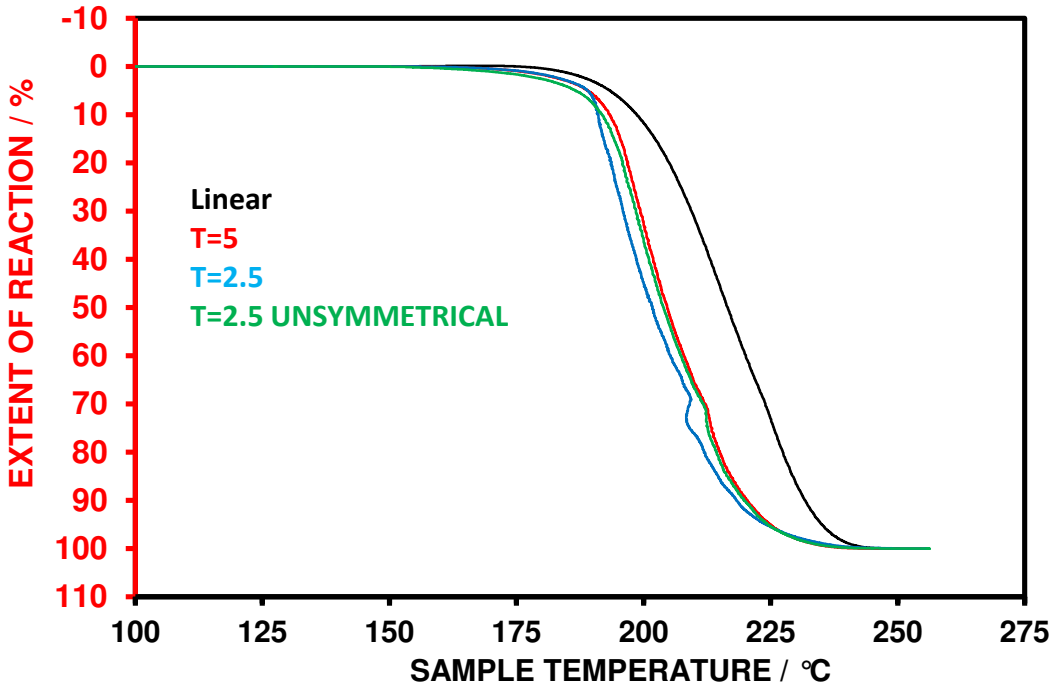

Fig. 3.26 Extent of reaction for the linear heating and proportional heating at several target levels of potassium dinitramide with respect to temperature

3.6 Exothermic Decomposition of Nitrocellulose

Nitrocellulose (also: cellulose nitrate, flash paper) is a highly flammable compound formed by nitrating cellulose through exposure to nitric acid or another powerful nitrating agent. When used as a propellant or low-order explosive, it is also known as guncotton. The power of guncotton made it suitable for blasting. As a projectile driver, it has around six times the gas generation of an equal volume of black powder and produces less smoke and less heating.

The thermal behaviour of nitrocellulose is of interest from a pyrotechnic viewpoint. It is added to certain compositions as a granulating agent but has also been found to modify the thermal behaviour of the zirconium – potassium perchlorate system [48]. Previous studies have shown that nitrocellulose decomposes exothermically in the region of 200 °C, via a vigorous bubbling reaction [51].

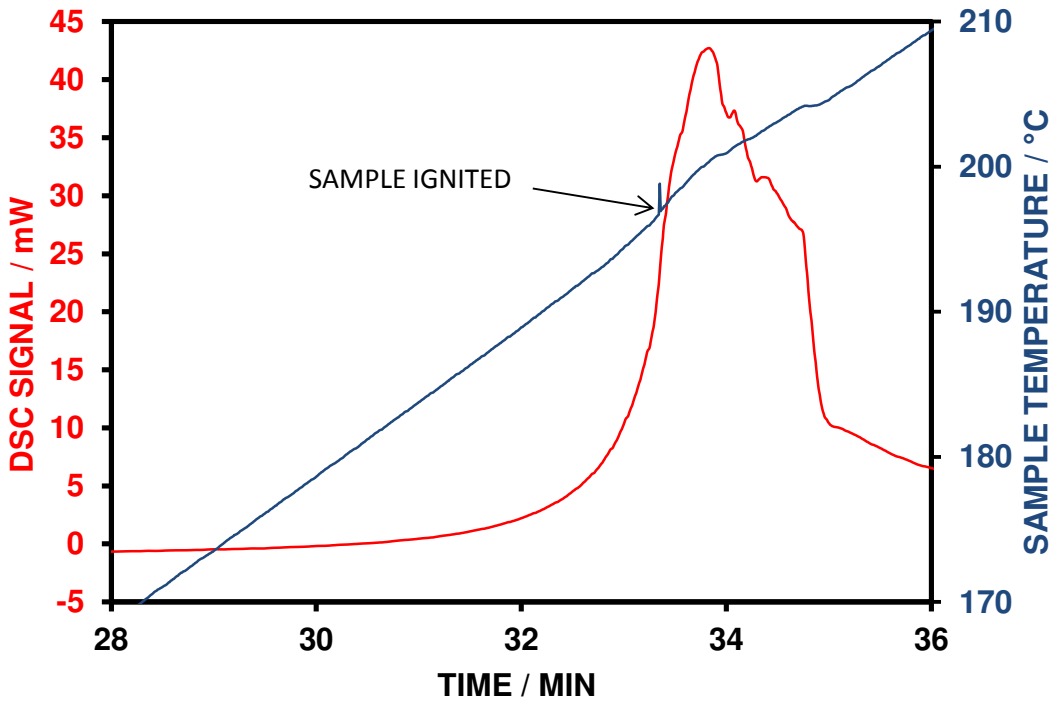

Fig. 3.27 DSC and temperature curves for nitrocellulose showing ignition (sample mass, 5 mg; heating rate, 5 °C min^{-1}; atmosphere, nitrogen)

When a sample mass as low as 2 mg is heated at 10 °C min^{-1} this reaction can frequently result in ignition and this is illustrated by the DSC curve in Fig. 3.27. An

example of the ignition is shown in Fig. 3.28 with photomicrographs of a 2.5mg sample of nitrocellulose (at 10 ℃ min^{-1}) both pre and post ignition shown in Figs. 3.29 and 3.30 respectively.

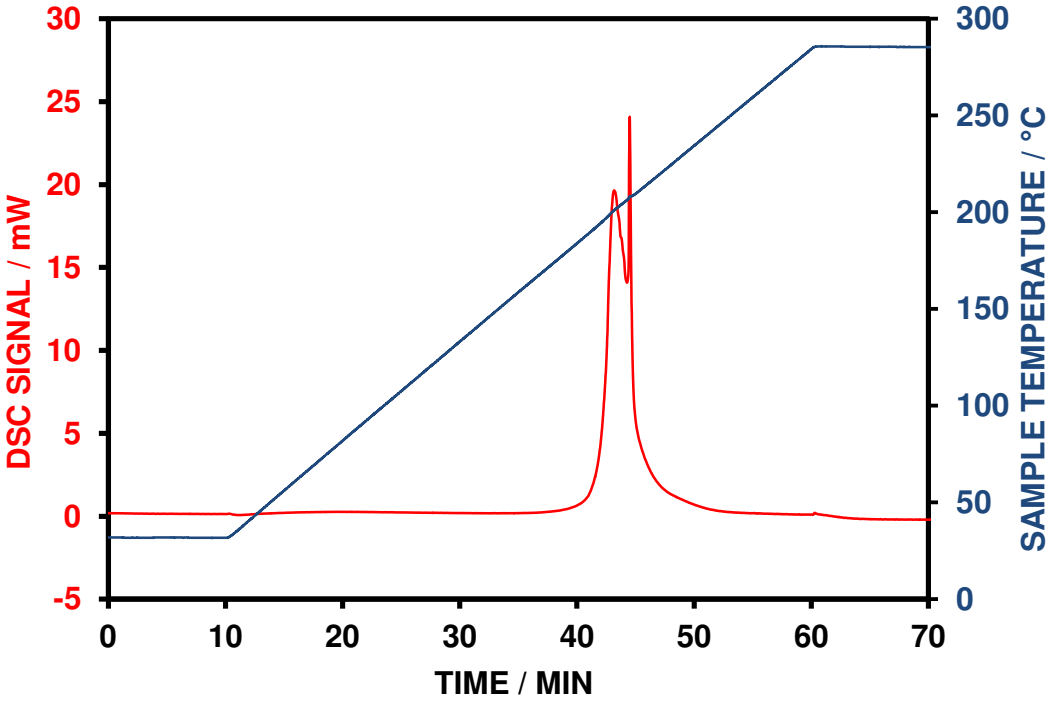

Fig. 3.28 DSC and temperature curves for nitrocellulose
(sample mass, 2 mg; heating rate, 5℃ min^{-1}; atmosphere, nitrogen)

Fig. 3.29 Photomicrograph of nitrocellulose prior to ignition
(sample mass, 2.5mg; heating rate, 10℃ min^{-1}; atmosphere, nitrogen)

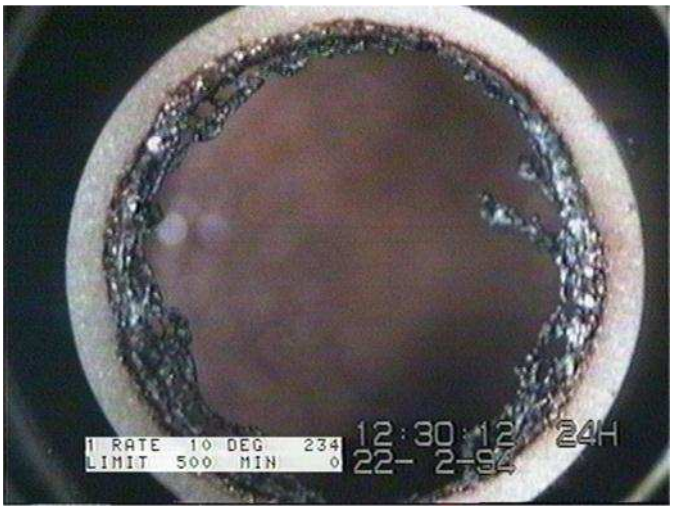

Fig. 3.30 Photomicrograph of nitrocellulose after ignition
(sample mass, 2.5mg; heating rate, 10℃ min^{-1}; atmosphere, nitrogen)

A series of proportional heating experiments were carried out using the symmetrical heating mode only and at target levels of 10, 5 and 2mW and sample masses of 2.5 mg.

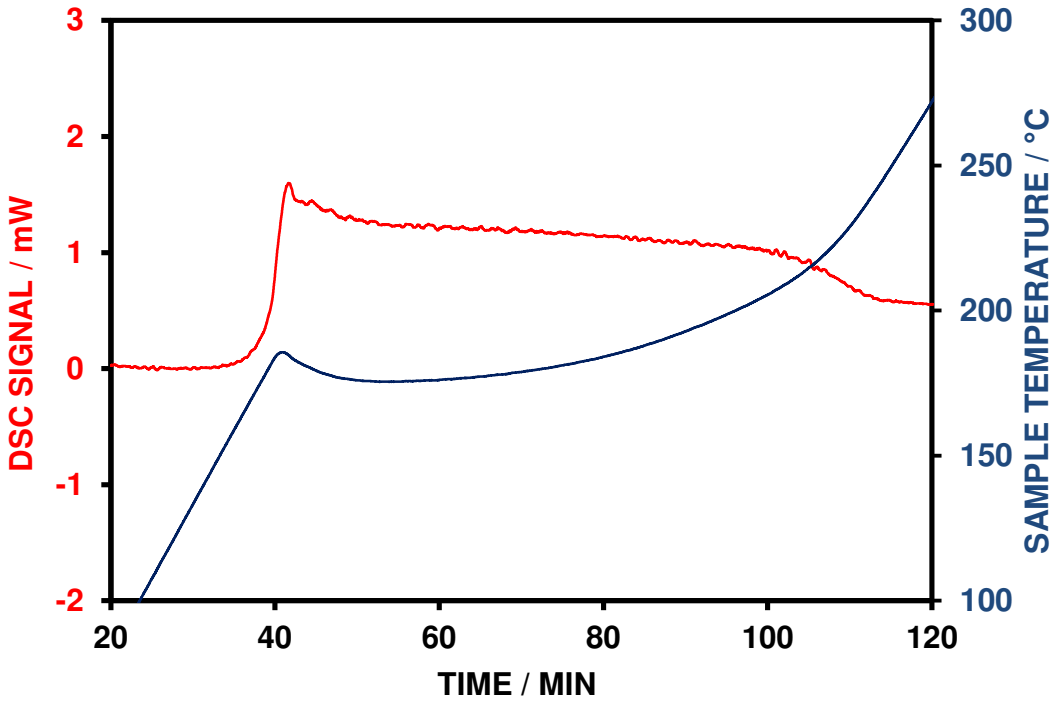

Fig. 3.31 DSC and temperature curves for the proportional heating of nitrocellulose
(sample mass, 2.5mg; heating rate, ±5℃ min^{-1}; target, 2mW; atmosphere, nitrogen)

Fig. 3.31 shows the overlay of DSC and temperature curves for a proportional heating experiment with a target used of 2mW and it can be seen that the ignition reaction has been eradicated and the decomposition reaction lengthened to over an 80 minute period. It can be seen from the temperature curve that there needed to be a significant element of cooling in order to attain sample control. The decomposition of nitrocellulose is well known to be autocatalytic and this is reflected in the shape of the temperature profile. The results showed similar trends in temperature profile to those obtained by Charsley et al using SC-TG [52] and by Paulik et al using quasi-isothermal thermogravimetry [53].

Based on the successful control at the 2mW target level, the same target level was repeated but with an increased mass of 5mg of nitrocellulose. The resulting DSC and temperature curves showed good control with no ignition reaction observed and the decomposition reaction extending over a period of 125 minutes. This is in contrast to the ignition reaction achieved using linear heating conditions at the 5 mg sample mass level.

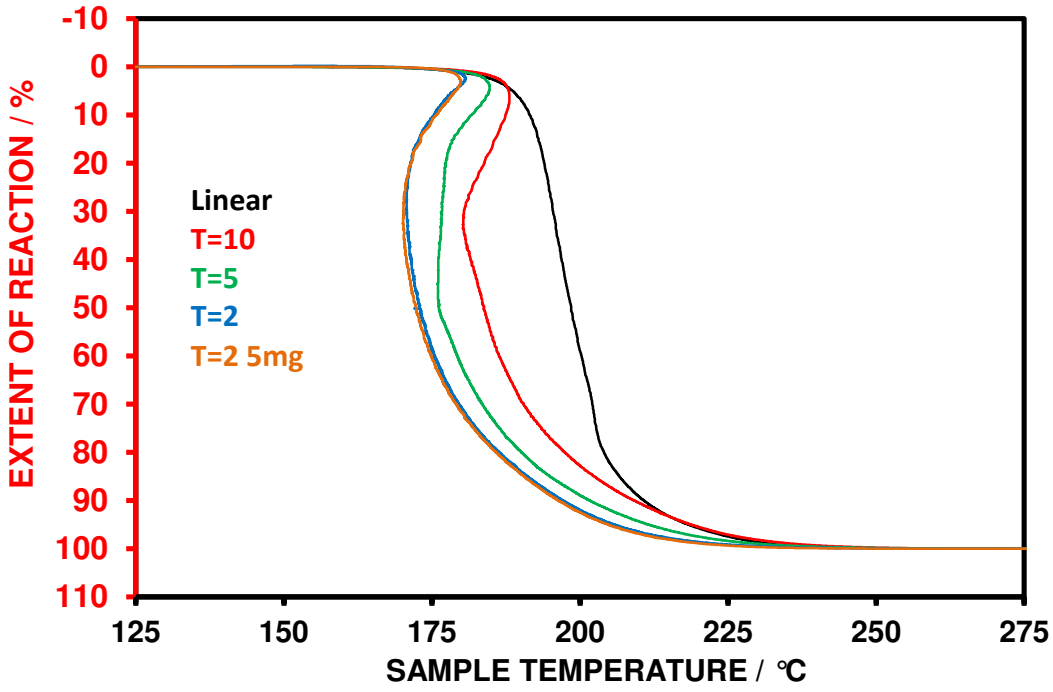

Fig. 3.32 Extent of reaction for the linear heating and proportional heating at several target levels of nitrocellulose with respect to temperature

Fig. 3.32 presents an overlay of the extent of reaction with respect to temperature at different target rates and it can be seen that by reducing the rate of the decomposition reaction reduces the likelihood of an ignition taking place. Raising the target level to 10 mW (Fig. 3.33), the reaction was controlled but an increased level of cooling was required to prevent thermal runaway. The control observed when increasing the sample mass would suggest an increase in the scope of DSC to study energetic materials without instrumental damage. It is of note that when using the same target level at two different mass levels, that the extent of reaction with respect for temperature produced near identical curves. This will require further investigation to establish if there is a relationship between sample mass and target level or if they act independently for some systems.

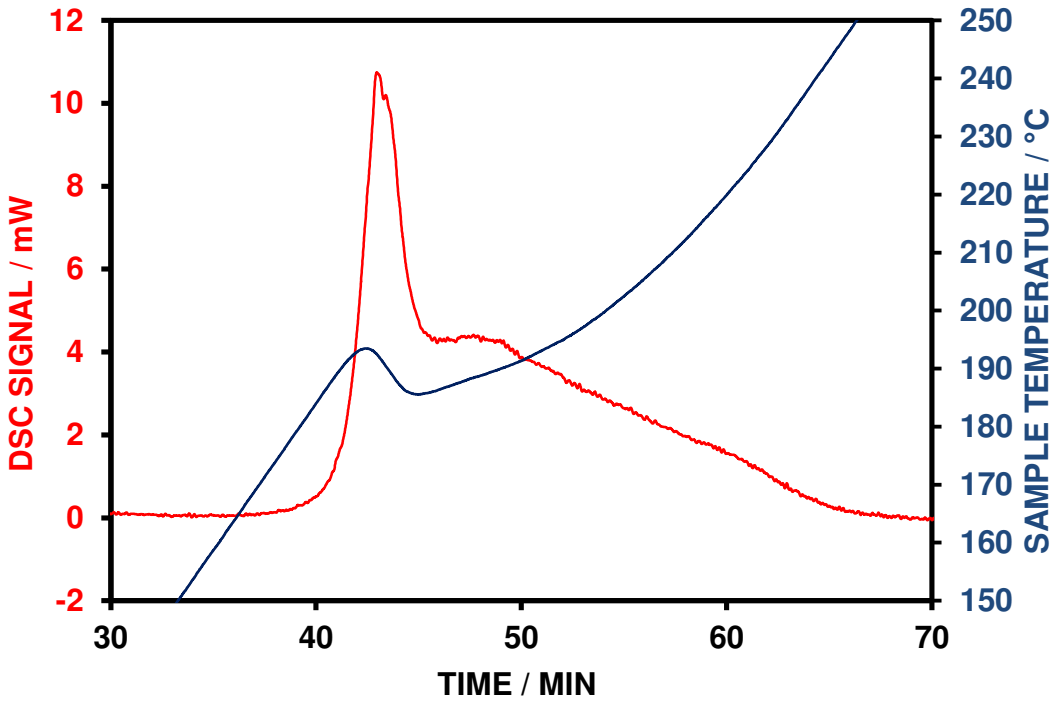

Fig. 3.33 DSC and temperature curves for the proportional heating of nitrocellulose
(sample mass, 2.5mg; heating rate, ±5℃ min^{-1}; target, 10mW; atmosphere, nitrogen)

3.7 Exothermic Oxidation of Carbon impregnated with Copper

The use of SC-DSC to study oxidation reactions was made by studying a copper impregnated carbon formed by the pyrolysis of a copper doped carboxymethyl cellulose sample in nitrogen at 400 ℃ [54]. In common with a number of activated carbon precursors, this system is very reactive and gives rise to highly exothermic reactions when heated in air. This is illustrated by the DSC curve obtained using a sample mass of 5 mg (Fig. 3.34).

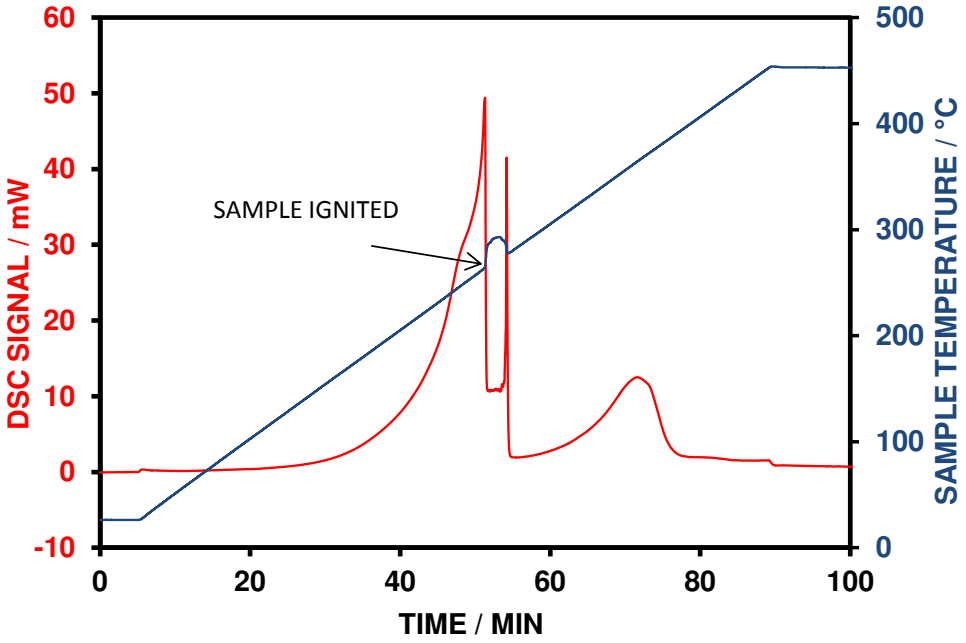

Fig. 3.34 DSC and temperature curves for the linear heating of a copper impregnated carbon sample
(sample mass, 4.86mg; heating rate, 5℃ min^{-1}; atmosphere, air)

The gasification reaction using aerial oxidation can therefore be difficult to control which can result in overheating and excessive burn-off leading to ignition and a non-uniform product. Reducing the sample mass to around 2mg also produced a sharp exothermic reaction and ignition and is shown in Fig. 3.35.

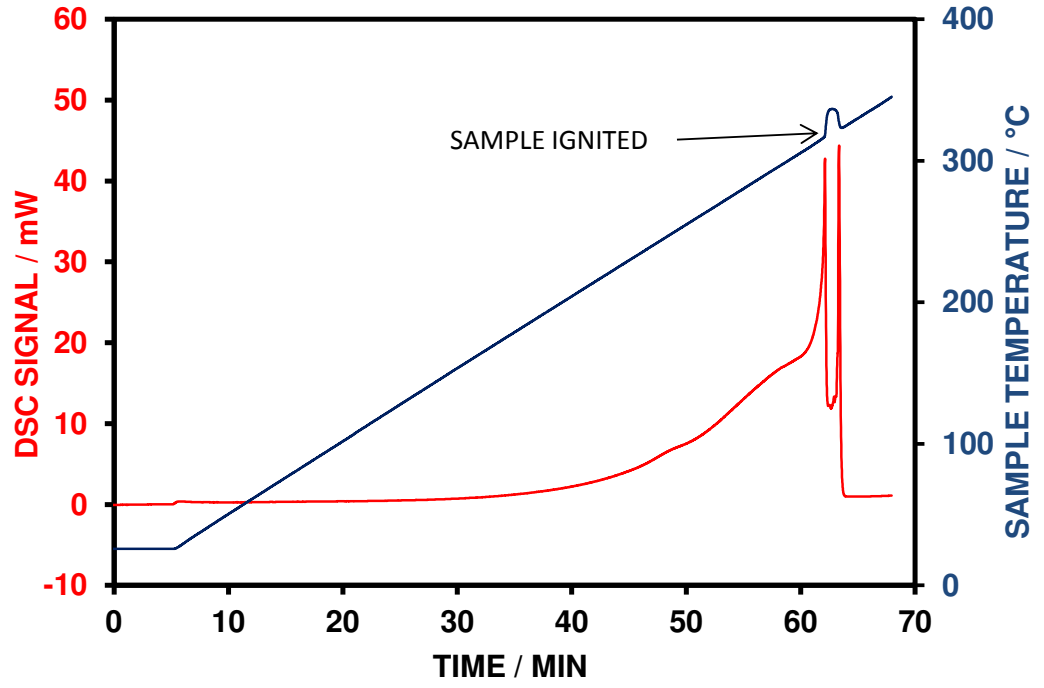

Fig. 3.35 DSC and temperature curves for the linear heating of a copper impregnated carbon sample

(sample mass, 2.06 mg; heating rate, 5℃ min^{-1}; atmosphere, air)

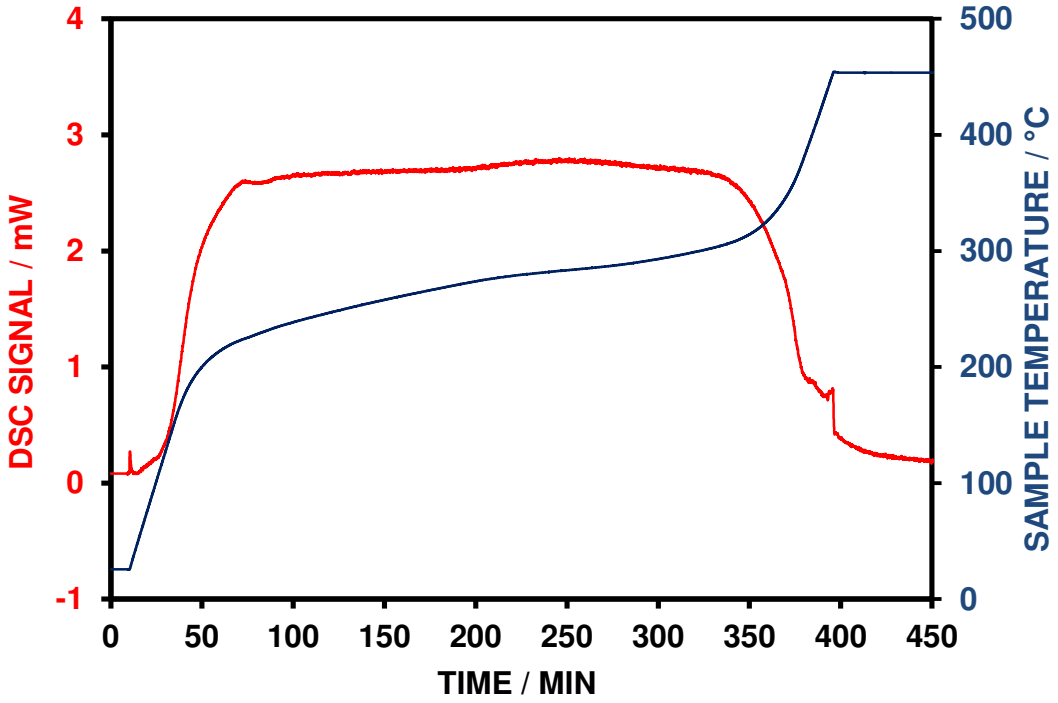

Fig. 3.36 DSC and temperature curves for the proportional heating of a copper impregnated carbon sample

(sample mass, 2.25 mg; heating rate, ±5℃ min^{-1}; target, 5mW; atmosphere, air)

An SC-DSC experiment using a 2mg sample mass of the doped carbon in air is given in Fig. 3.36. This shows that a well-controlled low temperature oxidation reaction has been obtained and that in order to achieve this, a low rate of heating has been used in the final stages. The chosen target rate has extended the oxidation reaction over a period of more than 340 minutes effectively eliminating self-heating problems. Thus, the technique offers the possibility of producing products of predetermined pore structure and surface area.

A series of proportional heating experiments were carried out using a variety of target levels from 5 mW to 25 mW with the symmetrical heating mode on 2 mg samples. An overlay plot for the linear heating experiment and the longest proportional heating experiment is shown in Fig. 3.37 and it can be seen that a good level of control can be achieved. The ignition reaction seen for the linear heating experiment did not occur for any of the sample controlled experiments.

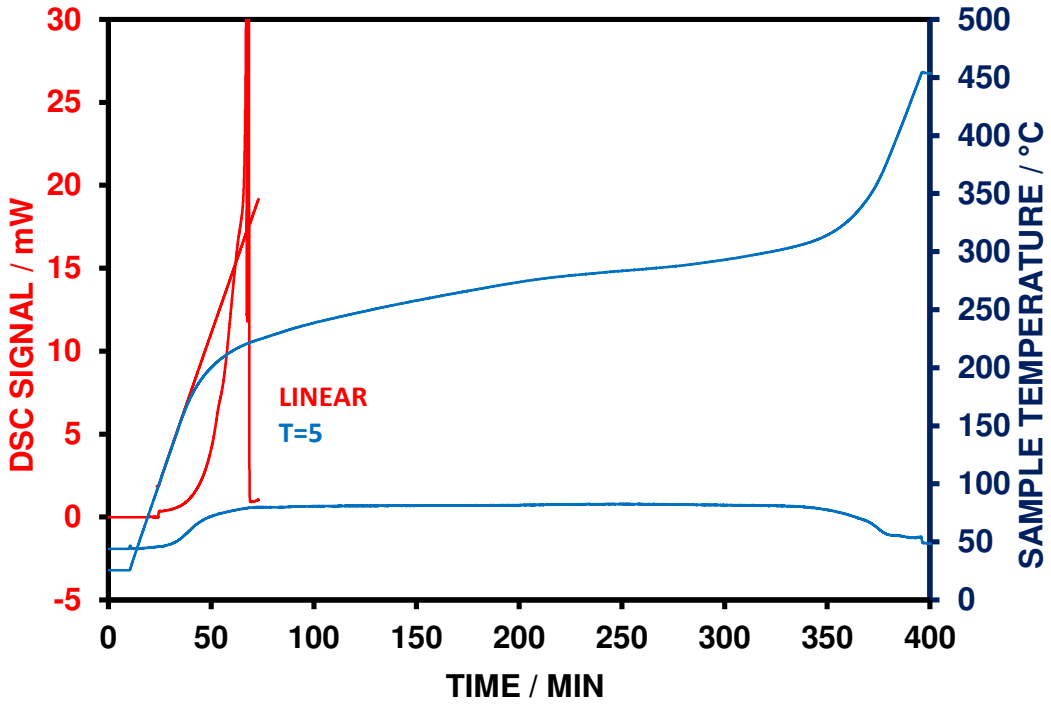

Fig. 3.37 Overlay of DSC and temperature curves for the linear heating and proportional heating of a copper impregnated carbon sample (sample mass, 2mg; heating rate, 5 °C min^{-1} and ±5 °C min^{-1}; atmosphere, air)

A plot of the extent of reaction with respect to temperature is shown in Fig. 3.38 and it can be seen that the oxidation reactions in all the experiments began and ended at almost the same temperatures in each case. The majority of the oxidation reaction carried out using a 5 mW target level occurred at around 15 ℃ lower than the linear heating experiment indicating control. However, reducing the target level did not show any significant benefits with respect to temperature. This suggests that although the time of the oxidation has been lengthened with reducing the target level, the oxidation reaction still requires the increase in temperature in order to proceed and therefore to oxidise the carbon, it appears that there is physical aspect to overcome which is provided by the temperature.

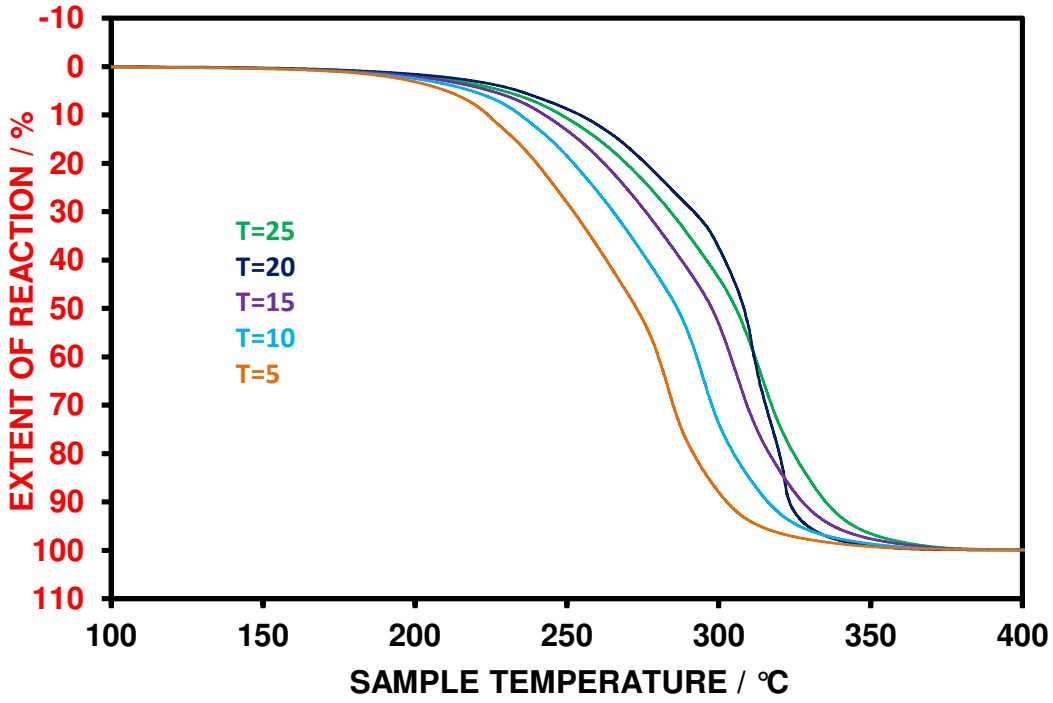

Fig. 3.38 Extent of reaction with respect to temperature for the proportional heating of a copper impregnated carbon sample at various target levels

Chapter 4 Applications: Reactions that take place without a Change in Mass

4.1 Aim and applications of SC-DSC to reactions without a mass change

The aim of this chapter is to evaluate the applicability of the sample controlled DSC technique to a wide range of reaction types. Discussed in this chapter will be reactions that occur without a change in sample mass such as aqueous fusion reactions, phase changes, fusion reactions and reactions in the solid state.

4.2 Exothermic Curing reaction of Araldite

Curing reactions are of interest in this study in that during the cross-linking process of the ingredients, there is a generation of heat without any appreciable mass change taking place. This makes such systems ideal candidates for thermal studies using a curing regime by DSC to establish the full cure of a thermoset material with the reheat of the fully cured material in many cases revealing a glass transition.

One such system is the thermal curing of Araldite ® which is a heavy duty adhesive. The system contains Bisphenol A-epoxy resins with a number average MW >700 to <1000. These are namely polyamide resin and epoxy phenol novolac resin. The system is a strong 2-component epoxy resin that when mixed in equal volumes provides a mixture that is workable for around 90 minutes reaching full strength after around 14 hours at ambient temperature [55].

Linear heating experiments were carried out on an Araldite ® sample that had been prepared by mixing equal volumes of the components for 30 seconds before weighing 30mg into an aluminium crucible. The crucible was sealed with an aluminium lid and immediately placed into the apparatus at 20℃. The temperature was then programmed to -20 ℃ which was aided by a mechanical cooling

attachment (MCA). The time taken from the start of mixing the components to achieving -20 ℃ within the instrument was 2 minutes. From a stable temperature of -20 ℃, the sample was heated at 5℃ min^{-1} to the end of the curing reaction. It can be seen from Fig. 4.1 that the experiment provided a broad single stage exothermic curing reaction having a peak temperature of around 100 ℃.

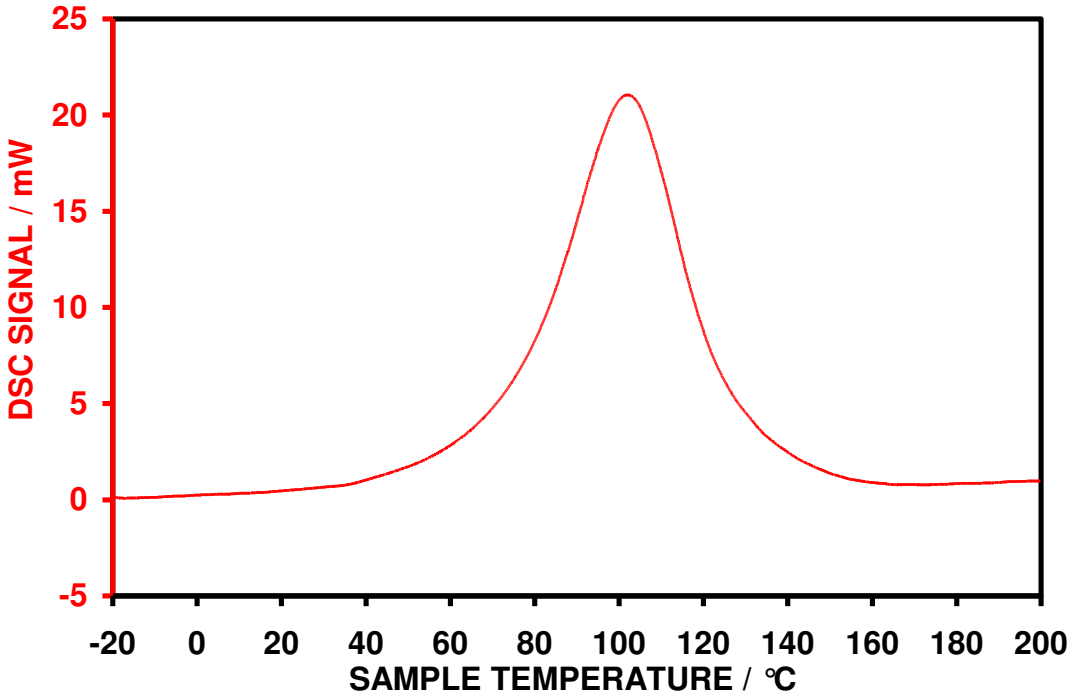

Fig. 4.1 Linear heating DSC curve for Araldite®
(sample mass, 30mg; heating rate, 5℃ min^{-1}; atmosphere, nitrogen)

A proportional heating experiment using symmetrical heating and a target level of 5 mW was carried out on a 30mg of a freshly mixed sample and is shown in Fig. 4.2. It can be seen that that there was control of the curing reaction from around 50 ℃ for a period of about 70 minutes before there appeared to be a small exothermic reaction superimposed towards the end of the curing peak.

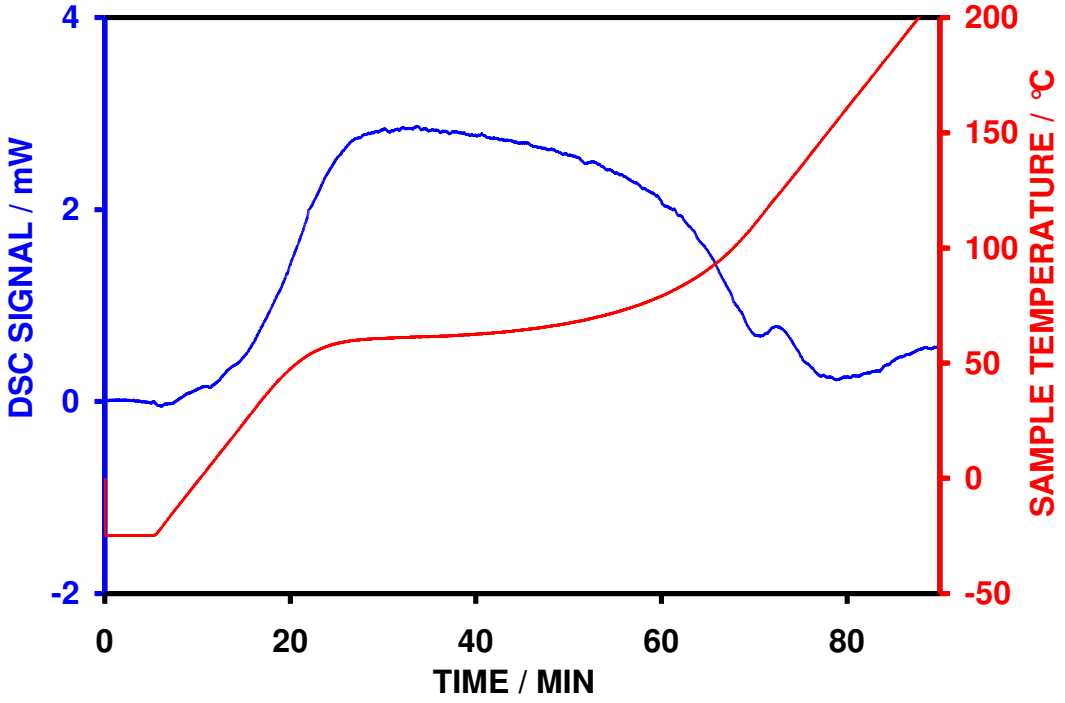

Fig. 4.2 DSC and temperature curves for the proportional heating of Araldite®
(sample mass, 30mg; heating rate, ±5°C min^{-1}; target, 5mW; atmosphere, nitrogen)

Unsymmetrical heating experiments were carried out on freshly mixed samples with a target level of 5 mW and 2mW and a good level of control was produced. Converting the exothermic peak areas into an extent of reaction, it can be seen that when plotted with respect to time that the curing reaction time has been lengthened and considerably more so when using the unsymmetrical heating mode and a lower target level. Using a target of 2mW in the unsymmetrical heating mode it was found that the time of curing reaction had been extended to around 100 minutes compared to around 12 minutes for the linear heating cure of the sample.

An extent of reaction plot with respect to sample temperature is shown in Fig. 4.3 and highlights the increased level of control obtained by using the unsymmetrical heating mode. It can be seen that when viewing the temperatures at 50% extent of reaction, that the sample temperature for the linear heating experiment was 91.5 °C compared to 48.5 °C for the similar extent of reaction for the unsymmetrically heated sample with a target level of 2 mW.

The use of sample control, symmetrically heating or not, has illustrated the reduced temperature range over which a reaction takes place under sample controlled conditions. The use of sample controlled DSC should allow the development of temperature profiles to enable samples to be cured at a selected rate.

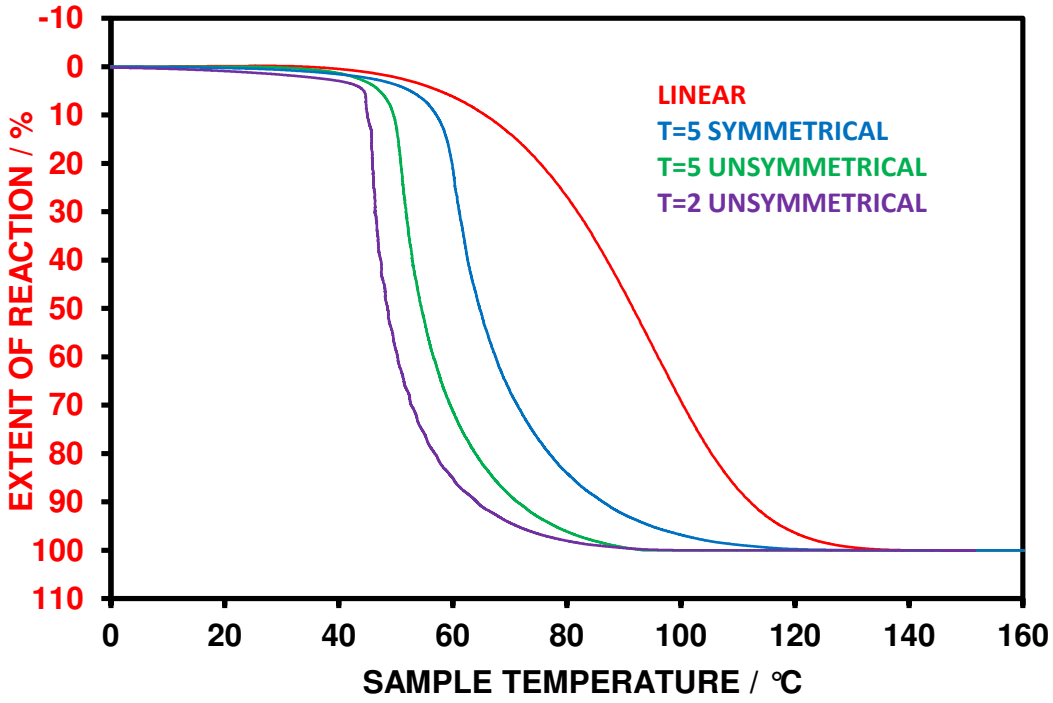

Fig. 4.3 Extent of reaction for the linear heating and proportional heating at several target levels of Araldite® with respect to temperature

4.3 Endothermic Aqueous Fusion of Magnesium Nitrate Hexahydrate

The reaction of magnesium nitrate hexahydrate is of interest due to two thermal events prior to 100 ℃. The first of these events is the solid-solid phase change in the region of 73 ℃ followed by the sample dissolving in its waters of crystallization at around 92 ℃. These events both take place reversibly without any mass changes when studied in a sealed system. It was found by Nagano, Ogawa, Mochida, Hayashi and Ogoshi [56] that the endothermic reactions on heating were completely reversible on cooling and that the heat-cool cycle of the material is repeatable for over 1000 cycles. Their study was to utilise the repeatability to use the latent heat storage of the phase changes in waste heat management such as the waste heat from generators. A study by Cantor [57] was carried out on a variety of salt hydrates including $Mg(NO_3)_2.6H_2O$ with the aim of using the materials for thermal energy storage.

A linear heating experiment for a 10mg sample is shown in Fig. 4.4. The sample is loaded in to an aluminium crucible and hermetically sealed with an aluminium lid.

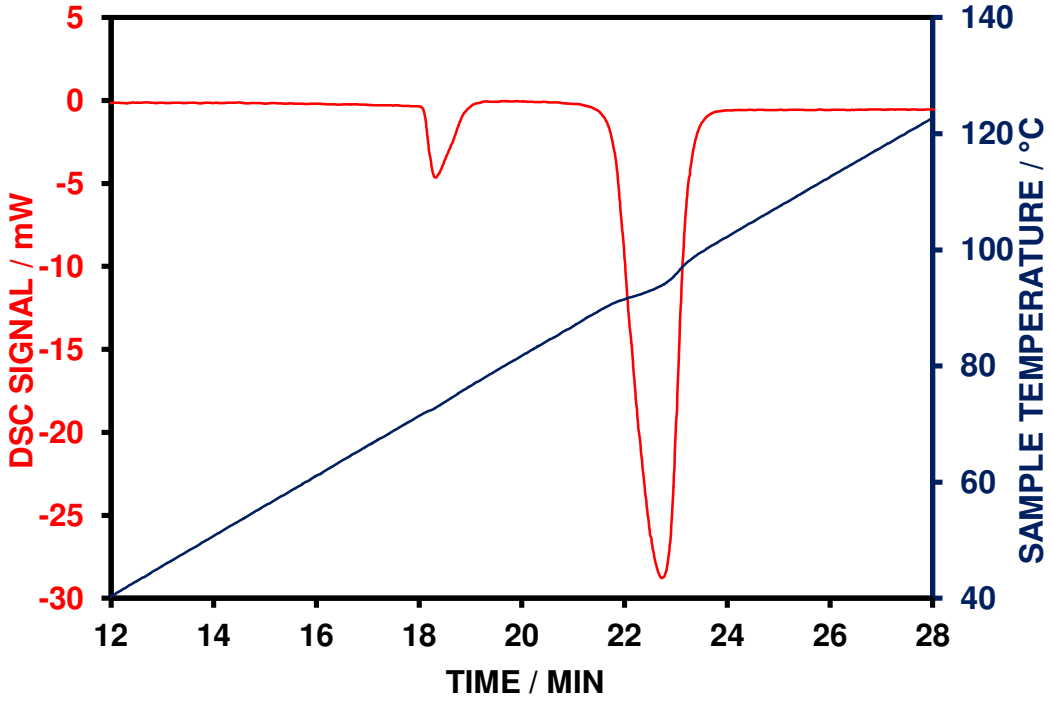

Fig. 4.4 DSC and temperature curves for the linear heating of magnesium nitrate hexahydrate
(sample mass, 10mg; heating rate, 5℃ min^{-1}; atmosphere, nitrogen)

It can be seen that the two endothermic peaks are present, the first being a small peak of less than 5 mW in height and the second peak being much larger with a peak height approaching 30 mW. In order to observe the reproducibility of the sample, three linear heating experiments were performed. It can be seen from Fig. 4.5 that the sample shows reasonable reproducibility without showing signs of decomposition and thus the same sample can be used for the rest of the investigation. The slight differences between the first heating and the repeat experiments are due to a better contact with the base of the crucible post aqueous fusion.

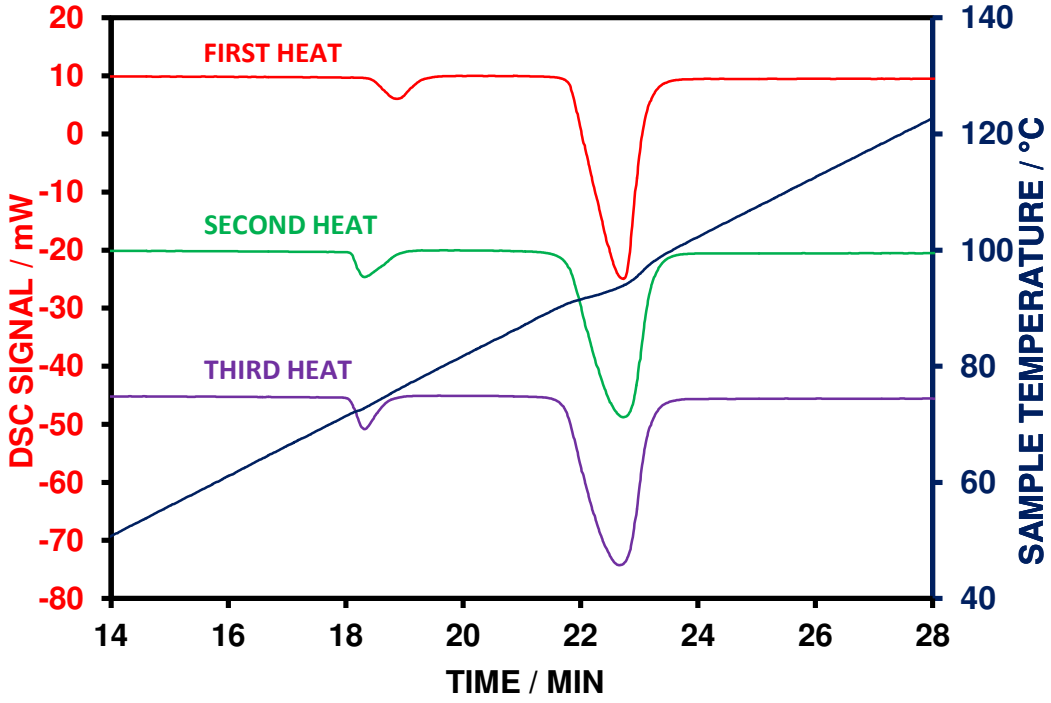

Fig. 4.5 DSC and temperature curves for three linear heating experiments of the same sample of magnesium nitrate hexahydrate
(sample mass, 10mg; heating rate, 5°C min^{-1}; atmosphere, nitrogen)

A proportional heating experiment was carried out on the sample with a target rate set to 10 mW and the symmetrical heating strategy used. It can be seen from Fig. 4.6 that heating through the first endothermic peak created a slight reduction in the heating rate but as the peak height was relatively small the maximum heating rate was resumed within 1 minute. This first endothermic peak will be ignored for the rest of this investigation. The second endothermic event however was seen to be split into four peaks for the aqueous fusion. The four peaks being produced for the

single event is due to the control system not being able to respond quickly enough as the target level is approached so that maximum cooling is required as the peak passes through the target setting. The cooling causes the reversal of the reaction to a small extent before proceeding through the reaction. This suggests that the resolidification on cooling is a slower step with respect to time than the actual dissolution reaction on heating.

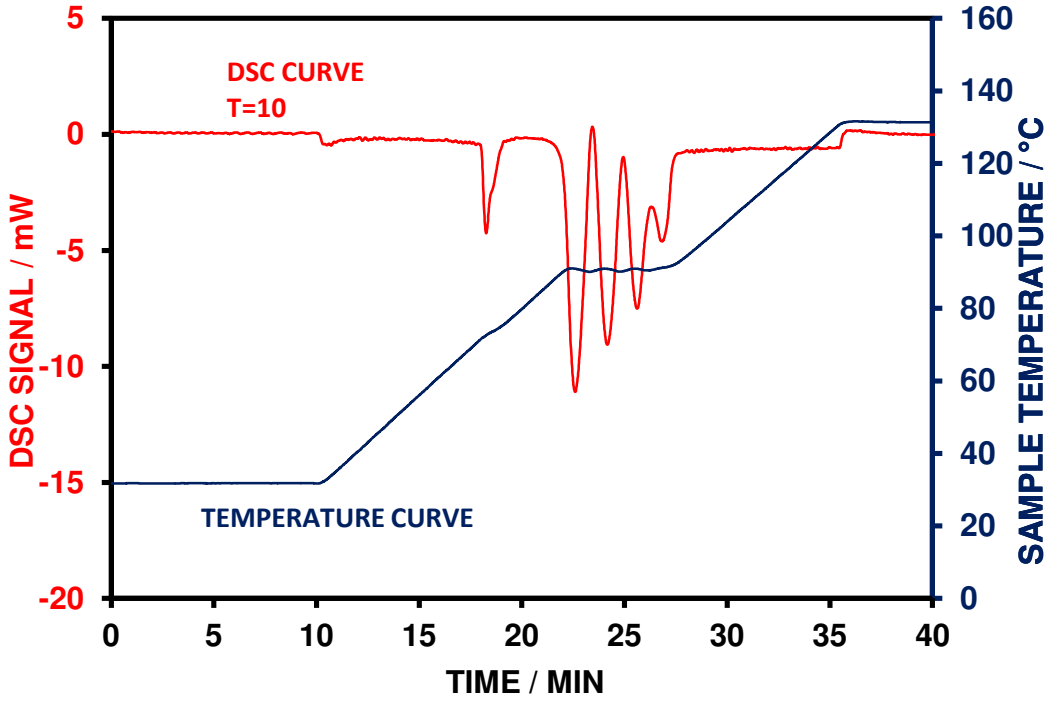

Fig. 4.6 DSC and temperature curves for the proportional heating of magnesium nitrate hexahydrate

(sample mass, 10mg; heating rate, ±5℃ min^{-1}; target, 10mW; atmosphere, nitrogen)

Reducing the target level to 5 mW however manages to control the dissolution event at an earlier stage and is shown in Fig. 4.7.

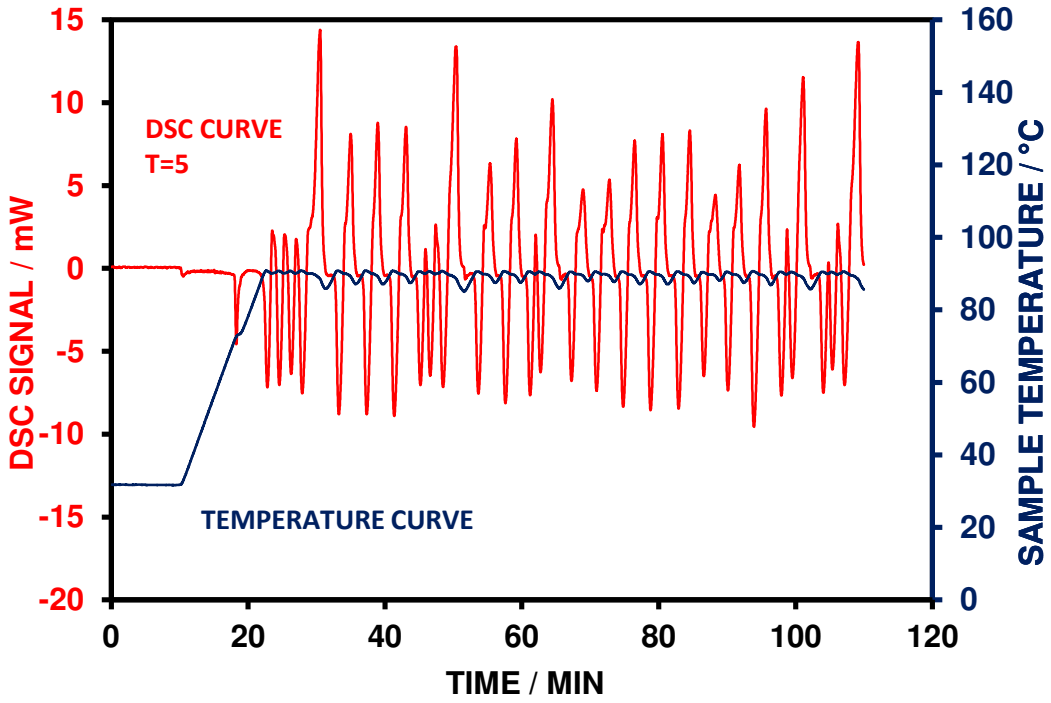

Fig. 4.7 DSC and temperature curves for the proportional heating of magnesium nitrate hexahydrate
(sample mass, 10mg; heating rate, ±5℃ min^{-1}; target, 5mW; atmosphere, nitrogen)

By carrying out the proportional heating experiments in the unsymmetrical heating mode, the oscillation effect was removed by not allowing the cooling effect to occur. An overlay of the experiments carried out on magnesium nitrate hexahydrate is shown in Fig. 4.8 where it can be seen that the best level of control without oscillations was for the unsymmetrically heated experiment with the target level set to 2 mW. The dissolution event can be seen to have been prolonged over a 5 minute period using the unsymmetrically heated, target of 2 mW experiment compared to 1 minute during linear heating. Apart from the oscillatory effect of the symmetrically heated sample, it also showed the elongation of the reaction period. An example of the control achieved can be seen in Fig. 4.9 when a target rate of 2 mW was used. It can be seen that the temperature profile was isothermal during the progress of the reaction.

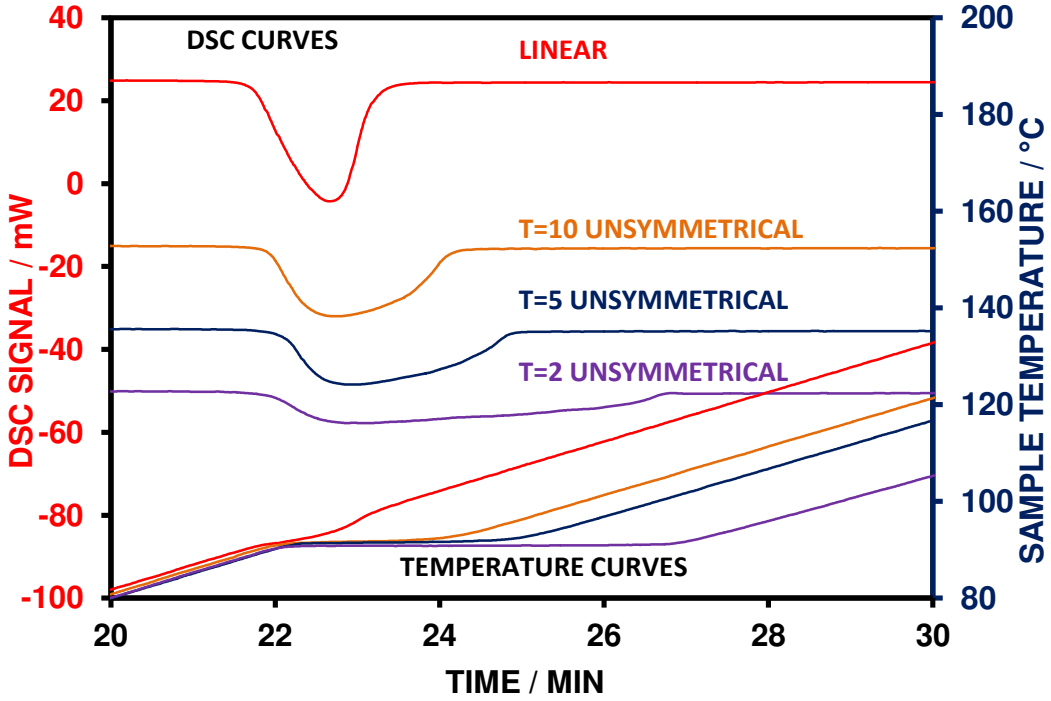

Fig. 4.8 Overlay of DSC and temperature curves for the linear and proportional heating experiments of magnesium nitrate hexahydrate

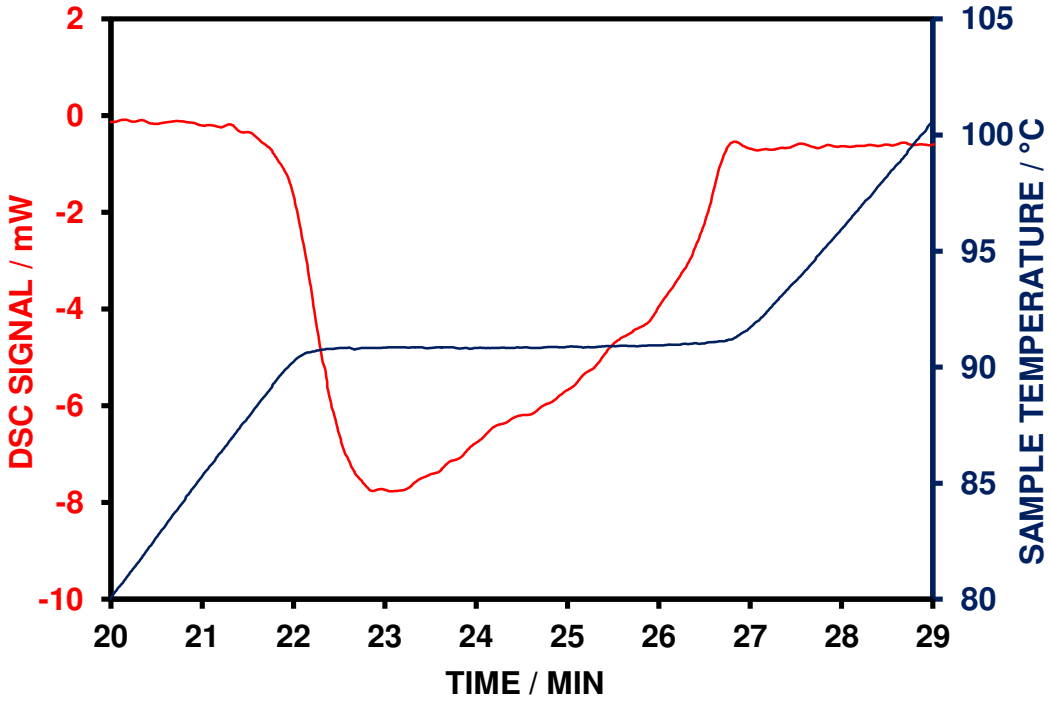

Fig. 4.9 SC-DSC and temperature curves for the proportional heating of magnesium nitrate hexahydrate

(sample mass, 10mg; heating rate, 5 and 0 ℃ min^{-1}; target, 2mW; atmosphere, nitrogen)

The effect of using proportional heating on the aqueous fusion reaction is more marked on the extent of reaction plotted with respect to temperature. It can be clearly seen in Fig. 4.10 that the temperature span of the reaction for the linear heating experiment was around 7 ℃ but this has been significantly reduced to less than 1 ℃ for the sample controlled experiments. The best example of the proportional heating strategy was observed for the unsymmetrically heated experiment with a target of 2 mW. It can be seen that as soon as the dissolution began, that the heating was arrested so as to provide a near isothermal holding of the temperature until completion of the reaction.

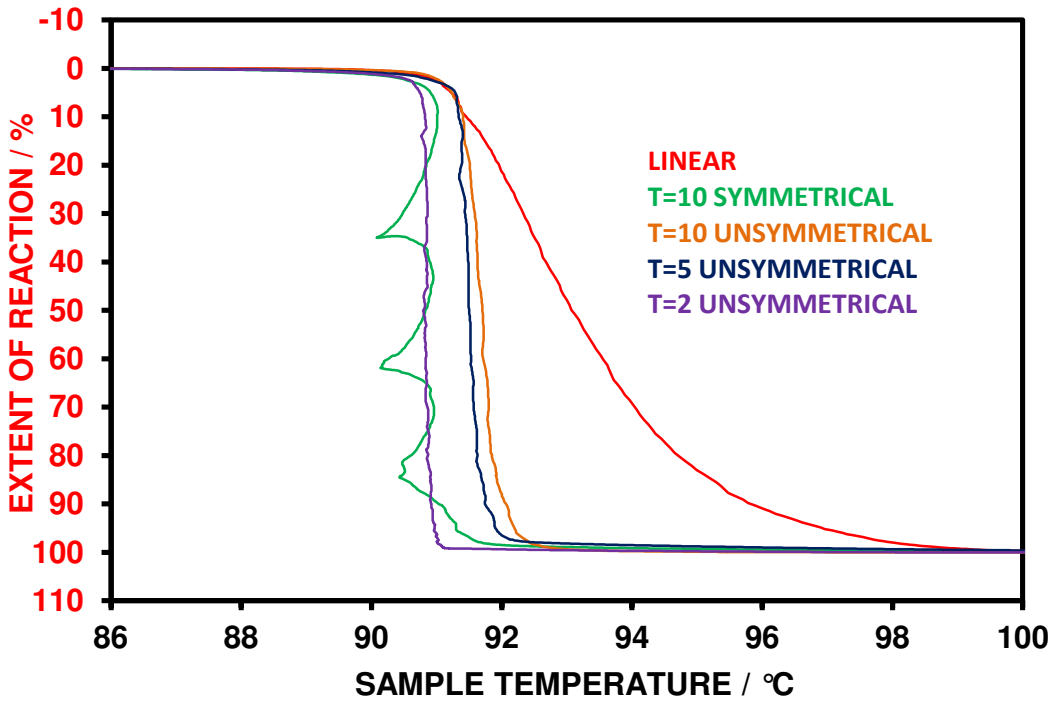

Fig. 4.10 Extent of reaction with respect to temperature for the aqueous fusion of magnesium nitrate hexahydrate

4.4 Exothermic Reaction in the Solid State for a 30% Zirconium – 69% Potassium Perchlorate – 1% Nitrocellulose Pyrotechnic composition.

The zirconium-potassium perchlorate-nitrocellulose (NC) pyrotechnic system, consisting of a mixture of finely divided zirconium, potassium perchlorate and nitrocellulose is commonly used as an ignition booster in many propellant systems. The zirconium powder acts as the fuel which is oxidised by the potassium perchlorate in a solid state reaction. The nitrocellulose acts as a binding agent so as the composition can be pelletised and shaped. Previous studies on the zirconium-potassium perchlorate-nitrocellulose pyrotechnic system, using simultaneous TG-DTA-mass spectrometry showed that zirconium and potassium perchlorate gave an exothermic solid state reaction in the region of 400°C, which overlapped with the decomposition of unreacted potassium perchlorate (Eq. 5) [50].

$$2\ Zr + KClO_4 \rightarrow 2\ ZrO_2 + 2\ KCl \qquad \text{(Eq. 5)}$$

This solid state reaction was followed quantitatively by scanning calorimetry (DSC) and chemical analysis but the studies were complicated by the decomposition of the unreacted potassium perchlorate which took place in the latter stages of the reaction. The system was therefore studied by sample controlled DSC with a view to increasing the extent of reaction taking place at lower temperatures.

A further complication is the ease of aerial oxidation of zirconium at elevated temperatures. As a precaution, to limit the effect of aerial oxidation after the sample was placed into the instrument, two small boats containing zirconium powder were placed in the DSC cell in a position so as to not influence the DSC signal. These were to act as oxygen scrubbers to remove extraneous oxygen from the DSC system. Loose fitting lids were also used on the sample and reference crucibles thereby promoting the oxidation of the scrubbers rather than the sample. A further enhancement of the instrument atmosphere was to evacuate the DSC cell to less than 10mBar and then reintroducing the inert gas slowly. The evacuation step was repeated three times before the start of each experiment. The efficiency of this scrubbing system was monitored by weighing at the end of each experiment.

A linear heating experiment was carried out on a 5mg sample and is presented in Fig. 4.11. It can be seen that the DSC curve comprises both endothermic and exothermic events. The large exothermic peak present is seen to start at around 260 ℃ albeit at a very low level which develops into a large three stage exothermic reaction. The exothermic reaction is seen to have two endothermic events superimposed, the first which a sharp endothermic event at around 300 ℃ for the solid-solid phase change of potassium perchlorate and the second endothermic reaction at around 506 ℃ which is due to the fusion reaction of the potassium perchlorate – potassium chloride eutectic formed in the reaction [51]. Following the eutectic fusion reaction is a final sharp exothermic event which is assumed to be the remainder of the pyrotechnic reaction that has been accelerated in the liquid state.

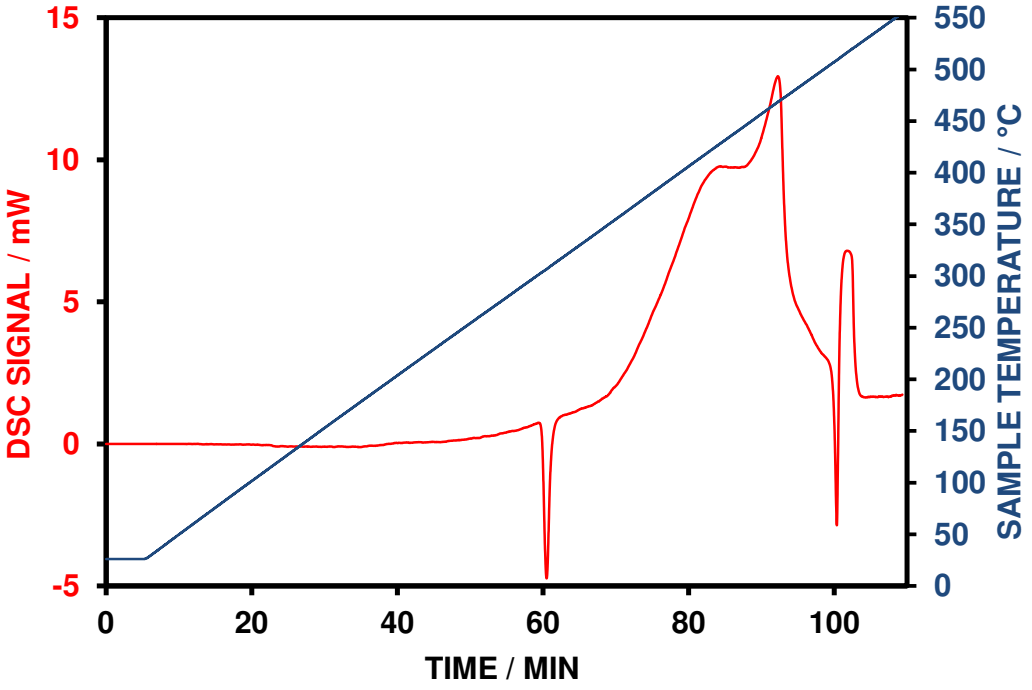

Fig. 4.11 DSC and temperature curves for the linear heating of a 30% zirconium – 69% potassium perchlorate – 1% nitrocellulose composition (sample mass, 5mg; heating rate, 5℃ min^{-1}; atmosphere, argon)

A series of proportional heating experiments were carried out using the symmetrical heating of ±5 ℃ min^{-1} and target levels of 10, 7.5, 5 and 2.5 mW. The DSC and temperature curves for the linear heating experiment and the proportional heating experiment using a target of 10mW are shown in Fig. 4.12 where it can be seen that the solid state reaction has been controlled significantly to extend the time of reaction.

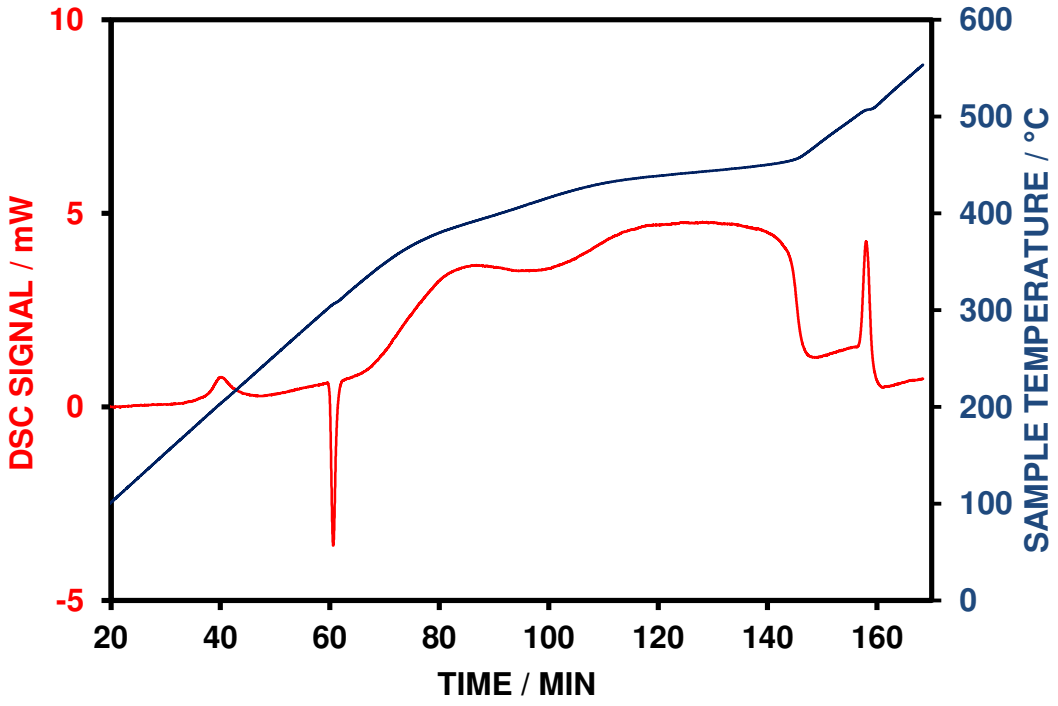

Fig. 4.12 DSC and temperature curves for the proportional heating of a 30% zirconium – 69% potassium perchlorate – 1% nitrocellulose composition (sample mass, 5mg; heating rate, ±5 ℃ min^{-1}; target, 10mW; atmosphere, argon)

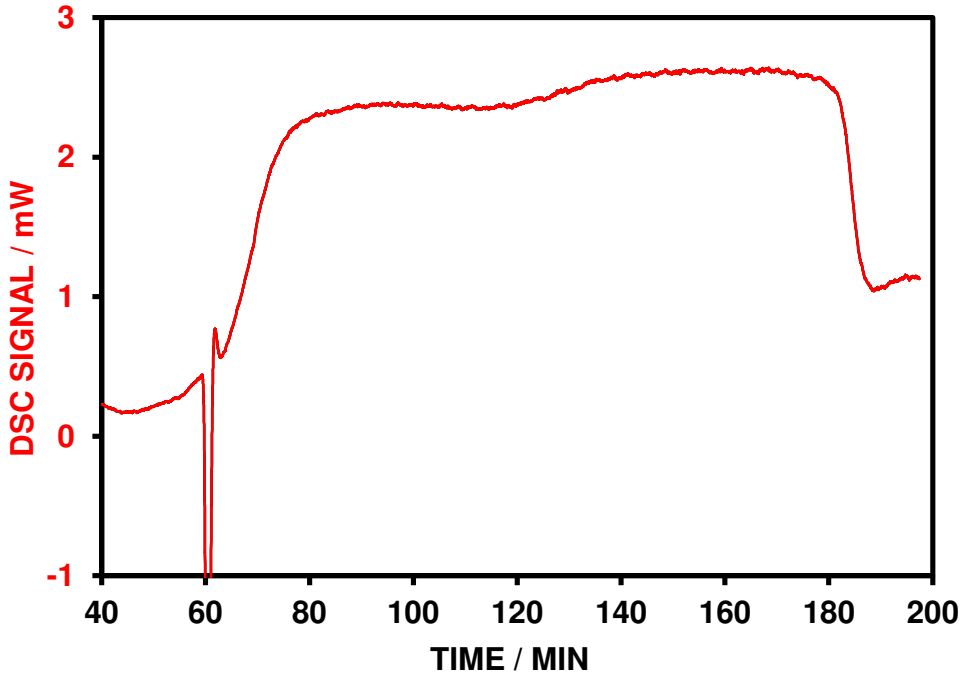

Fig. 4.13 DSC and temperature curves for the proportional heating of a 30% zirconium – 69% potassium perchlorate – 1% nitrocellulose composition (sample mass, 5mg; heating rate, ±5 ℃ min^{-1}; target, 5mW; atmosphere, argon)

The extension of time of control through the exothermic reaction is more marked for the experiment carried out with a target of 5 mW. This is shown in Fig. 4.13 and it can be seen that the exothermic reaction has been extended to over two hours.

It can be seen from the proportional heating experiments that no cooling of the reaction was for target levels of 5 mW and greater with the sample temperature rising, although at a reduced heating rate, throughout the exothermic reaction. The exothermic peak areas for the sample controlled experiments were converted to give the extent of reaction and plotted with respect to sample temperature (Fig. 4.14) and show the lowering of the completion of the reaction temperature to 425 ℃ compared 506 ℃ for the linear heating experiment.

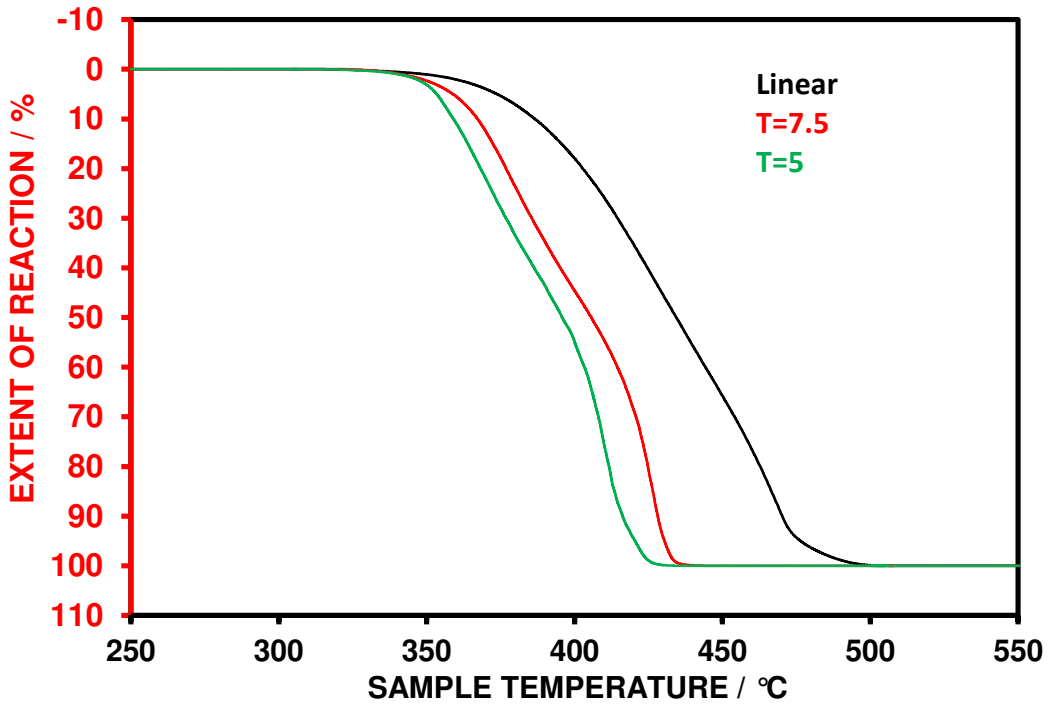

Fig. 4.14 Extent of reaction for the linear heating and proportional heating at several target levels of a 30% zirconium – 69% potassium perchlorate – 1% nitrocellulose with respect to temperature

Estimation of Potassium Perchlorate reacted through the Exothermic Reaction

Previous studies on the quantification of the reaction between zirconium and potassium perchlorate with extent of reaction were carried out by Charsley et al by DSC and chemical analysis [56] and they found a good correlation in the reduction of perchlorate to a stoichiometric rise in the chloride formed. The aim of this section is to use the DSC peak area for the potassium perchlorate at around 300 ℃ as an alternative to the use of the more cumbersome chemical analysis methods. As the exothermic solid state reaction proceeds, the level of potassium perchlorate will be reduced and the level of potassium chloride will increase. The potassium perchlorate can be followed by conducting a reheat of the residue from the pyrotechnic reaction under linear heating conditions. The potassium perchlorate solid-solid phase change occurs in the region of 300 ℃ and the reheat of the sample should reveal if there is any potassium perchlorate remaining in the residue.

An example plot of the first heat under proportional heating conditions and the Residue reheat is shown in Fig. 4.15. In order to use the area of the potassium perchlorate peak to assess its consumption, several mass levels of a potassium perchlorate sample was run under linear heating conditions. A reheat of these samples were also run so as to have a similar thermal history as to the pyrotechnic samples. The calibration plot of potassium perchlorate with respect to mass is shown in Fig. 4.16 with the resulting area with respect to mass tabulated in Table 4.1.
It can be seen from Fig. 4.16 that there was a linear trend for both the first and reheat of potassium perchlorate with mass.

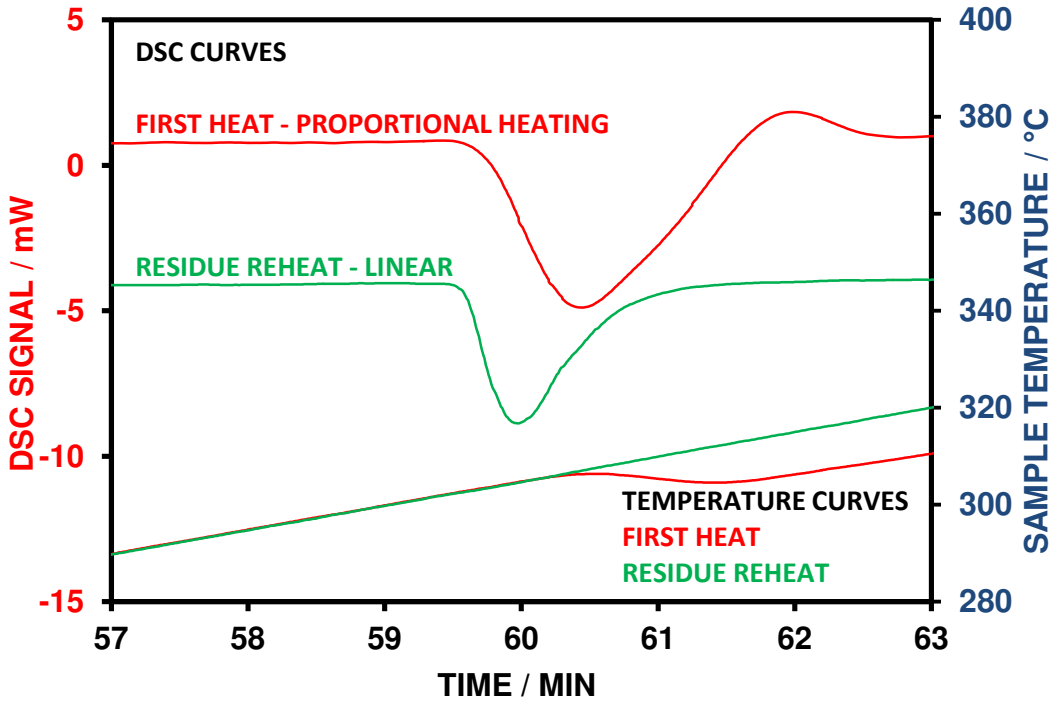

Fig. 4.15 Example plot of a first heat and residue reheat for a 30% zirconium – 69% potassium perchlorate – 1% nitrocellulose composition

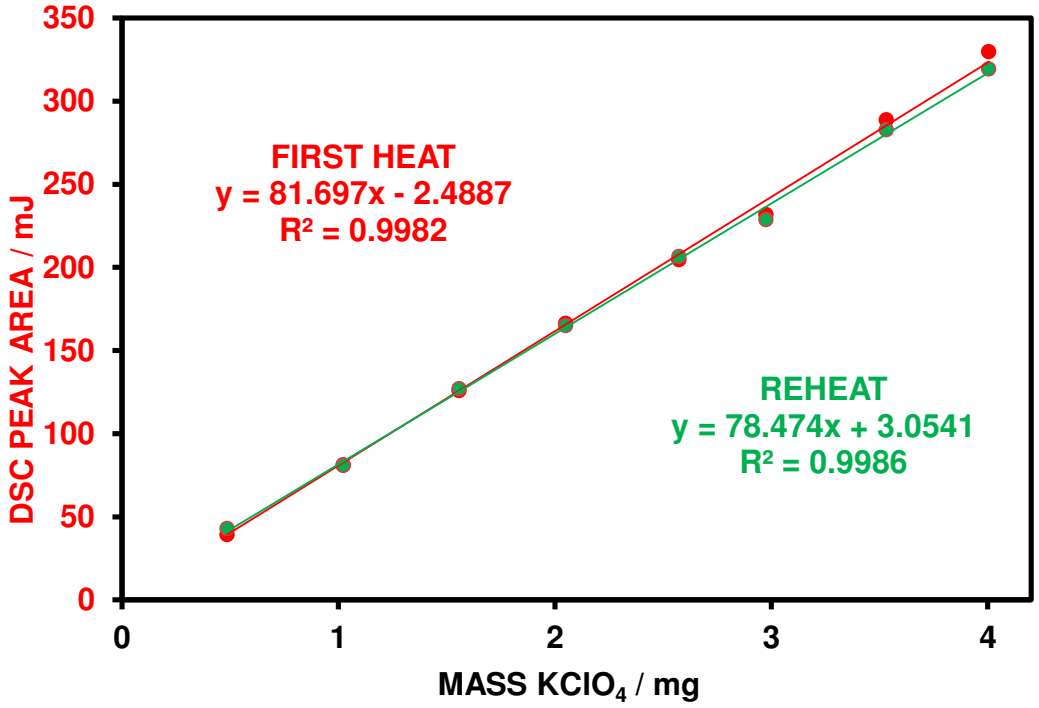

Fig. 4.16 Calibration plot of DSC peak area of potassium perchlorate with respect to sample mass for the first heat and reheat under linear heating conditions (heating rate, 5℃ min^{-1}; atmosphere, argon)

Table 4.1

DSC peak area determinations for potassium perchlorate at several masses (heating rate, 5 °C min^{-1}; atmosphere, argon)

	DSC Peak Areas / mJ	
Sample mass / mg	First Heat	Reheat
0.486	39.2	42.9
1.023	81.2	80.8
1.558	125.8	127.1
2.05	166.3	164.9
2.573	204.6	206.6
2.976	231.7	228.6
3.532	288.7	282.7
4.005	329.7	319.3

A series of experiments were carried out on the pyrotechnic composition using the symmetrically heated proportional heating strategy with a target level of 5 mW. The aim of these experiments was to manually quench the reaction at several temperatures along the solid-state exothermic reaction and then using the residues to assess the level of potassium perchlorate consumption.

The series of proportional heating experiments can be seen plotted with respect to time in Fig. 4.17 which showed that the time period during the reaction to a set temperature was not uniform with the experiment quenched at 434 °C being similar in time as the experiment quenched at 460 °C and this may reflect the inhomogeneity of the composition.

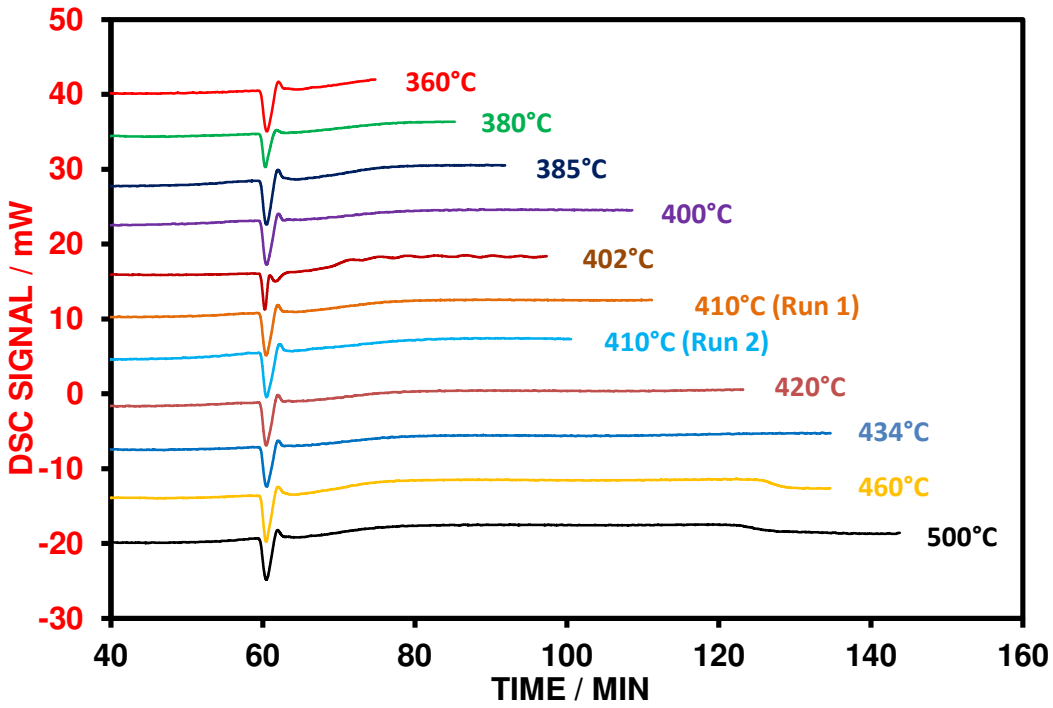

Fig. 4.17 Overlay of DSC curves with respect to time for a series of proportional heating experiments to set temperatures for a 30% zirconium – 69% potassium perchlorate – 1% nitrocellulose composition (sample mass, 5mg; heating rate, ±5 ℃ min^{-1}; target, 5 mW; atmosphere, argon)

The exothermic peak area for the solid state pyrotechnic reaction is shown in Fig. 4.18 as a function of the maximum temperature achieved by the samples. It can be seen that the pyrotechnic reaction proceeds in an almost linear trend until the sample heated to around 434 ℃. Above 434 ℃ the rate of evolution of heat appears to slow. This reduction in the rate of exothermicity is assumed to be the nearing of completion of the solid state reaction. A third order trend with an R^2 value of 0.95 was seen for the exothermic area determination with increasing temperature.

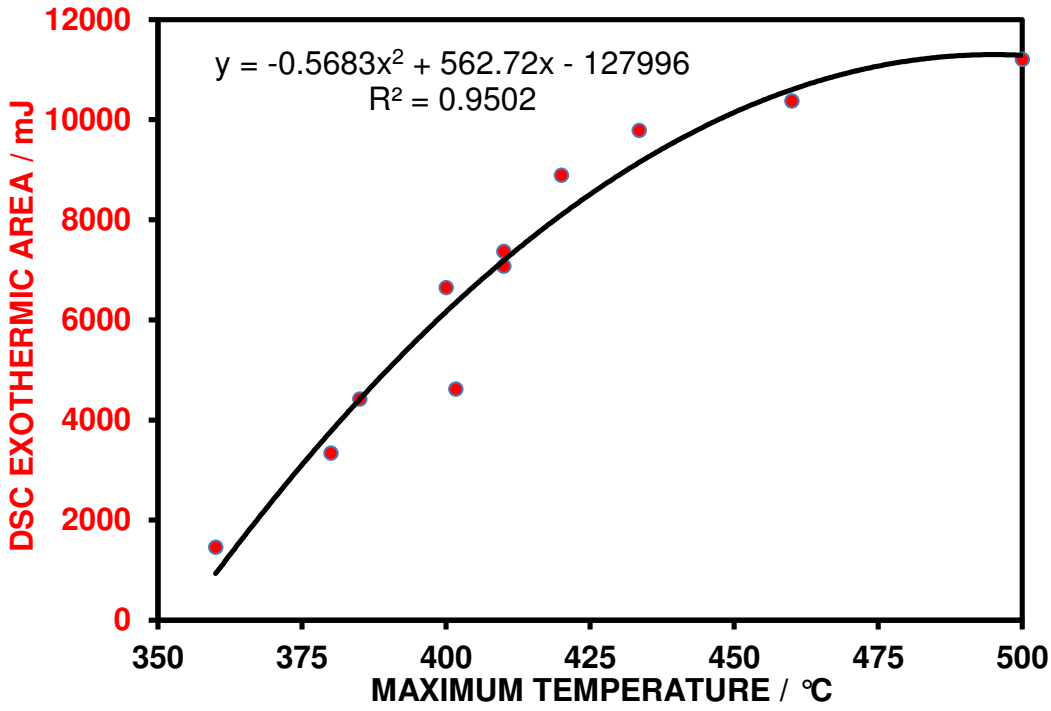

Fig. 4.18 Plot of exothermic peak area for the proportional heating experiments for a 30% zirconium – 69% potassium perchlorate – 1% nitrocellulose composition (sample mass, 5mg; heating rate, ±5 ℃ min^{-1}; target, 5 mW; atmosphere, argon)

The linear reheat experiments on the residues all showed the peak corresponding to potassium perchlorate at 300 ℃. The area measurements were taken and these are presented in Table 4.2. It can be seen that in all the experiments that there was a reduction in the peak are indicating consumption of potassium perchlorate. However a plot of the consumption of potassium perchlorate with respect to the maximum temperature achieved provided an R^2 value of 0.76 as can be seen in Fig. 4.19. A possible contribution to this low linearity may be due to the inhomogeneity of the supplied mixture. To conclude, it can be seen that using the sample controlled strategy of proportional heating that the solid state pyrotechnic reaction, involving negligible mass change was able to be controlled.

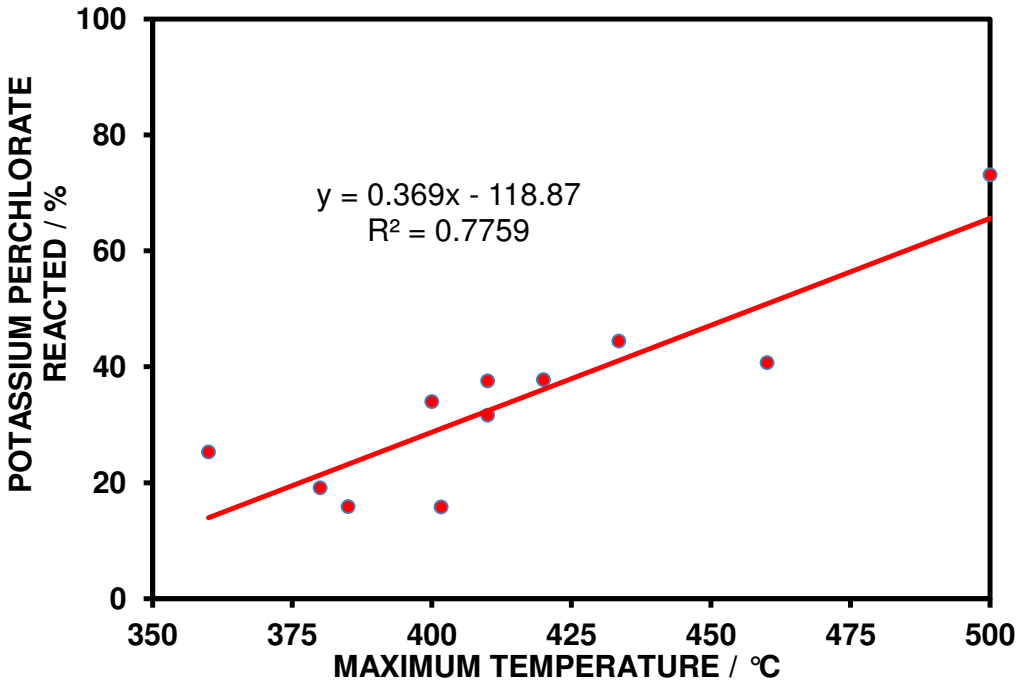

Fig. 4.19 Estimation of potassium perchlorate reacted for a series of proportional heating experiments carried out to set temperatures for a 30% zirconium – 69% potassium perchlorate – 1% nitrocellulose composition (sample mass, 5mg; heating rate, ±5 ℃ min^{-1}; target, 5 mW; atmosphere, argon)

Table 4.2

Estimation of potassium perchlorate reacted for a series of proportional heating experiments carried out to set temperatures for a 30% zirconium – 69% potassium perchlorate – 1% nitrocellulose composition (sample mass, 5mg; heating rate, ±5 ℃ min^{-1}; target, 5 mW; atmosphere, argon)

Maximum temperature / ℃	Potassium perchlorate reacted / %
360	25.3
380	19.1
385	15.9
400	34.0
402	15.8
410	31.6
410	37.5
420	37.8
434	44.4
460	40.7
500	73.1

Although the correlation of the results from this study on the pyrotechnic composition was poor, the investigation has shown that using sample controlled DSC to carry out to treat and then quantify may be viable but the concept will need more work in order to quantify how the reaction mechanism is affected by using the proportional heating method.

4.5 Endothermic Fusion Reaction of Indium

A linear heating experiment for a high purity sample of indium is shown in Fig. 4.20 where a sharp fusion reaction can be seen. The enthalpy of the fusion reaction is small relative to the organic fusion reactions but is widely used as it is easy to handle and the same sample can be repeated many times.

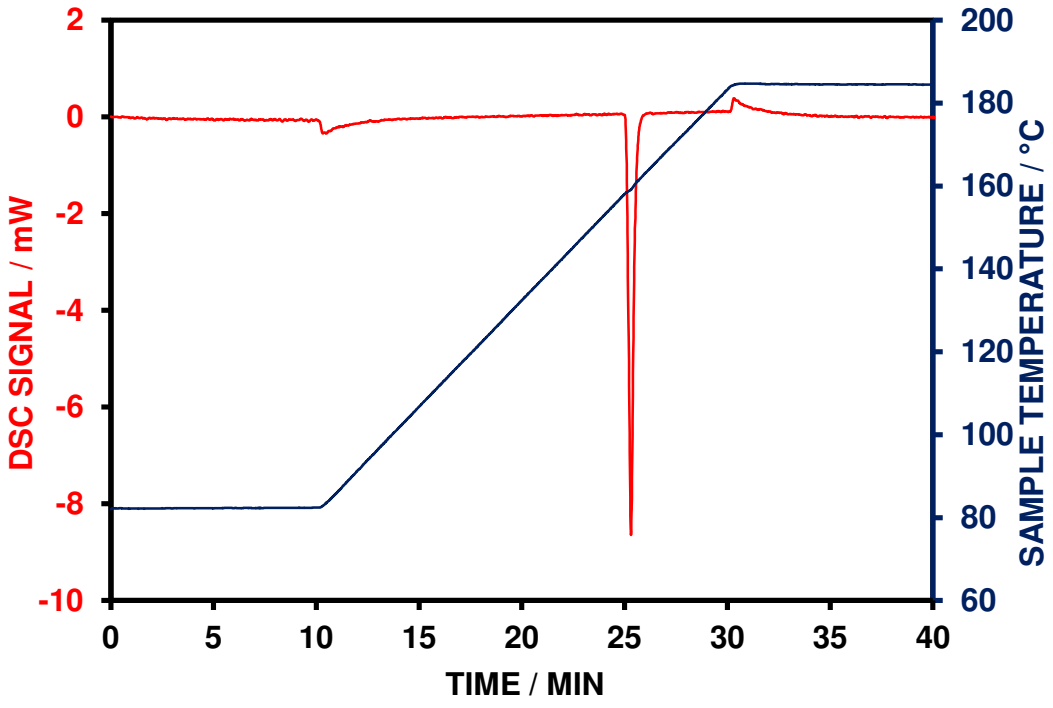

Fig. 4.20 DSC and temperature curves for the linear heating of indium (sample mass, 5mg; heating rate, 5℃ min^{-1}; atmosphere, nitrogen)

As the indium sample can be cycled several times through its fusion reaction, then the same sample was reheated using the proportional heating method in the symmetrical heating mode. It can be seen from Fig. 4.21 that the fusion reaction took place with only a small level of control occurring. A replay experiment, using the heating profile of the proportional heating experiment produced exactly the same

DSC and temperature profile showing the repeatable nature of the fusion reaction and can be seen in Fig. 4.22.

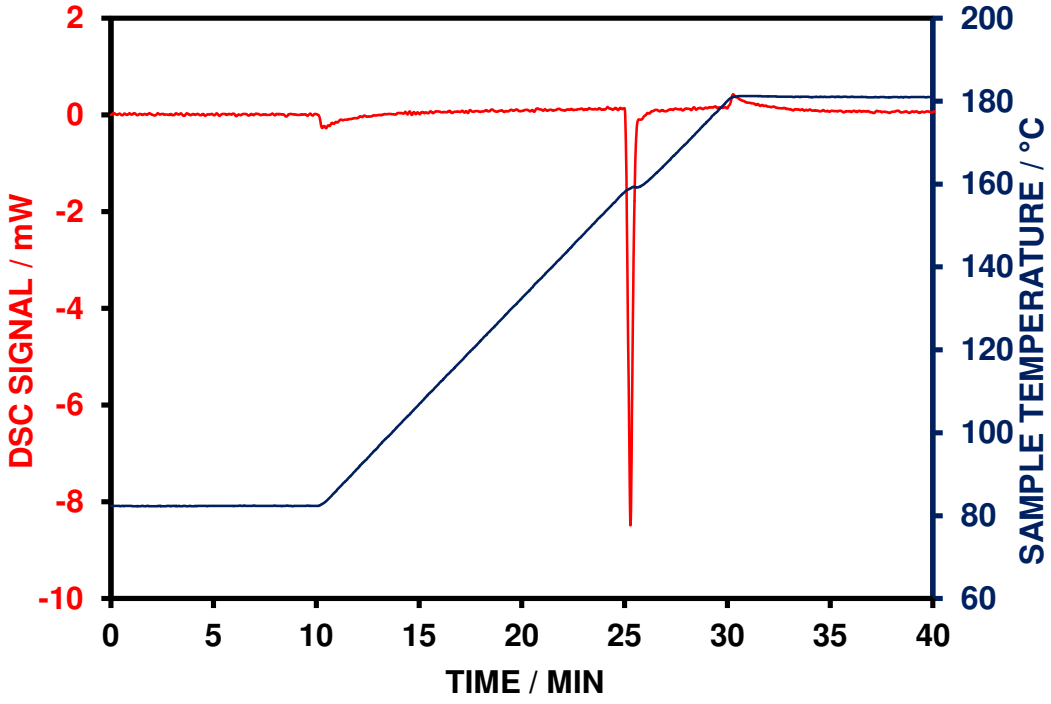

Fig. 4.21 DSC and temperature curves for the proportional heating of indium (sample mass, 5mg; heating rate, ±5℃ min^{-1}; target, 5mW; atmosphere, nitrogen)

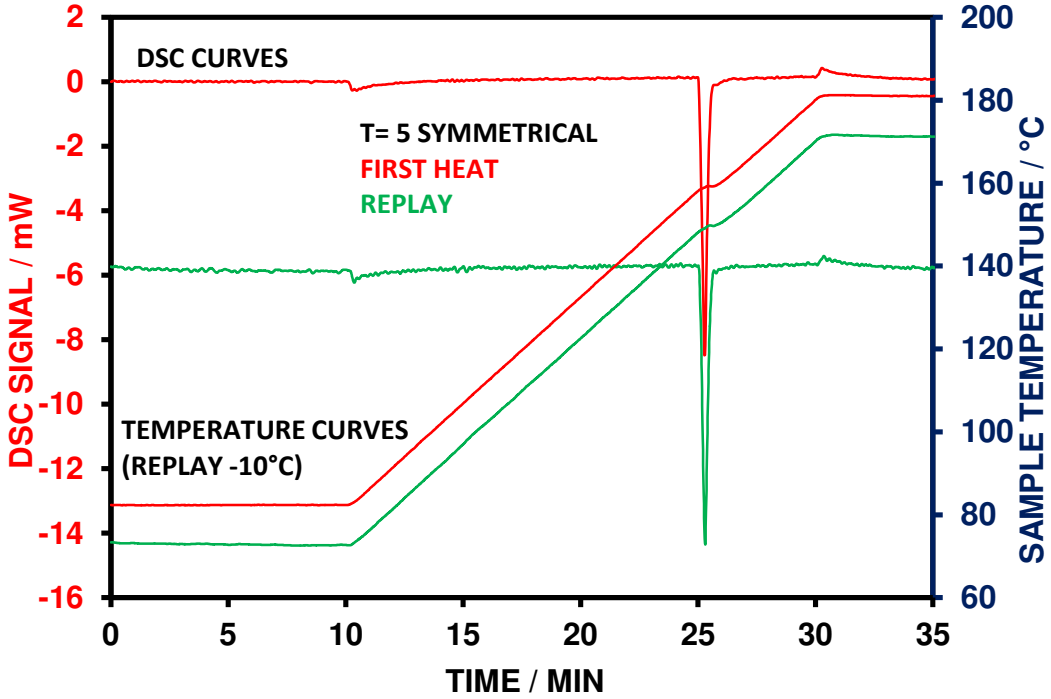

Fig. 4.22 DSC and temperature curves for the initial heating and replay of the proportional heating of indium
(sample mass, 5mg; heating rate, ±5℃ min^{-1}; target, 5mW; atmosphere, nitrogen)

Several proportional heating experiments were carried out in both symmetrical and unsymmetrical heating modes which produced fusion reactions that were very similar with only small deflections observed on the temperature curves.

The extent of reaction was plotted with respect to temperature in Fig. 4.23 where it can be seen that the proportional heating experiments had narrowed the temperature range for the majority of the fusion reaction compared to the linear heating experiment.

A possible reason for the small level of control offered by proportional heating in these experiments lies in the small enthalpy and hence peak size produced by the fusion reaction. Coupled with the good heat transfer properties of Indium which produce small thermal gradients in the sample, it means that the reaction progresses at a rate that is faster than the measuring circuit can respond thus the reaction proceeds to near completion before control can occur. A possible improvement in the study of indium could be by increasing the sample mass thereby increasing the amount of peak height and area to allow control at an earlier stage of the fusion reaction.

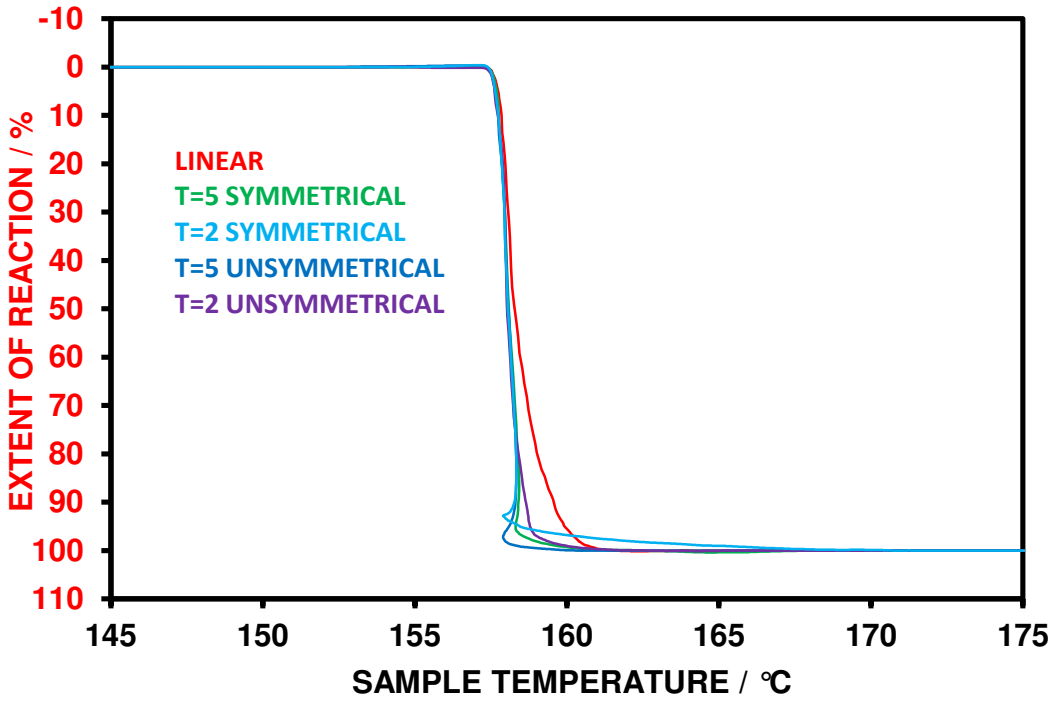

Fig. 4.23 Extent of reaction with respect to temperature for the fusion reaction of indium

4.6 Endothermic Fusion Reaction of Tin

A linear heating experiment for a high purity sample of tin is shown in Fig. 4.24 where a sharp fusion reaction can be seen.

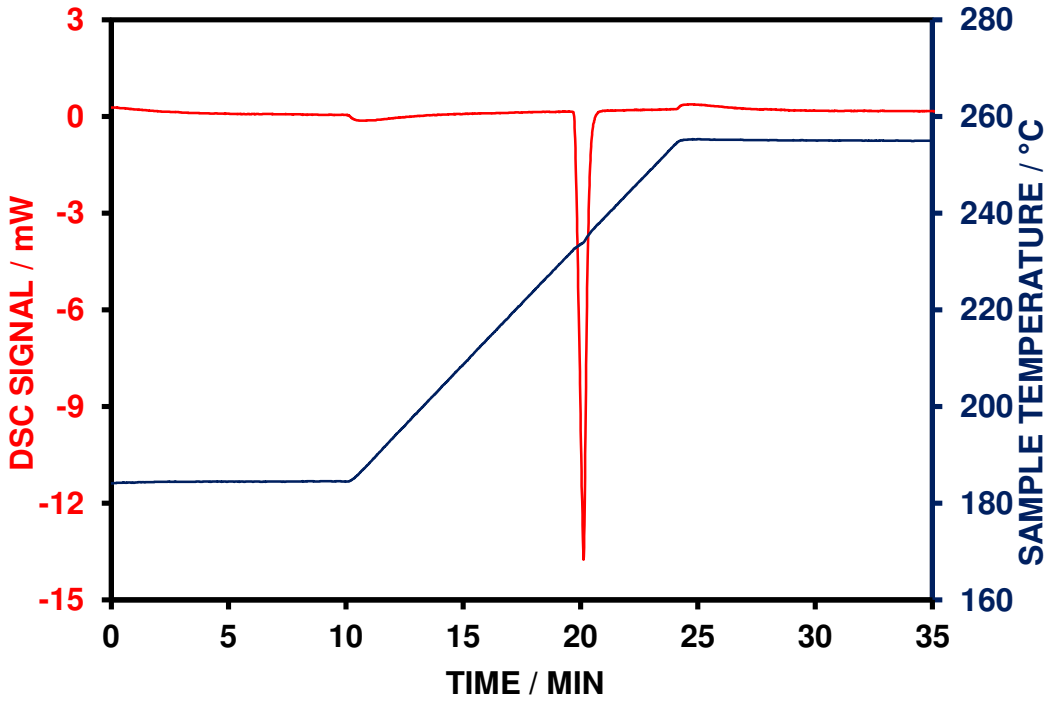

Fig. 4.24 DSC and temperature curves for the linear heating of tin (sample mass, 5mg; heating rate, 5℃ min^{-1}; atmosphere, nitrogen)

As the tin sample can be recycled through its fusion reaction, then the same sample was reheated using the proportional heating method in the symmetrical heating mode. It can be seen from Fig. 4.25 that the fusion reaction took place with only a small level of control occurring. Cooling was employed during the fusion reaction but the transition had already progressed before the response was in effect. The replay of the proportional heating experiment produced exactly the same DSC and temperature profile showing the repeatable nature of the fusion reaction and can also be seen in Fig. 4.26.

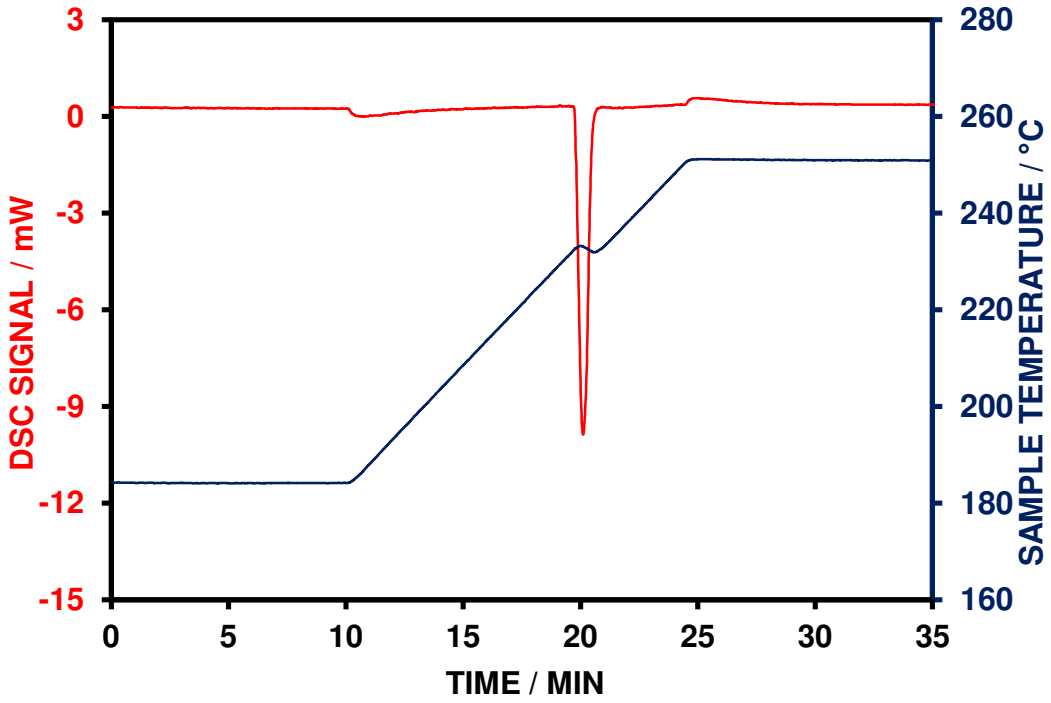

Fig. 4.25 DSC and temperature curves for the proportional heating of tin (sample mass, 5mg; heating rate, ±5℃ min^{-1}; target, 5mW; atmosphere, nitrogen)

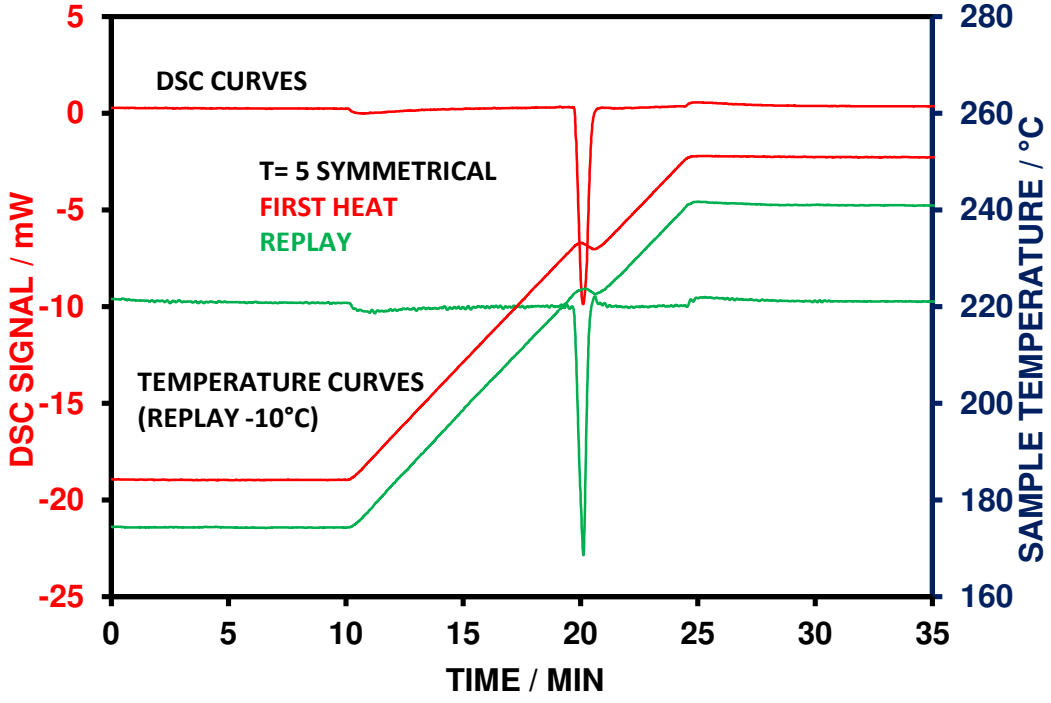

Fig. 4.26 DSC and temperature curves for the initial heating and replay of the proportional heating of tin (sample mass, 5mg; heating rate, ±5℃ min^{-1}; target, 5mW; atmosphere, nitrogen)

Several proportional heating experiments were carried out in both symmetrical and unsymmetrical heating modes and can be seen in the overlay plot in Fig. 4.27. It can be seen that the fusion reactions observed by DSC all appeared to be very similar except for the experiment with the target level set to 2 mW, with only small deflections observed on the temperature curves. In the case of the symmetrically heated sample at 2 mW it appears that the target level was sufficiently low to reduce the heating rate early in the fusion reaction so as to cause the fusion to reverse. This resulted in a series of heating and cooling to produce oscillations during the fusion reaction. The experiment at a target level of 2 mW did not reach completion.

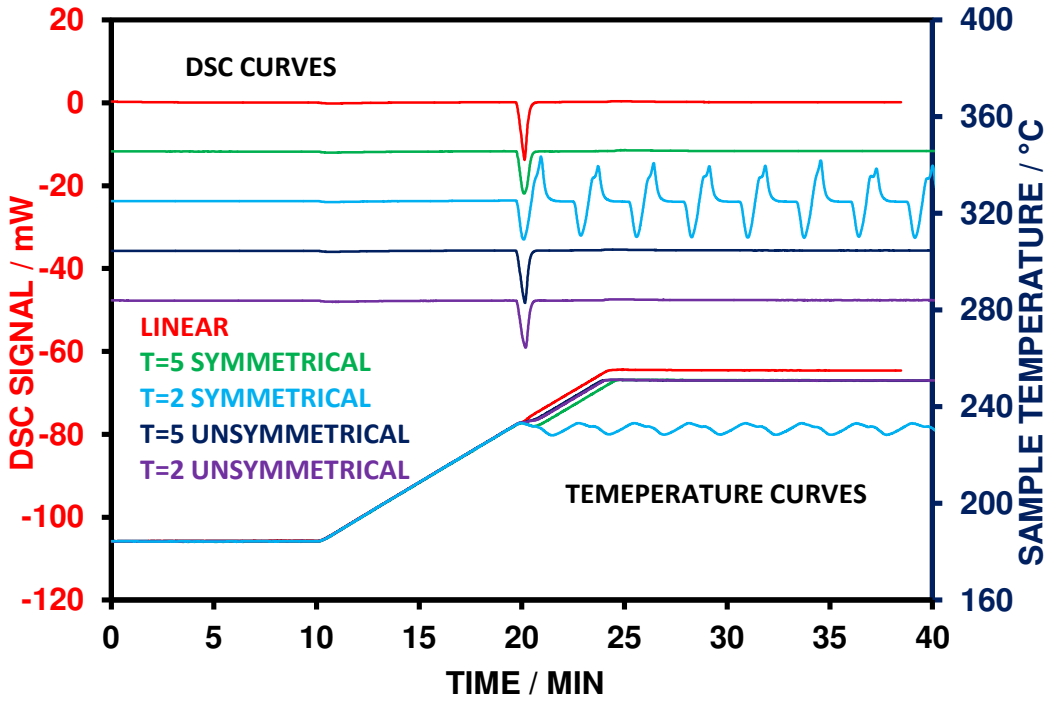

Fig. 4.27 Overlay of DSC and temperature curves for the linear and proportional heating of tin

The effect of cooling is shown in Fig. 4.28 where the extent of reaction is plotted with respect to temperature. It can be seen that in the symmetrically heated mode, that the sample was cooled by around 1.5 ℃ once the fusion had begun.

As with the indium sample studied previously it appears that the magnitude of the peak height is the major issue in allowing sample control to take place. It appears control may be improved by increasing the size of the peak for the fusion reaction by

gaining a response to the DSC signal from earlier in the transition. Increasing the mass of the sample would therefore suggest the possibility of better control.

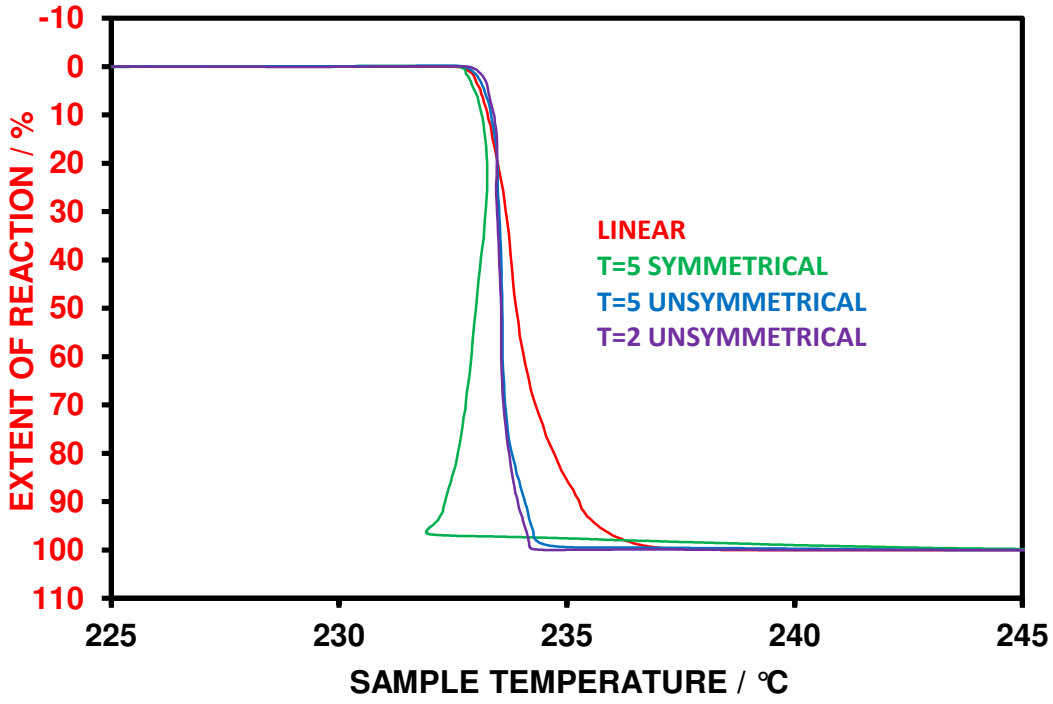

Fig. 4.28 Extent of Reaction with respect to temperature for the fusion reaction of tin

4.7 Endothermic Fusion Reaction of Benzil

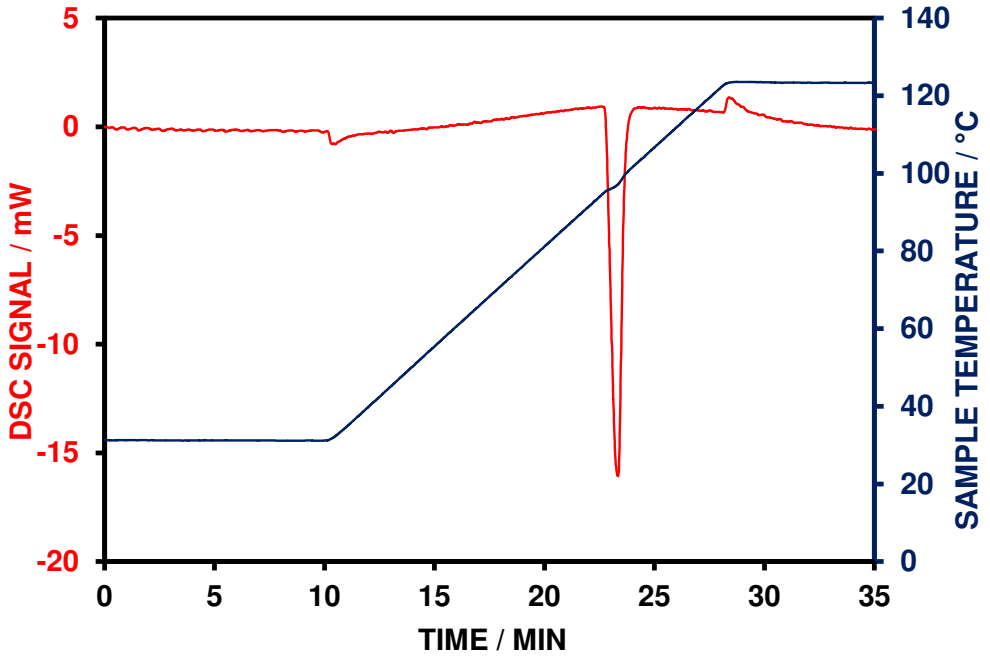

Fig. 4.29 DSC and temperature curves for the linear heating of benzil (sample mass, 2.5mg; heating rate, 5℃ min^{-1}; atmosphere, nitrogen)

A linear heating DSC curve for benzil is shown in Fig. 4.29 which shows the endothermic fusion reaction. It can also be seen that the fusion reaction has caused heat to be withdrawn from the temperature sensor creating an inflection in the temperature curve.

A proportional heating experiment was carried out in the symmetrical heating mode using a target level of 5 mW and it can be seen from Fig. 4.30 that the fusion reaction occurred rapidly and could not be controlled for the majority of the reaction. The temperature curve indicates that cooling had taken place before the heating was resumed. The proportional heating experiment was repeated but using a target level of 2 mW. By using the lower target level, it caused the cooling to start much earlier in the fusion reaction and initiated the cooling. The cooling and reheating then continued to cycle and it can be seen from Fig. 4.31 that there appeared to be an equilibrium between the solid phase and the liquid phase. The proportional heating experiments were repeated using the unsymmetrical heating mode and this was found to have eliminated the cycling effect seen previously with the fusion reaction showing evidence of control albeit very slight.

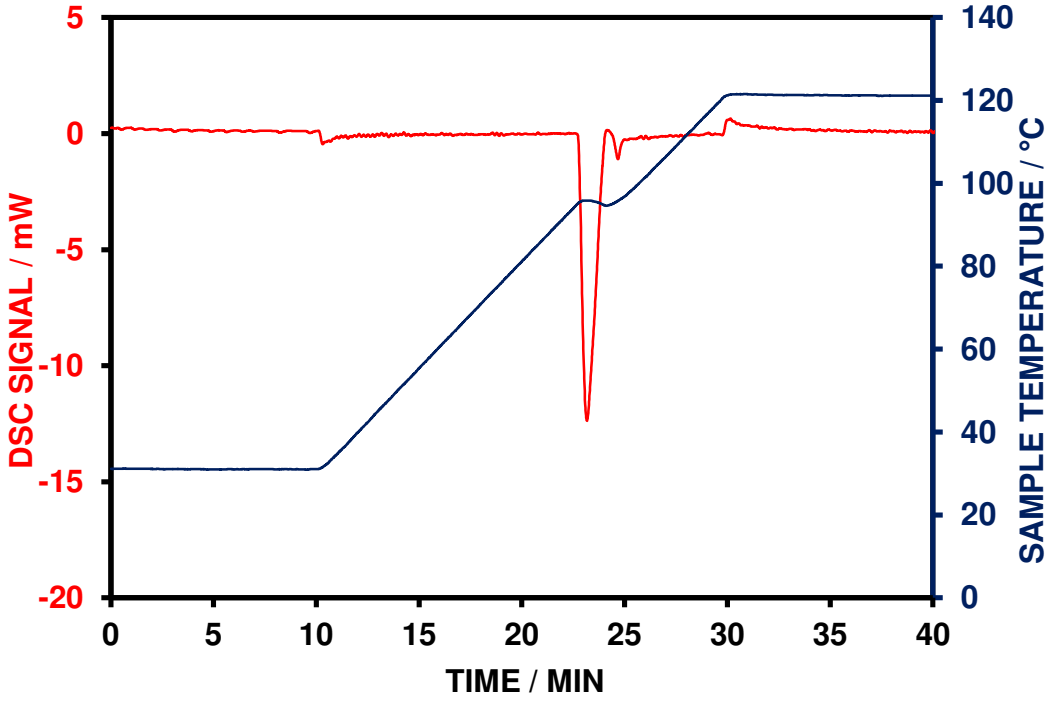

Fig. 4.30 DSC and temperature curves for the proportional heating of benzil (sample mass, 2.5mg; heating rate, ±5 °C min^{-1}; target, 5mW; atmosphere, nitrogen)

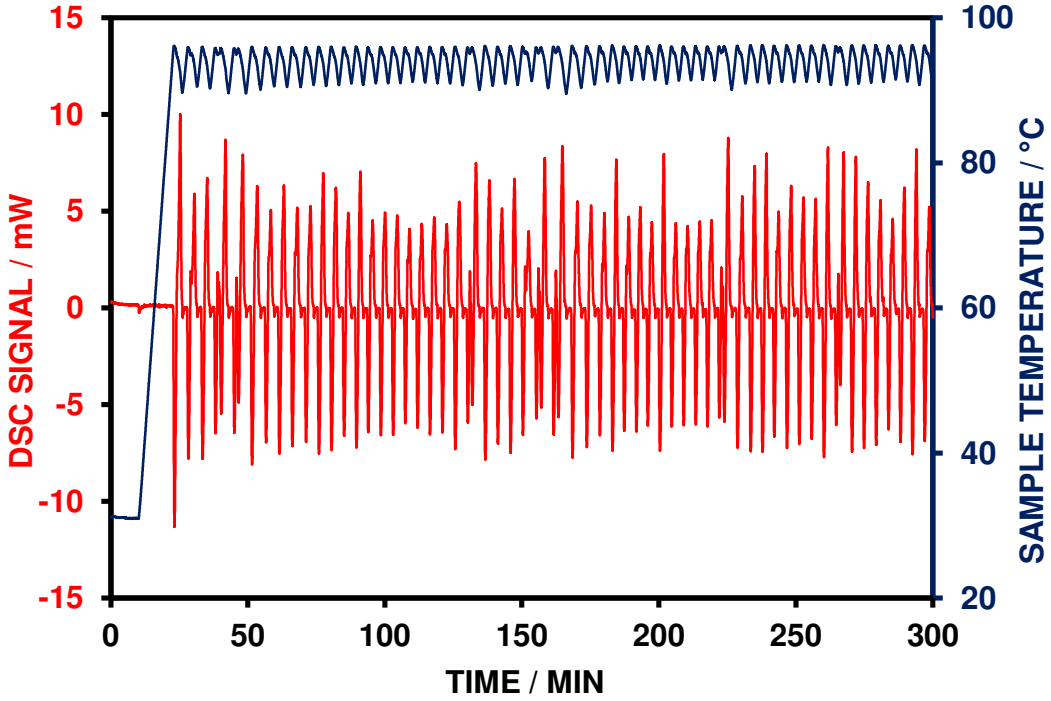

Fig. 4.31 DSC and temperature curves for the proportional heating of benzil (sample mass, 2.5mg; heating rate, ±5℃ min^{-1}; target, 2mW; atmosphere, nitrogen)

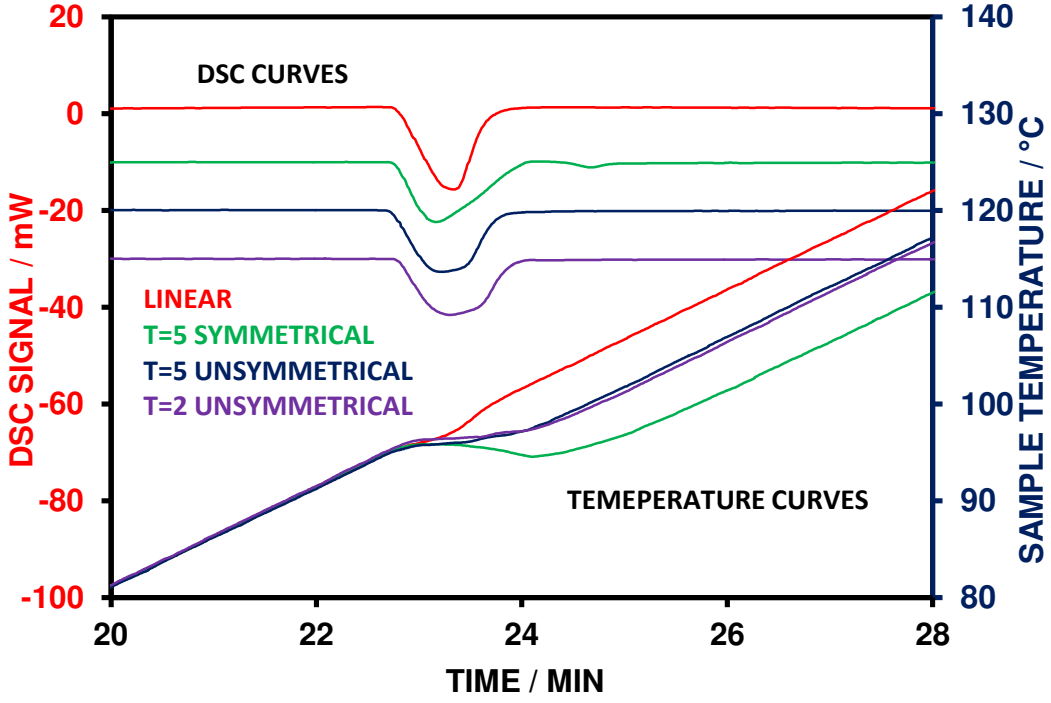

Fig. 4.32 DSC and temperature curves for the fusion reaction of benzil

An overlay of the DSC and temperature curves is shown in Fig. 4.32 that shows that the heating in the unsymmetrical mode only has a slight effect relative to the linear heating experiment, whereas the symmetrical heating, when cooling is employed, is

seen to delay the completion of the fusion by around 1 minute. By plotting the extent of reaction with respect to temperature (Fig. 4.33) it can be seen that the temperature range of the fusion reaction has been reduced in particularly over the first 90% of the fusion event therefore suggesting that it may be possible to control the fusion reactions of organic compounds.

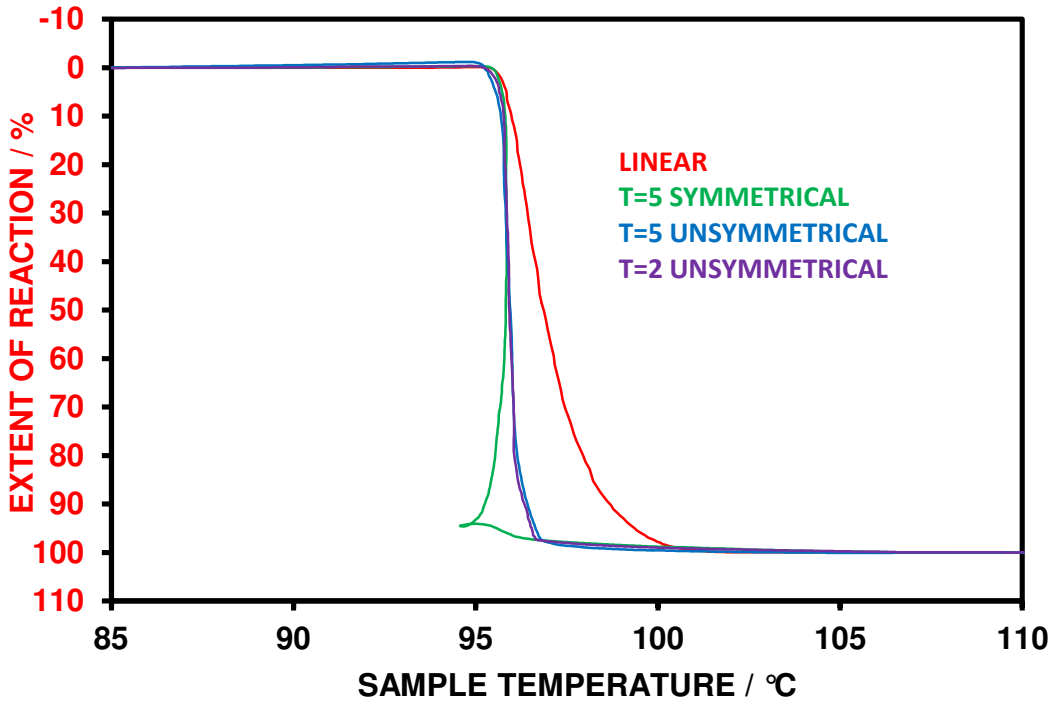

Fig. 4.33 Extent of reaction for the linear heating and proportional heating at several target levels of benzil with respect to temperature

4.8 Endothermic Fusion Reaction of Diphenylacetic Acid

Diphenylacetic acid, like benzil is an organic material that is widely used as a temperature and enthalpy calibration material. Its importance in thermal analysis is due to having a fusion temperature that is close to that of indium, a metallic standard, and thus is a viable alternative when calibrating thermal analysis equipment at around 150 ℃.

A linear heating of a sample of diphenylacetic acid is shown in Fig. 4.34 where it can be seen that at around 147 ℃. The arrest seen in the temperature curve is indicative of a high heat of fusion.

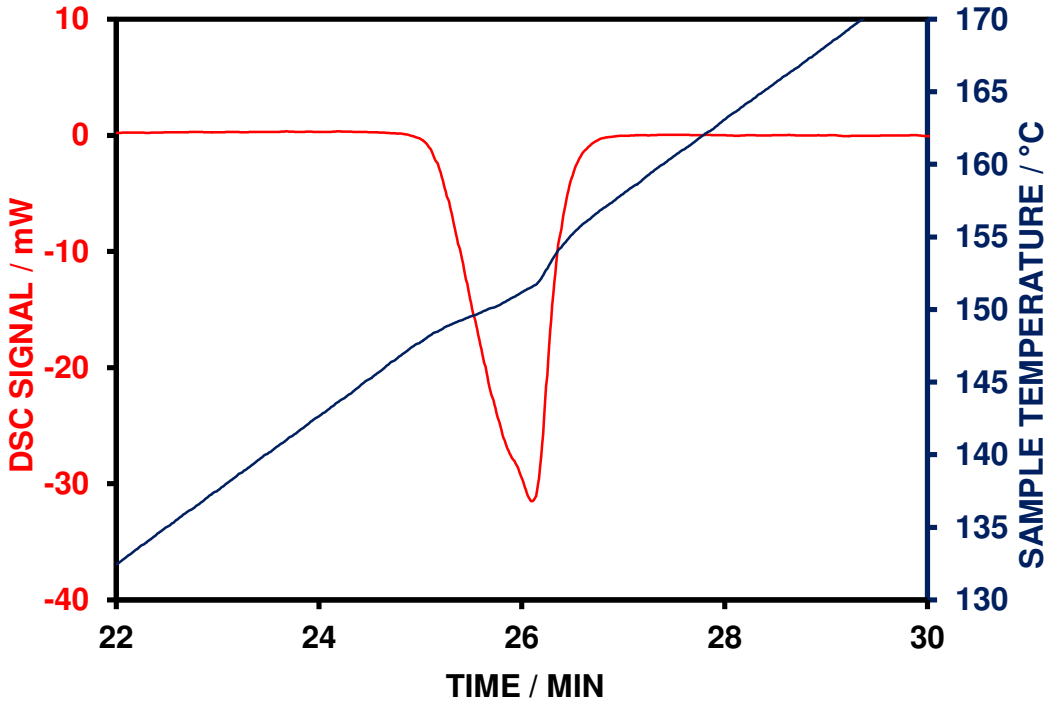

Fig. 4.34 DSC and temperature curves for the linear heating of diphenylacetic acid

(sample mass, 2.5mg; heating rate, 5℃ min^{-1}; atmosphere, nitrogen)

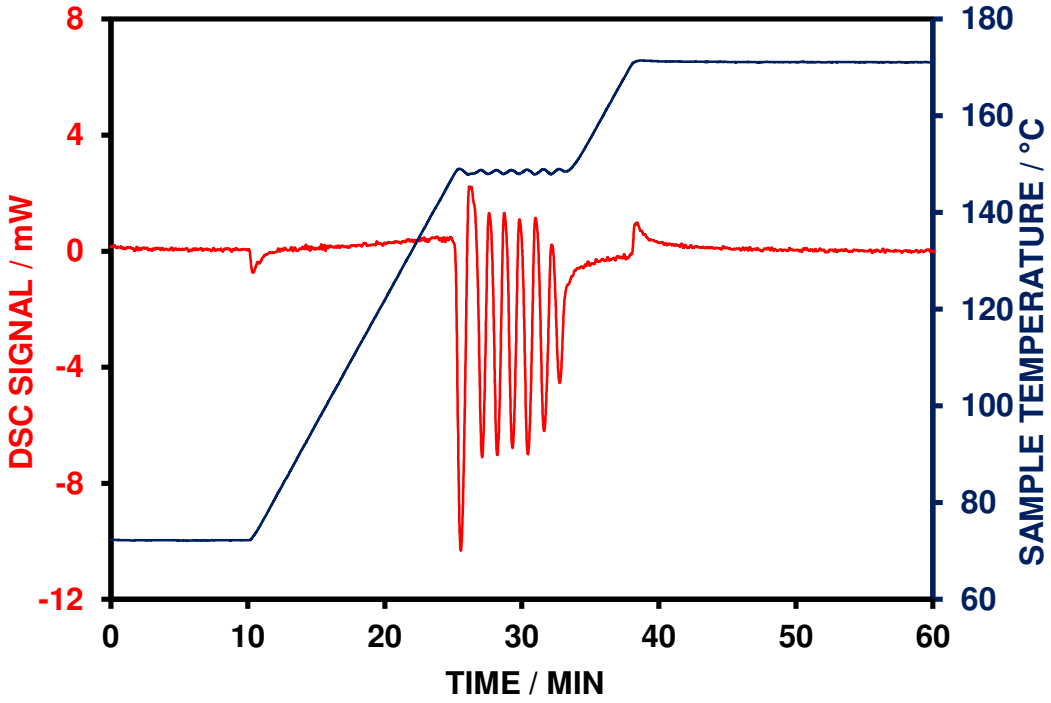

Fig. 4.35 DSC and temperature curves for the proportional heating of diphenylacetic acid

(sample mass, 2.5mg; heating rate, ±5℃ min^{-1}; target, 5mW; atmosphere, nitrogen)

A proportional heating experiment was performed using the symmetrical heating mode and is presented in Fig. 4.35. It can be seen that as the sample progresses through the fusion reaction, that cooling of the sample occurs. However the cooling did not seem to progress so as to completely reform the solid. Instead it appears that only a small level of resolidifcation occurred before heating was resumed. This continued for a period of around 10 minutes by which time the fusion reaction had been progressing towards completion.

Reducing the target level to 2 mW in the symmetrical heating mode (Fig. 4.36) showed the oscillations corresponding to the partial melting and resolidification of diphenylacetic acid. A possible explanation for the completion of the fusion reaction at 5 mW may lie in the rates at which fusion occurs compared to that of the resolidification. If the heat absorbed by the sample for the fusion event cannot be lost efficiently then a portion of the sample will remain in the fused state and the heating will resume so the fusion reaction will be completed in small increments.

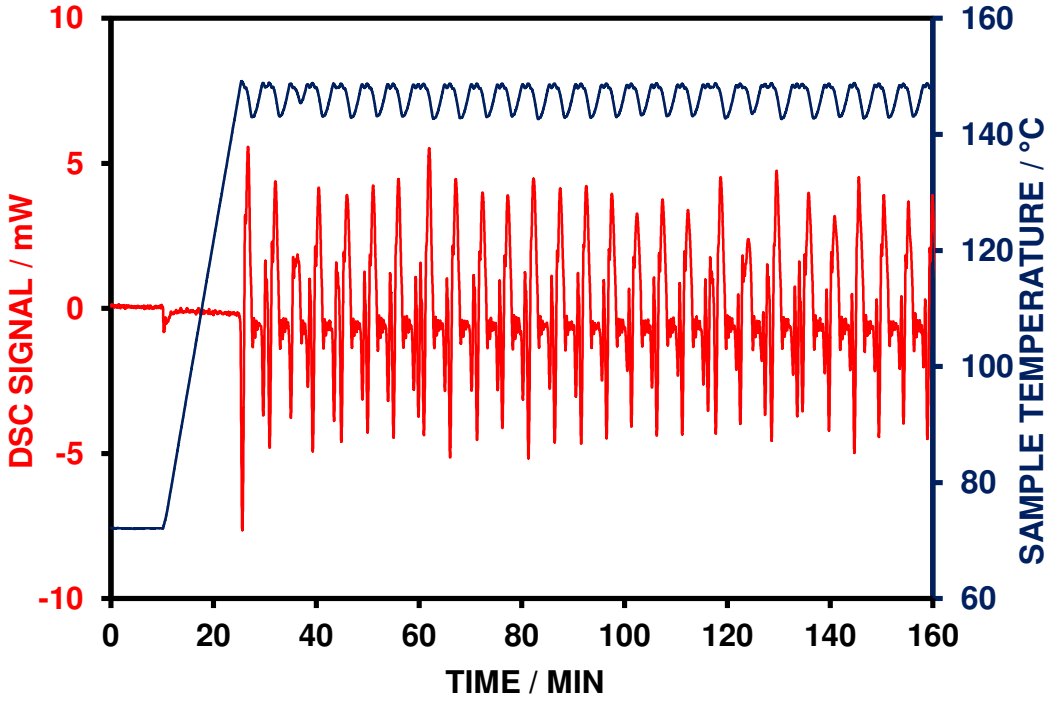

Fig. 4.36 DSC and temperature curves for the proportional heating of diphenylacetic acid

(sample mass, 2.5mg; heating rate, ±5°C min^{-1}; target, 2mW; atmosphere, nitrogen)

In addition to the symmetrical heating experiments, studies were also carried out in the unsymmetrical heating mode and it can be seen from the overlay plot of all the experiments on diphenylacetic acid in Fig. 4.37 that the magnitude of the fusion peak has been reduced in height and the time period increased.

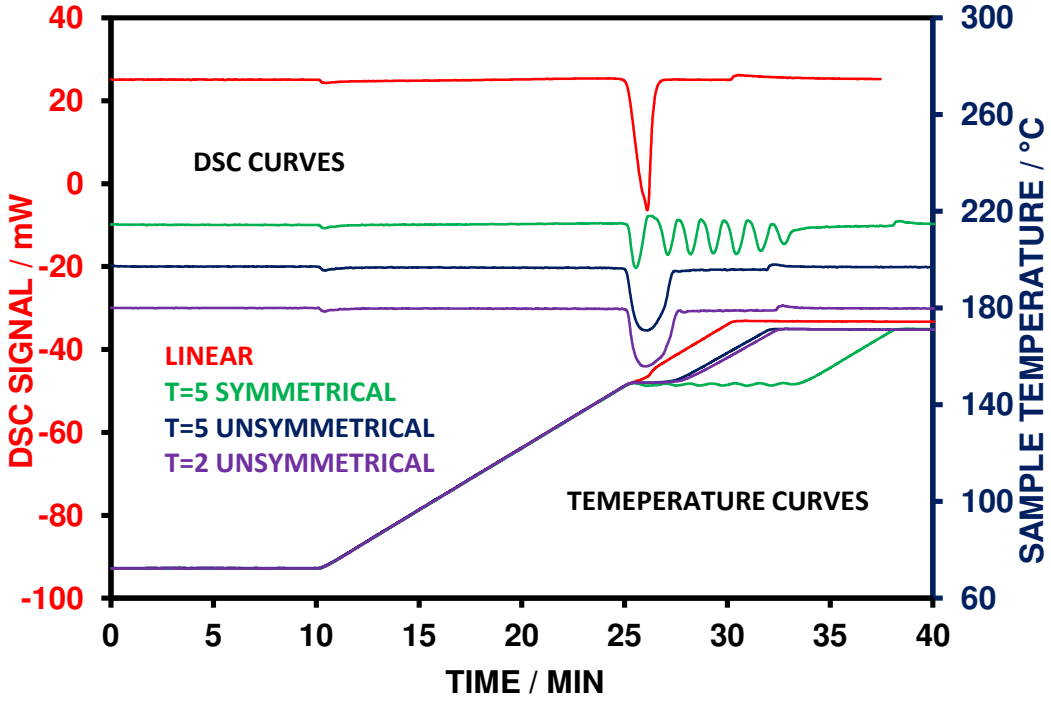

Fig. 4.37 Overlay of DSC and temperature curves for the fusion reaction of diphenylacetic acid

The extent of reaction with respect to temperature is shown in Fig. 4.38 and shows that the proportional heating experiments have reduced the temperature range of the fusion reaction with the linear experiment completing at around 6 ℃ higher temperature than for all the proportional heating experiments. The symmetrically heated experiment that provided the shallow oscillations is seen to form a spiral which was centred around 147 ℃ and completely before the temperature of the unsymmetrical heating experiments, which is very close to the equilibrium temperature of fusion for diphenylacetic acid.

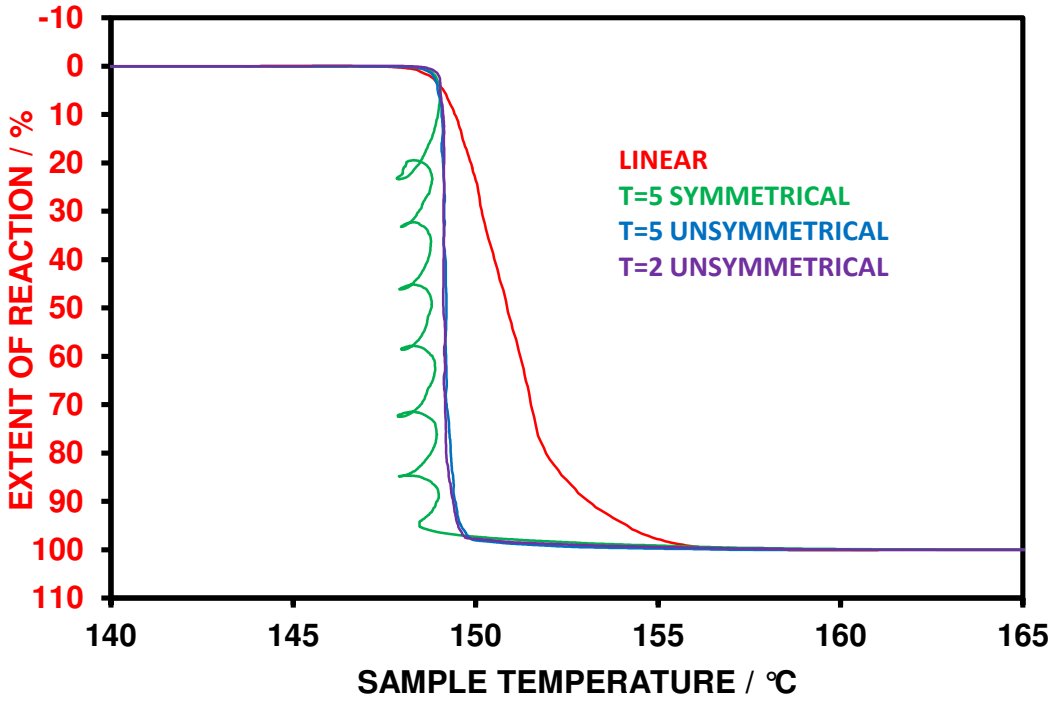

Fig. 4.38 Extent of reaction for the linear heating and proportional heating at several target levels of diphenylacetic acid with respect to temperature

4.9 Phase changes of hydrocarbon based waxes

In order to explore the resolving power of sample controlled experiments, a series of experiments were carried out on hydrocarbons namely tetradecane and hexadecane. These two hydrocarbons have transition temperatures between 0 ℃ and 20 ℃ whereby on cooling through the transition, the samples solidify with the evolution of heat and absorb heat on melting without any change in sample mass. The potential use of the materials is in the construction industry whereby these types of hydrocarbons are impregnated in to wall cavities in buildings to aid in temperature control. As the external temperature cools to below the solidification of the hydrocarbon, energy will be released to the surroundings and vice versa so as to aid in maintaining the temperature of the surrounding climate.

The linear heating and cooling curves for the tetradecane and hexadecane materials are shown in Figs 4.39 and 4.40 respectively where it can be seen that both produce endothermic reactions on cooling and exothermic reactions on heating. The thermal

hysteresis effect can be seen with the temperature difference between heating and cooling being the order of 5 to 10 ℃.

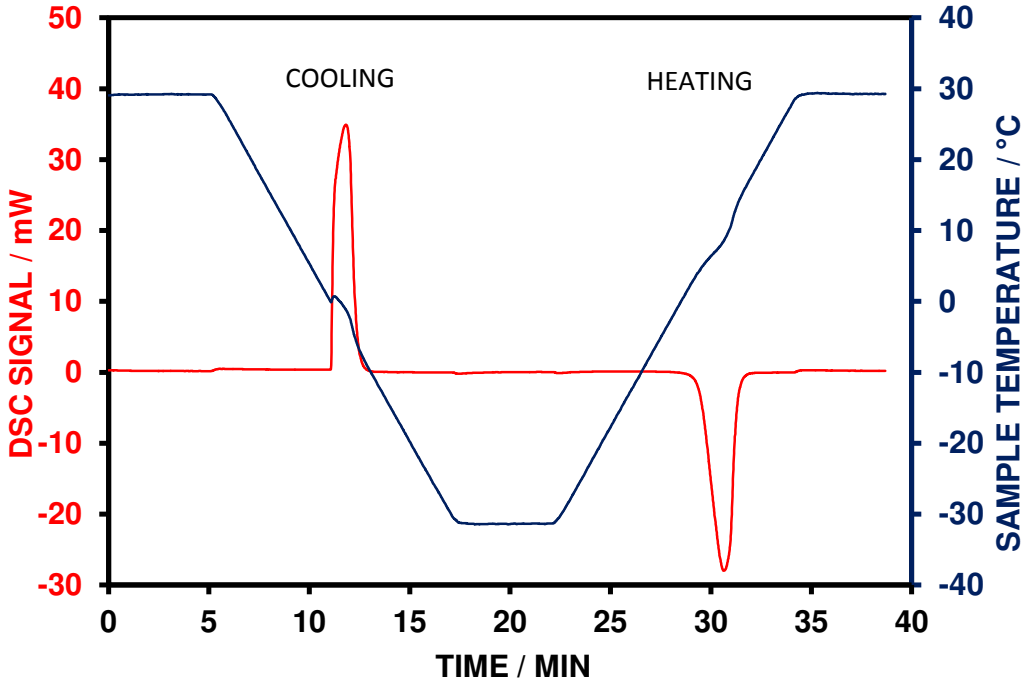

Fig. 4.39 DSC and temperature curves for the linear cooling and heating of tetradecane (sample mass, 10mg; cooling/heating rate, 5℃ min^{-1}; atmosphere, nitrogen)

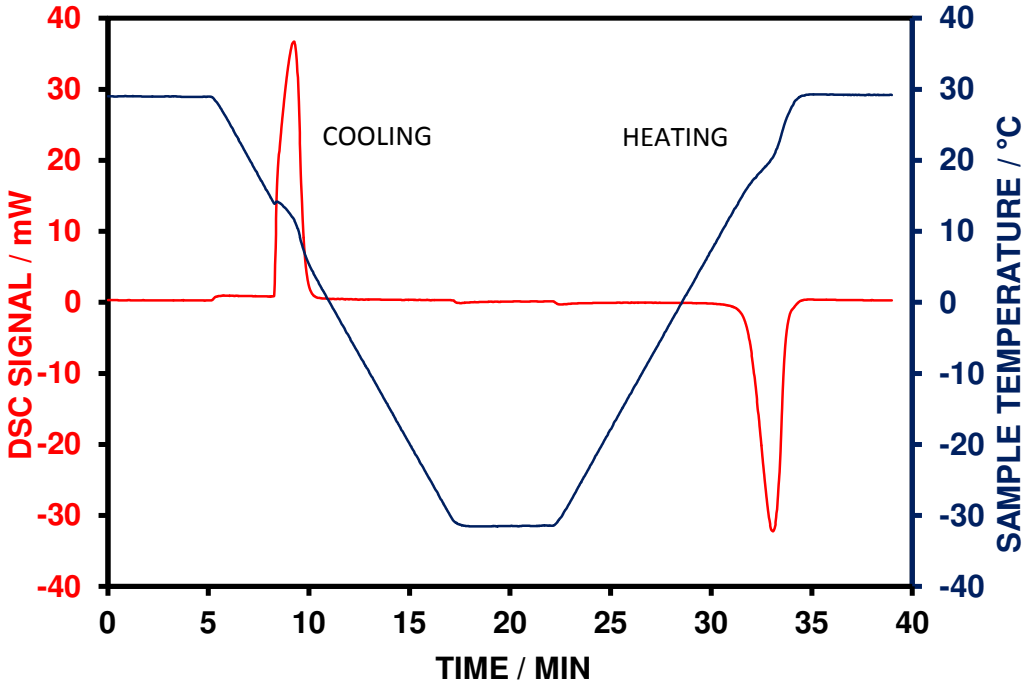

Fig. 4.40 DSC and temperature curves for the linear cooling and heating of hexadecane (sample mass, 10mg; cooling/heating rate, 5℃ min^{-1}; atmosphere, nitrogen)

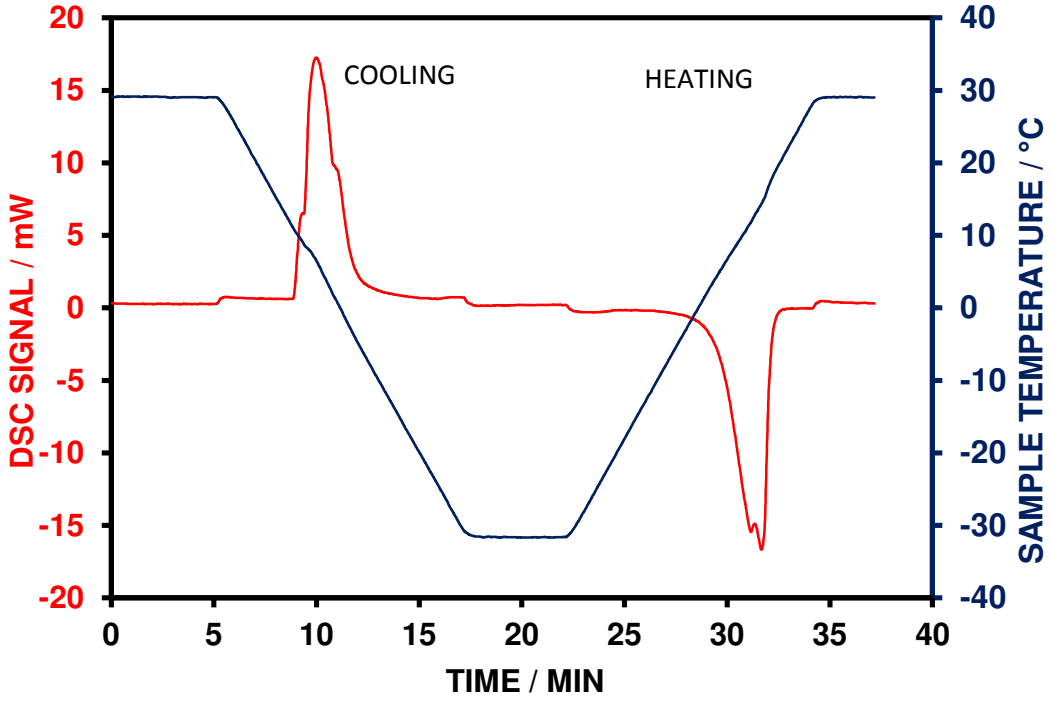

Fig. 4.41 DSC and temperature curves for the linear cooling and heating of 22% tetradecane-78% hexadecane (sample mass, 10mg; cooling/heating rate, 5°C min^{-1}; atmosphere, nitrogen)

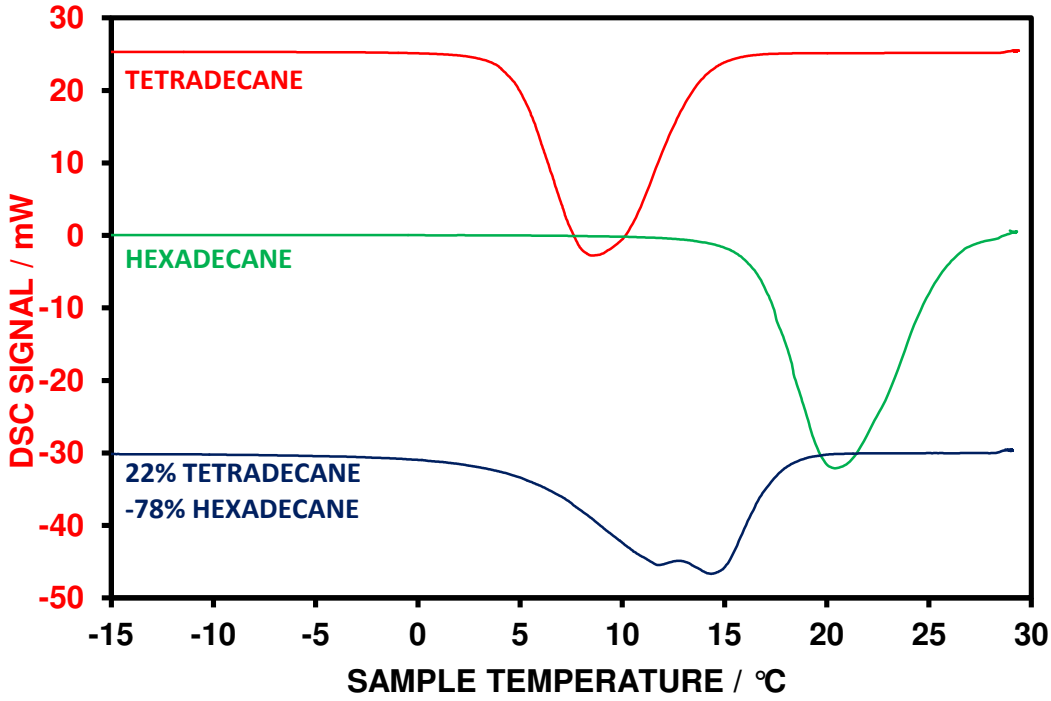

Fig. 4.42 Overlay of linear heating curves with respect to temperature for tetradecane, hexadecane and a 22% tetradecane – 78% hexadecane mixture (sample mass, 10mg; heating rate, 5°C min^{-1}; atmosphere, nitrogen)

As these two hydrocarbons are around 12 ℃ (peak temperature) apart and slightly overlap, a mixture of the two hydrocarbons seems suitable to explore the resolving power of the sample controlled technique.

A 22% tetradecane-78% hexadecane mixture as suggested by He [59] was prepared and a linear heating experiment is shown in Fig. 4.41. It can be seen that the exothermic and endothermic transitions are still evident although it appears to have merged the two materials together to form a single event with a doublet peak. Plotting the overlay of DSC signals with respect to temperature showed that mixing the two ingredients has produced two broad overlapping peaks and this is shown in Fig. 4.42.

A proportional heating experiment carried out in the symmetrical heating mode was carried out on the mixture using a target level of 10 mW. It appeared that there was a small level of separation between the two ingredients but complete resolution did not occur. Lowering the target level to 5 mW appeared to extend the fusion reaction but eliminated the obvious breakpoint observed at the 10 mW target level. However, it can be seen that around half way into the DSC fusion peak, that slight oscillations occur and this may reflect the fusion of that component relative to the other before the oscillations take effect. Reducing the target further to 2 mW produced the oscillation effect for the simultaneous fusion and solidification but the fusion reaction did proceed to completion. It can be seen from the target of 2 mW DSC curve that there appears to be a break in the cycling period close to half way through the reaction which is indicative of resolution between the two components. The experiments performed using the symmetrical heating mode is shown in Fig. 4.43 whereas in Fig. 4.44, the set of proportional heating experiments were repeated using the unsymmetrical mode of heating. It can be seen from this set of experiments that the level of control was not improved by using the heating only control. Using a target of 10 mW, there appeared to be three peaks formed which then increased in number with reducing the target level. The SC-DSC curves are shown using a more sensitive y-axis scale in Fig. 4.45. The use of the unsymmetrical heating mode did not appear to be suitable for this investigation.

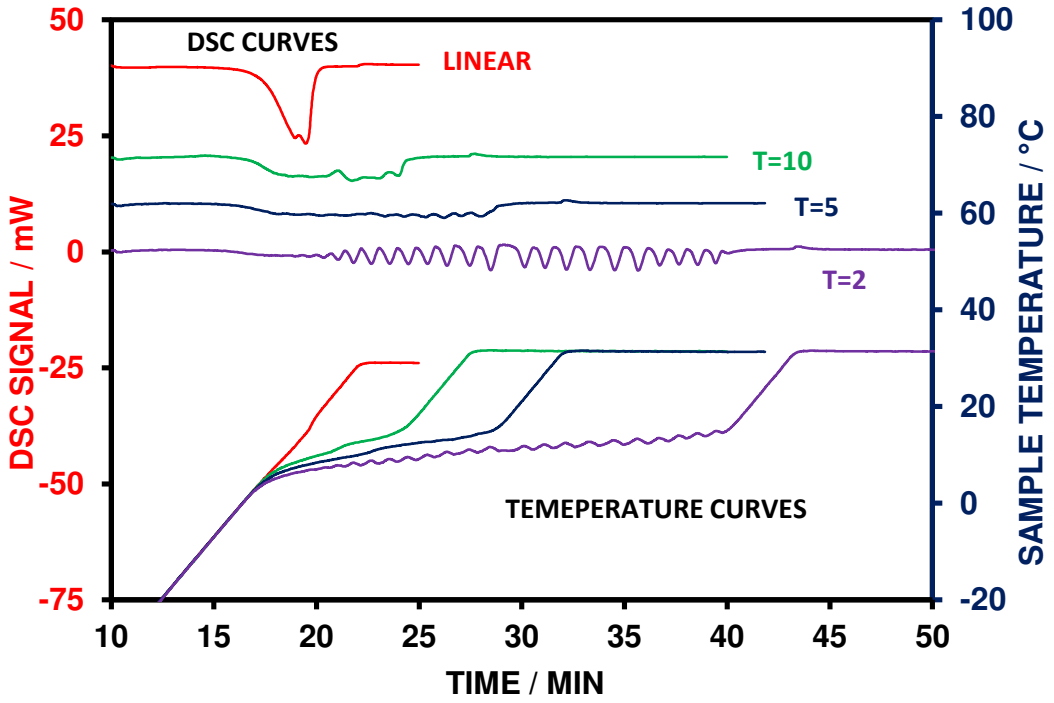

Fig. 4.43 Overlay of linear and proportional heating curves with respect to time for a 22% tetradecane – 78% hexadecane mixture
(sample mass, 10mg; heating rate, ±5℃ min^{-1}; atmosphere, nitrogen)

Plotting the extent of reaction with respect to temperature for the unsymmetrically controlled samples (Fig. 4.46) did not appear to promote any resolution taking place but it can be seen that the fusion reactions contained several differences above the 50% reaction level which would require further investigation to ascertain how they are created.

From the experiments carried out using the hydrocarbon system, it does not appear to be possible to resolve the two components in the mixture. By relating the linear heating curves for the two ingredients and the 22% tetradecane - 78% hexadecane mixture, it appears that there is a eutectic formation of the mixture occurring. This would explain the changing of the temperature range of the mixture relative to its components and also the presence of a near single peak rather than the two discrete peaks expected. It appears that sample controlled studies may not be suitable for this system of hydrocarbons. The opportunity for resolution of hydrocarbons may rest with using hydrocarbons that are immiscible and do not interact with each other to form eutectic peaks.

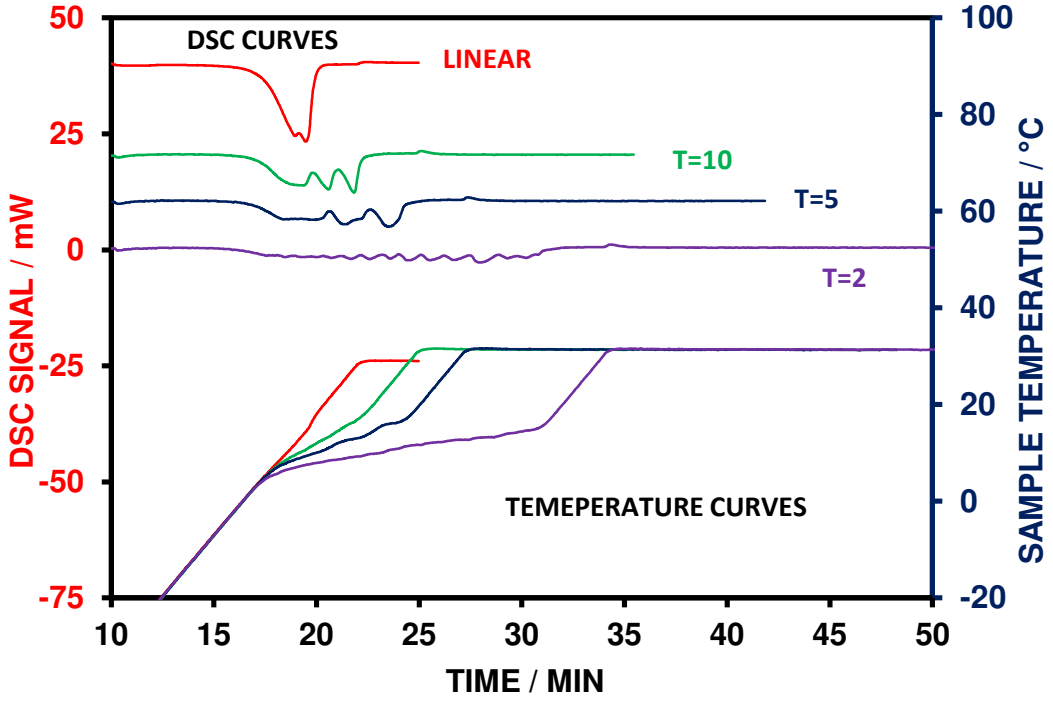

Fig. 4.44 Overlay of linear and proportional heating curves with respect to time for a 22% tetradecane – 78% hexadecane mixture
(sample mass, 10mg; heating rate, +5 and 0 ℃ min^{-1}; atmosphere, nitrogen)

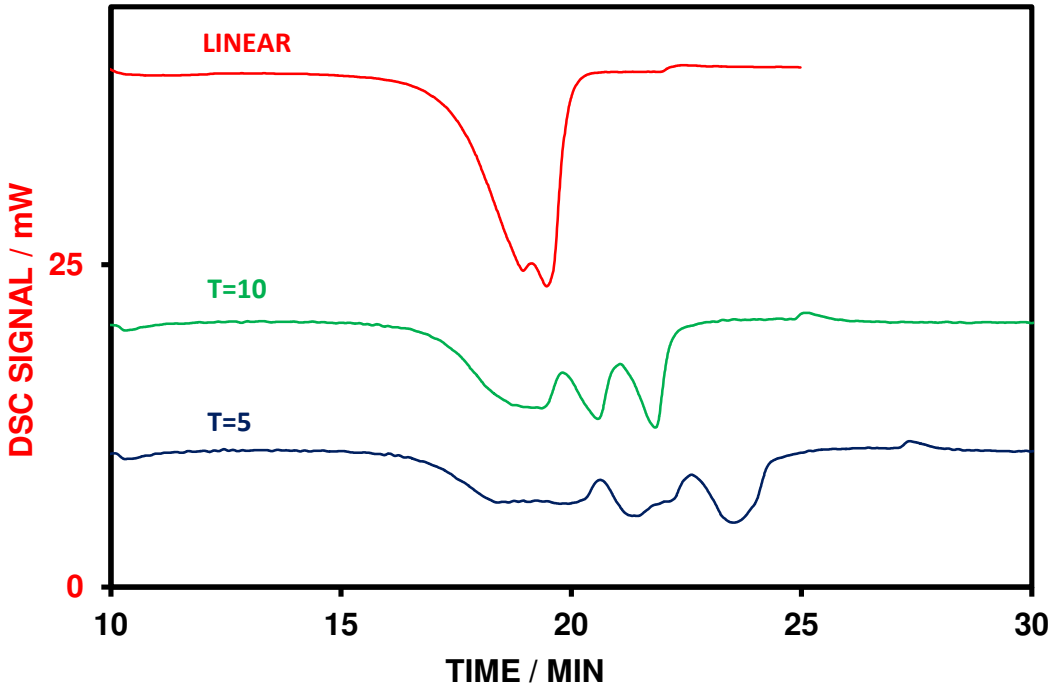

Fig. 4.45 Expanded overlay of linear and proportional heating curves with respect to time for a 22% tetradecane – 78% hexadecane mixture
(sample mass, 10mg; heating rate, +5 and 0 ℃ min^{-1}; atmosphere, nitrogen)

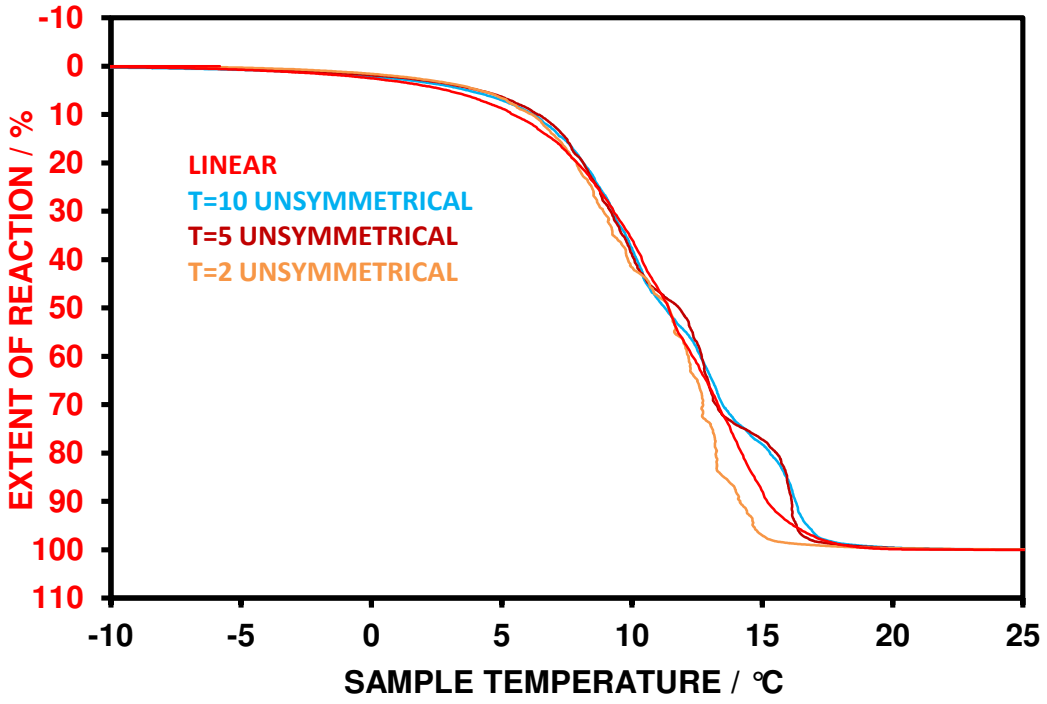

Fig. 4.46 Extent of reaction with respect to temperature for the fusion reaction of a 22% tetradecane – 78% hexadecane mixture

4.10 Application of the Replay Function

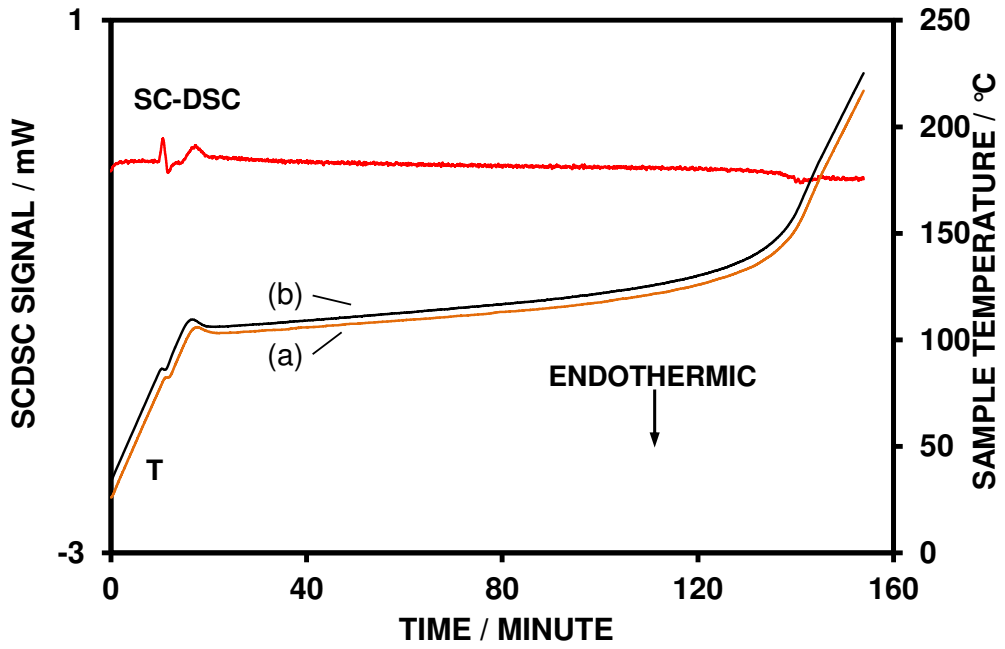

Fig. 4.47 SC-DSC empty pan baseline obtained using replayed temperature profile from a decomposition reaction of sodium bicarbonate with (a) sodium bicarbonate SC-DSC temperature profile and (b) the replayed temperature profile shown displaced by +3 ℃

For several of the systems examined, the replay of the temperature profile was carried out. This is of interest as the baseline of the DSC cell is heating rate dependent and many sample controlled experiments will have varying heating rates, therefore the replicating of the temperature programme using empty crucibles without a sample in place should offer the true baseline of the system for that particular temperature profile. The use of the true baseline may be of benefit in attempting to produce accurate enthalpy determinations.

Fig. 4.47 shows the temperature plot from an SC-DSC experiment on sodium bicarbonate and the replayed temperature plot which can be seen to have closely followed the original. The SC-DSC empty pan baseline obtained in the replayed experiment is also plotted and demonstrates the good baseline stability of the SC-DSC system. This is particularly important since the heating programme is controlled by the magnitude of the deviation of the DSC signal from the baseline [60].
The replay function for several of the systems in this study was examined with the true baseline subtracted. The baseline area was compared with that of the linear heating experiment and subtracted for selected reactions. It was found that there was a reasonable correlation of the enthalpies produced. These are listed in Table 4.3.

The value of the replay function is that the heating profile may be applied to modify or control industrial processes where heating is involved. The application to replicate the heating profile will act to eliminate or at least reduce the deleterious effects of thermal and concentration gradients caused by heating the bulk materials too fast.

Table 4.3

Comparison of DSC Peak Area Determinations of Linear and Proportional Heating Experiments on Various Samples

	DSC Peak Areas / mJ mg^{-1}	
Sample	Linear	Sample Control
Sodium hydrogen carbonate	684	652
Calcium oxalate monohydrate	474	480
Strontium nitrite monohydrate	170	177
Potassium dinitramide	446	454

Chapter 5 Conclusions and Suggestions for Further Work

5.1 Conclusions and Suggestions for Further Work

A new system has been developed, which for the first time, has enabled the benefits of sample controlled thermal analysis to be extended to the widely used technique of DSC. The system was based on a Du Pont 910 heat flux DSC cell which was chosen not only for its sensitivity and baseline stability but also for its relative ease of interfacing to the available in-house control and data processing system. Careful optimisation of the instrument parameters during the development stages has minimised the potential problem of shifts in the DSC baseline when the temperature programme is changed. This has enabled the rate of heating to be controlled directly from the DSC signal and has also allowed controlled cooling to be incorporated.

The problem of making baseline corrections to sample controlled experiments has been addressed by the implementation of a facility to replay the temperature programme for an experiment. This has enabled a baseline to be determined under the same experimental conditions as for the sample and has demonstrated the good baseline stability of the SC-DSC system. This is of particular important since the heating programme is controlled by the magnitude of the deviation of the DSC signal from the baseline. This replay facility will enable an accurate buoyancy correction to be applied in SC-TG experiments for the first time.

The potential of the new SC-DSC system has been evaluated by studying a wide range of reaction types. The first part consisted of reactions taking place with a change in mass, including endothermic dehydration, dehydroxylation and decomposition reactions and exothermic decomposition and oxidation reactions. The results were compared with those obtained by sample controlled thermogravimetry. Similar profiles were obtained using both techniques and the ability of SC-DSC to provide direct information on reaction mechanisms was demonstrated in the studies on the dehydration of the calcium oxalate and strontium nitrate monohydrates and

the decomposition of sodium bicarbonate. In all of these cases the SC-DSC curves showed clear evidence of a nucleation and growth reaction. Similarly, SC-DSC studies confirmed the autocatalytic nature of the exothermic decomposition reaction of nitrocellulose.

SC-DSC was also found to be successful in preventing the ignition reactions in the decomposition of nitrocellulose and the oxidation of a copper impregnated carbon which were found to occur under linear heating conditions. This should enable the reactions to be studied in more detail than is possible with conventional thermal analysis techniques and SC-DSC will be a suitable technique for comparing different batches of the same material.

The second part of the instrument evaluation has focussed on the applicability of the technique to study both endothermic and exothermic reactions that took place without a change in mass and which were outside the scope of the existing sample controlled techniques. The studies on fusion reactions showed that the best results were obtained when samples were not allowed to cool thus avoiding the effects of supercooling. While it proved difficult to control the rapid fusions of metal and organic DSC standards with the present equipment, promising results were obtained for the fusion of a mixture of tetradecane and hexadecane and for the aqueous fusion of magnesium nitrate hexahydrate, which both took place over a broader temperature range. Thus, when using SC-DSC in the heating only mode the temperature range of the aqueous fusion of the nitrate was reduced from 7°C in a DSC experiment at 5 °C min^{-1} to less than 1 °C. Both of these samples are used as phase change materials and SC-DSC should be a valuable additional technique for investigating these types of systems.

The potential of the SC-DSC technique to study the metal-oxidant based pyrotechnic systems which react without a significant change in mass has been demonstrated by studies on a zirconium-potassium perchlorate-nitrocellulose pyrotechnic composition. Not only was SC-DSC able to prevent an ignition reaction in this highly reactive system but caused the reaction to take place over a markedly lower temperature range than in DSC studies. In the case of the lowest target rate chosen, the exothermic reaction was extended over a period of some two hours and the reduced

rate and the significantly lower temperatures, compared with DSC, will enable the reaction to be followed quantitatively, without interference from the decomposition of the potassium perchlorate. This has been demonstrated in a preliminary study where samples were removed at set temperature intervals and the amount of perchlorate reacted determined by DSC analysis.

Another important area where it is now possible to make sample controlled studies is in the curing of polymeric samples. This is illustrated by the ability of the SC-DSC technique to control the rate of exothermic curing reaction of an epoxy resin. The use of SC-DSC should therefore allow the development of temperature profiles to enable polymer samples to be cured at selected rates. These could then be approximated for use with larger scale preparative system that lack SC-TA control.

Since the aim of the present work was to develop the new technique of SC-DSC and apply it to a wide range of reaction types, the experimental conditions used had to be restricted. It would therefore be of value to investigate a greater range of variables including sample size, heating and cooling rates and target values using a number of the systems already investigated. In view of the potential of the SC-DSC for studies on phase change materials it will be necessary to evaluate the relationship between the equilibrium melting temperature for a given transition and the values obtained from SC-DSC studies. In addition, the reproducibility of the measurements obtained by SC-DSC would also be further investigated and compared with those obtained previously by sample controlled TG.

The SC-DSC studies carried out in the present work have been carried out using proportional heating and it would be of interest to evaluate the constant rate and stepwise isothermal methods. The latter method may be of particular value for the study of the fusion of phase change materials. The possibility of using the derivative DSC signal to control the reaction should also be investigated and may reduce any problems due to baseline shifts when working at lower target rates. In addition, this approach would enable second order transitions such as glass transitions to be investigated.

The studies to date have shown that for reactions taking place with a change in mass similar profiles are given by SC-DSC and sample controlled TG. It would be of value to make a quantitative comparison of the two techniques by developing a simultaneous sample controlled TG-DSC system. This would allow the TG and DSC curves to be compared directly under sample controlled conditions and reaction rate could be controlled by either the DSC or derivative TG signals. This would be of particular interest for systems where more than one reaction is taking place at the same time e.g in the aerial oxidation of carbonaceous systems.

In conclusion, the newly developed technique of SC-DSC has been shown to be capable of being applied to a wide range of reaction types and has extended considerably the range of reactions that fall within the scope of sample controlled thermal analysis, particularly those taking place without a change in mass. Since the system can be calibrated directly using DSC temperature standards, it also offers the important advantage of accurate measurement of the sample temperature which is not always possible in existing SC-TA systems. Further enhancement of the SC-DSC technique would obtained by taking advantage of the improved performance of the latest DSC equipment compared to the unit used in the present studies.

Chapter 6 REFERENCES

[1] Differential scanning calorimetry, G. Höhne, W. F. Hemminger, H. -J. Flammersheim, Springer-Verlag Berlin Heidelberg, 2nd Editn, 2003.

[2] Thermal analysis of polymers: Fundamentals and Applications. Eds. J. D. Menczel, R. B. Prime, Wiley, Hoboken, 2009.

[3] Thermal analysis of pharmaceuticals, Eds. D. Q. M. Craig, M. Reading, 2006, CRC Press, Boca Raton, 2007.

[4] Applications of thermal analysis and coupled techniques in pharmaceutical industry, D. Giron, J.Therm. Anal & Calorim. 68 (2002) 335.

[5] Sir William Chandler Roberts-Austen — His role in the development of binary diagrams and modern physical metallurgy, F. X. Kayser, J. W. Patterson, J. Phase Equilib., 19 (1) (1998) 11.

[6] Differential thermal analysis (DTA) and differential scanning calorimetry (DSC) as a method of material investigation; G. Klančnik, J. Medved, P. Mrvar; Materials and Geoenvironment, 57 (1) (2010) 127.

[7] A theory of differential thermal analysis and new methods of measurement and interpretation, S.L.Boersma, J. Am. Ceram. Soc., 38 (1955) 281.

[8] Sample controlled thermal analysis, Eds. O. T. Sørensen & J. Rouquerol, Kluwer Academic Publishers, Dordrecht, 2003.

[9] L. Erdey, F. Paulik, J. Paulik, Hungarian Patent 152197, 1962.

[10] Differential thermal analysis under quasi-isothermal, quasi isobaric conditions, F. Paulik, E. Bessenyey-Paulik, K. Walther-Paulik, Part 1, Thermochim. Acta, 402 (2003) 105. Part 2, Thermochim. Acta, 424 (2004) 75.

[11] Vacuum thermal analysis apparatus, with controlled residual pressure and with constant decomposition rate. J. Rouquerol; In R. F. Schwenker Jr. and P. D. Garn, Ed., Therm. Anal., (1969) 281. Academic Press, New York.

[12] A general introduction to SC-TA and to rate-controlled SC-TA, J. Rouquerol, J. Therm. Anal. Calorim. 72 (2003) 1081.

[13] A new high performance evolved gas analysis system for catalyst characterisation. P. A. Barnes, G. M. B. Parkes, E. L. Charsley, Anal. Chem., 66 (1994) 2226.

[14] Special trends in thermal analysis, F. Paulik, John Wiley & Sons Ltd, Chichester, 1995.

[15] Development and applications of sample controlled thermomicroscopy. E. L. Charsley, C. Stewart, P. A. Barnes, G. M. B. Parkes, J.Therm. Anal. Calorim. 72 (2003) 1087.

[16] Gas concentration programming – a new approach to sample controlled thermal analysis, G. M. B. Parkes, P. A. Barnes, E. L. Charsley, Thermochim. Acta. 320 (1998) 297.

[17] Characterisation of the components of pyrotechnic systems by sample controlled thermogravimetry, E. L. Charsley, J. J. Rooney, H. A. White, B. Berger, T. T .Griffiths, Proceedings 31st North American Thermal Analysis Society Conference, Albuquerque, New Mexico, Ed. M.Rich, NATAS, 2003, 133.

[18] SC-TA and adsorbents, P.Llewellyn, F.Rouquerol and J.Rouquerol, in: Sample Controlled Thermal Analysis, Eds. O. T. Sorensen, J. Rouquerol, Kluwer Academic Publishers, Dordrecht, (2003) 135.

[19] Comparison of new thermal and reactant gas blending methods for the controlled oxidation of carbon; E. A. Dawson, G. M. B. Parkes, P. A. Barnes, M. J. Chinn, P. R. Norman, Thermochim. Acta, 335 (1999) 141.

[20] An investigation of the porosity of carbons prepared by constant rate activation in air; E. A. Dawson, G. M. B. Parkes, P. A. Barnes and M. J. Chin, Carbon, 41 (2003) 571.

[21] Applications of new high resolution evolved-gas analysis systems for the characterisation of catalysts using rate-controlled thermal analysis, P. A. Barnes, G. M. B. Parkes, D. R. Brown, E. L. Charsley, Thermochim. Acta, 269-270 (1995) 665.

[22] Catalyst characterisation and preparation using sample controlled thermal techniques—high resolution studies and the determination of the energetics of surface and bulk processes, E. A. Fesenko, P. A. Barnes, G. M. B. Parkes, E. A. Dawson, M. J. Tiernan, Top. Catal., 19 (2002) 283.

[23] Mineralogical evolution of portland cement blended with silica nanoparticles and its effect on mechanical strength, J. I. Tobón, J. J. Payá, M. V. Borrachero, O. J. Restrepo, Construction and Building Materials, 36 (2012) 736.

[24] SC-TA and ceramics, O. T. Sørensen, J. M. Criado, in: Sample Controlled Thermal Analysis, Eds. O. T. Sorensen, J. Rouquerol, Kluwer Academic Publishers, Dordrecht, (2003)102.

[25] SC-TA and ceramics, O. T. Sørensen, J. Therm. Anal. Calorim., 72 (2003) 1093.

[26] High-resolution TG for the characterization of diesel fuel additives, A. Zanier, J. Therm. Anal. Calorim., 64 (2001) 377.

[27] Study of gypsum dehydration by controlled transformation rate thermal analysis (CRTA), E. Badens, P. Llewellyn, J. M. Fulconis, C. Jourdan, S. Veesler, R. Boistelle, F. Rouquerol, J. Solid State Chem., 139 (1998) 37.

[28] The effect of humidity on thermal decomposition of zinc acetylacetonate monohydrate, T. Arii, A. Kishi, Humidity controlled thermal analysis: J. Therm. Anal. Calorim., 83 (2006) 253.

[29] Applications of sample-controlled thermal analysis (SC-TA) to kinetic analysis and synthesis of materials, L. A. Pérez-Maqueda, J. M. Criado, P. E. Sánchez-Jiménez, M. J. Diánez, J. Therm. Anal. Calorim., 120 (2015) 45.

[30] Mechanism for hydrotalcite decomposition- a controlled rate thermal analysis study, R. L. Frost, V. Vagvoelgyi, S. J. Palmer, J. Kristof, E. Horvath, Journal of Colloid and Interface Sci. 318(2) (2008) 302.

[31] Controlled rate thermal analysis of sepiolite, R. L. Frost, J. Kristof, E. Horváth, J. Therm. Anal. Calorim., 98(3) (2009) 749

[32] Application of high resolution thermogravimetry to the study of thermal stability of poly(vinyl chloride) resins, N. Gonzalez, A. Mugica, M. J. Fernandez-Berridi, Polym. Degrad. Stab., 91 (2006) 629.

[33] SC-TA & kinetics, J. M.Criado, L. A. Perez-Maqueda, in: Eds. O.T. Sorensen, J.Rouquerol, Sample Controlled Thermal Analysis, Kluwer Academic Publishers, Dordrecht, 2003, 62.

[34] Applications of sample-controlled thermal analysis (SC-TA) to kinetic analysis and synthesis of materials, L. A. Pérez-Maqueda, J. M. Criado, P. E. Sánchez-Jiménez, M. J. Diánez, J. Therm. Anal. Calorim., 120 (2015) 45.

[35] Du Pont 990 Differential scanning calorimeter operator's manual; TA Instruments Ltd, section 4.5.

[36] The Engineering Toolbox; Thermal Conductivity of Aluminium. http://www.engineeringtoolbox.com/thermal-conductivity-metals-d_858.html

[37] Significance of the kinetics of thermal decomposition of $NaHCO_3$ evaluated by thermal analysis; H. Tanaka and H. Takemoto; J. Therm. Anal., 38 (1992) 429.

[38] A new method of analyzing thermogravimetric data, T. Ozawa, Bull. Chem. Soc. Jpn. 38 (1965) 1881.

[39] Use of solid insertion probe mass spectrometry and constant rate thermal analysis in the study of materials: Determination of apparent activation energies and mechanisms of solid-state decomposition reactions. M. J. Tiernan, P. A. Barnes and G. M. B. Parkes*;* J. Phys. Chem. B*,* 103 (33) (1999) 6944.

[40] The thermal decomposition of $NaHCO_3$. Renewed studies by DSC, SEM and FT-IR; L. Dei and G. T. T. Guarini; J. Therm. Anal., 50 (1997), 773.

[41] Correlation between the shape of controlled-rate thermal analysis curves and the kinetics of solid state reactions. J. M. Criado, A. Ortega, F. Gotor. Thermochim. Acta. 157 (1990) 171.

[42] A method of assessing solid state reactivity illustrated by thermal decomposition experiments on sodium bicarbonate, H. Tanaka; Thermochim. Acta, 255 (1995) 255.

[43] Investigation under quasi-isothermal and quasi-isobaric conditions by means of the derivatograph. F. Paulik, J. Paulik, J. Therm. Anal., 5 (1973) 253.

[44] A study of calcium oxalate monohydrate using dynamic differential scanning calorimetry and other thermoanalytical techniques; K. J. Kociba, P. K. Gallagher; Thermochim. Acta. 282/283 (1996) 277.

[45] Kinetics and mechanism of the thermal dehydration of calcium oxalate monohydrate; H. Tanaka, S. Oshima, S. Ichiba, H. Negita; Thermochim. Acta. 48 (1981) 137.

[46] An investigation of strontium nitrite and its role in the ageing of the magnesium–strontium nitrate pyrotechnic system using isothermal microcalorimetry and thermal analysis techniques; I. M. Tuukkanen, E. L. Charsley, S. J. Goodall, P. G. Laye, J. J. Rooney, T. T. Griffiths, H. Lemmetyinen; Thermochim. Acta. 443 (2006) 116.

[47] Thermal decomposition of strontium nitrite monohydrate**;** P. K. Gallagher Thermochim. Acta 75 **(**1984**)** 121.

[48] The thermal behaviour of potassium dinitramide. Part 2. Mechanism of thermal decomposition. M. Lei, Z-R. Lui, Y-H. Kong, C-M. Yin, B-Z. Wang, Y. Wang, P. Zhang; Thermochim. Acta 335 (1999) 113.

[49] Thermal studies on potassium dinitramide in the liquid state, E. L. Charsley, P. G. Laye, H. M. Markham, J. J. Rooney, B. Berger, P. Folly, R. P. Claridge, T. T. Griffiths, Proc, 36th Int. Ann. Conf. ICT/ 32nd Int. Pyrotechnic Seminar on Karlsruhe, Fraunhofer-Institut Chemische Technologie, 2005, V34.

[50] Characterisation of the zirconium-potassium perchlorate-nitrocellulose pyrotechnic system by simultaneous thermogravimetry-differential thermal analysis-mass spectrometry, B. Berger, E. L. Charsley, S. B. Warrington, Propellants, Explos., Pyrotech., 20 (1995) 266.

[51] Thermomicroscopy studies on the zirconium-potassium perchlorate-nitrocellulose pyrotechnic system, B. Berger, A. J. Brammer, E. L. Charsley, Thermochim. Acta, 269/270 (1995) 639.

[52] The characterization of the components of pyrotechnic systems by sample controlled thermogravimetry, E. L. Charsley, J. J. Rooney, H. A. White, B. Berger, T. T. Griffiths, Proceedings 31st North American Thermal Analysis Society Conference, Albuquerque, New Mexico, Ed. M.Rich, NATAS, 2003, 133.

[53] TG and TGT investigations of the decomposition of nitrocellulose under quasi isothermal conditions. F. Paulik and J. Paulik and M. Arnold; J. Therm. Anal., 12 (1977) 383.

[54] A study of the activation of carbon using sample controlled thermal analysis. E. A. Dawson, G. M. B. Parkes, P. A. Barnes, M. J. Chinn, P. R. Norman. J. Therm. Anal. Calorim. 56 (1999) 267.

[55] Huntsman Advanced Materials, B-3078, Everberg.

[56] Thermal characteristics of $Mg(NO_3).6H_2O$; Nagano, Ogawa, Mochida, Hayashi, Ogoshi; Appl. Therm. Eng., 24 (2004) 221.

[57] DSC study of the melting and solidification of salt hydrates; S. Cantor; Thermochim. Acta, 33 (1979) 69.

[58] Quantitative studies on the zirconium-potassium perchlorate-nitrocellulose pyrotechnic system using differential scanning calorimetry and chemical analysis, B. Berger, E. L. Charsley, J. J. Rooney, S.B.Warrington, Thermochim. Acta, 255 (1995) 227.

[59] Doctoral thesis. Department of Chemical Engineering and Technology Energy Processes. Bo He, KTH Stockholm, Sweden, 2004.

[60] Development and applications of a sample controlled DSC system; E. L. Charsley, P. G. Laye, G. M. B. Parkes, J. J. Rooney; J. Therm. Anal. Calorim. 105 (2011) 699.

Chapter 7 Conferences Attended, Presentations and Publications

7.1 Conferences Attended

Royal Society of Chemistry; Thermal Methods Group- TAC 2005
University of Huddersfield, Huddersfield; November 2005

Royal Society of Chemistry; Thermal Methods Group- TAC 2006
London School of Pharmacy, London; April 2006

Royal Society of Chemistry; Thermal Methods Group- TAC 2007
University of Strathclyde, Glasgow; April 2007

Royal Society of Chemistry; Thermal Methods Group- TAC 2008
National Physical Laboratory (NPL), London; April 2008

Royal Society of Chemistry; Thermal Methods Group- TAC 2009
University of Bath, Bath; April 2009

Royal Society of Chemistry; Thermal Methods Group- TAC 2011
Queens University, Belfast; April 2011

Royal Society of Chemistry; Thermal Methods Group- TAC 2012
Nottingham University, Nottingham; April 2012

7.2 Oral Presentation

University of Huddersfield; School of Applied Sciences Research Seminar
University of Huddersfield, Huddersfield; January 2012

7.3 Presentations

7.3.1 Research Festival, University of Huddersfield, March 12th 2008

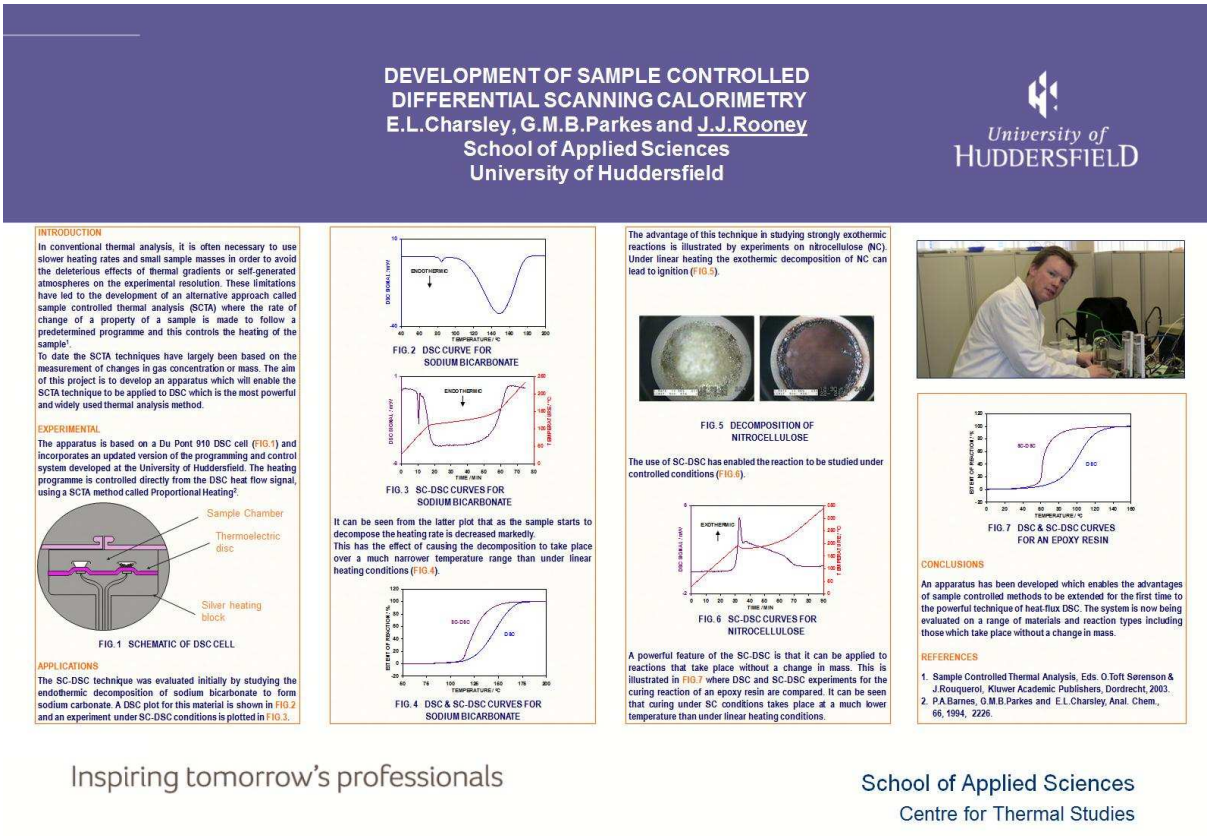

DEVELOPMENT OF SAMPLE CONTROLLED DIFFERENTIAL SCANNING CALORIMETRY

E.L.Charsley, G.M.B.Parkes and J.J.Rooney
School of Applied Sciences
University of Huddersfield

University of HUDDERSFIELD

INTRODUCTION

In conventional thermal analysis, it is often necessary to use slower heating rates and small sample masses in order to avoid the deleterious effects of thermal gradients or self-generated atmospheres on the experimental resolution. These limitations have led to the development of an alternative approach called sample controlled thermal analysis (SCTA) where the rate of change of a property of a sample is made to follow a predetermined programme and this controls the heating of the sample[1].

To date the SCTA techniques have largely been based on the measurement of changes in gas concentration or mass. The aim of this project is to develop an apparatus which will enable the SCTA technique to be applied to DSC which is the most powerful and widely used thermal analysis method.

EXPERIMENTAL

The apparatus is based on a Du Pont 910 DSC cell (FIG.1) and incorporates an updated version of the programming and control system developed at the University of Huddersfield. The heating programme is controlled directly from the DSC heat flow signal, using a SCTA method called Proportional Heating[2].

FIG.1 SCHEMATIC OF DSC CELL

APPLICATIONS

The SC-DSC technique was evaluated initially by studying the endothermic decomposition of sodium bicarbonate to form sodium carbonate. A DSC plot for this material is shown in FIG.2 and an experiment under SC-DSC conditions is plotted in FIG.3.

FIG.2 DSC CURVE FOR SODIUM BICARBONATE

FIG.3 SC-DSC CURVES FOR SODIUM BICARBONATE

It can be seen from the latter plot that as the sample starts to decompose the heating rate is decreased markedly. This has the effect of causing the decomposition to take place over a much narrower temperature range than under linear heating conditions (FIG.4).

FIG.4 DSC & SC-DSC CURVES FOR SODIUM BICARBONATE

The advantage of this technique in studying strongly exothermic reactions is illustrated by experiments on nitrocellulose (NC). Under linear heating the exothermic decomposition of NC can lead to ignition (FIG.5).

FIG.5 DECOMPOSITION OF NITROCELLULOSE

The use of SC-DSC has enabled the reaction to be studied under controlled conditions (FIG.6).

FIG.6 SC-DSC CURVES FOR NITROCELLULOSE

A powerful feature of the SC-DSC is that it can be applied to reactions that take place without a change in mass. This is illustrated in FIG.7 where DSC and SC-DSC experiments for the curing reaction of an epoxy resin are compared. It can be seen that curing under SC conditions takes place at a much lower temperature than under linear heating conditions.

FIG.7 DSC & SC-DSC CURVES FOR AN EPOXY RESIN

CONCLUSIONS

An apparatus has been developed which enables the advantages of sample controlled methods to be extended for the first time to the powerful technique of heat-flux DSC. The system is now being evaluated on a range of materials and reaction types including those which take place without a change in mass.

REFERENCES

1. Sample Controlled Thermal Analysis, Eds. O.Toft Sørenson & J.Rouquerol, Kluwer Academic Publishers, Dordrecht, 2003.
2. P.A.Barnes, G.M.B.Parkes and E.L.Charsley, Anal. Chem., 66, 1994, 2226.

Inspiring tomorrow's professionals

School of Applied Sciences
Centre for Thermal Studies

7.3.2 Poster presentation, Royal Society of Chemistry; Thermal Methods Group – TAC 2009; University of Bath. April 2009

DEVELOPMENT OF SAMPLE CONTROLLED DIFFERENTIAL SCANNING CALORIMETRY

E. L. Charsley, G.M.B.Parkes and J.J.Rooney
School of Applied Sciences, University of Huddersfield,
Queensgate, Huddersfield HD1 3DH, UK

INTRODUCTION

In conventional thermal analysis, it is often necessary to use slower heating rates and small sample masses in order to avoid the deleterious effects of thermal gradients or self-generated atmospheres on the experimental resolution. These limitations have led to the development of an alternative approach called sample controlled thermal analysis (SCTA) where the rate of change of a property of a sample is made to follow a predetermined programme and this controls the heating of the sample[1].

To date the SCTA techniques have largely been based on the measurement of changes in gas concentration or mass. The aim of this project is to develop an apparatus which will enable the SCTA technique to be applied to DSC which is the most powerful and widely used thermal analysis method.

EXPERIMENTAL

The apparatus is based on a Du Pont 910 DSC cell and incorporates an updated version of the programming and control system developed at the University of Huddersfield. The heating programme is controlled directly from the DSC heat flow signal, using a SCTA method called Proportional Heating[2].

APPLICATIONS

The SC-DSC technique was evaluated initially by studying the endothermic decomposition of sodium bicarbonate to form sodium carbonate. A DSC plot for this material is shown in FIG. 1 and an experiment under SC-DSC conditions is plotted in FIG. 2. It can be from the latter plot that as the sample starts to decompose the heating rate is decreased markedly.

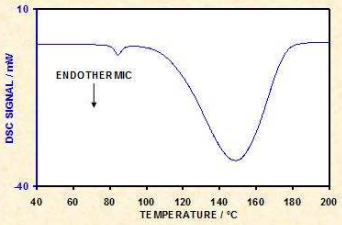

FIG. 1 DSC CURVE FOR SODIUM BICARBONATE

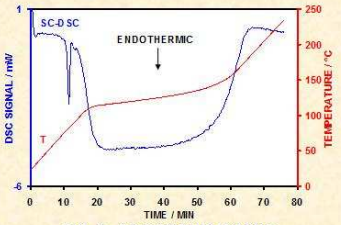

FIG. 2 SC-DSC CURVES FOR SODIUM BICARBONATE

This has the effect of causing the decomposition to take place over a much narrower temperature range than under linear heating conditions (FIG. 3)

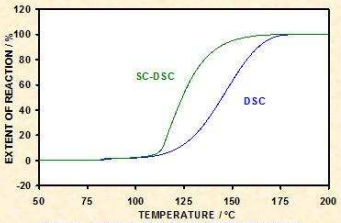

FIG. 3 DSC & SC-DSC CURVES FOR SODIUM BICARBONATE

The advantage of this technique in studying strongly exothermic reactions is illustrated by experiments on nitrocellulose (NC). Under linear heating the exothermic decomposition of NC can lead to ignition (FIG. 4).

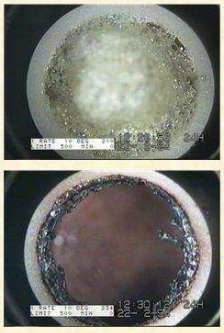

FIG. 4 DECOMPOSITION OF NITROCELLULOSE

The use of SC-DSC has enabled the reaction to be studied under controlled conditions (FIG. 5).

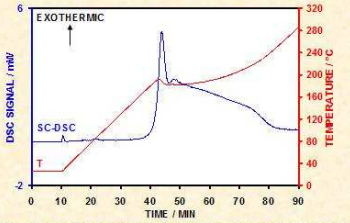

FIG. 5 SC-DSC CURVES FOR NITROCELLULOSE

A powerful feature of the SC-DSC is that it can be applied to reactions that take place without a change in mass. This is illustrated in FIG. 6 where DSC and SC-DSC experiments for the curing reaction of an epoxy resin are compared. It can be seen that curing under SC conditions takes place at a much lower temperature than under linear heating conditions.

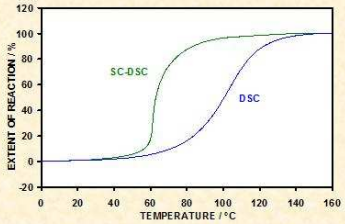

FIG. 6 DSC & SC-DSC CURVES FOR AN EPOXY RESIN

CONCLUSIONS

An apparatus has been developed which enables the advantages of sample controlled methods to be extended for the first time to the powerful technique of heat-flux DSC. The system is now being evaluated on a range of materials and reaction types including those which take place without a change in mass.

REFERENCES

1. Sample Controlled Thermal Analysis, Eds. O. Toft Sørenson & J.Rouquerol, Kluwer Academic Publishers, Dordrecht, 2003.
2. P.A.Barnes, G.M.B.Parkes and E.L.Charsley, Anal. Chem., 66, 1994, 2226.

7.4 Publications

7.4.1 Development and applications of a sample controlled DSC system; E. L. Charsley, P. G. Laye, G. M. B. Parkes, J. J. Rooney; J. Therm. Anal. Calorim, (2011) 105, 699.

J Therm Anal Calorim (2011) 105:699–703
DOI 10.1007/s10973-010-1196-8

Development and applications of a sample controlled DSC system

E. L. Charsley · P. G. Laye ·
G. M. B. Parkes · J. J. Rooney

ESTAC2010 Conference Special Issue

Abstract The development of a new sample controlled thermal analysis technique based on a heat flux DSC is described. The performance of the system is demonstrated by studies on the decomposition of sodium bicarbonate and the oxidation of a copper impregnated carbon. The ability of the technique to study reactions which take place without a change in mass is illustrated by the curing of an epoxy resin with a polyaminoamide hardener.

Keywords Sample controlled · DSC · Sodium bicarbonate · Carbon · Epoxy resin

Introduction

In conventional thermal analysis, it is often necessary to use slow heating rates and small sample masses in order to reduce the deleterious effects of thermal gradients or self-generated atmospheres on the experimental resolution. These limitations have led to the development of an alternative approach called sample controlled thermal analysis (SCTA) where the rate of change of a property of a sample is made to follow a pre-determined programme and this controls the heating of the sample [1].

E. L. Charsley (✉) · P. G. Laye · J. J. Rooney
Centre for Thermal Studies, IPOS,
School of Applied Sciences, University of Huddersfield,
Queensgate, Huddersfield HD1 3DH, UK
e-mail: e.l.charsley@hud.ac.uk

G. M. B. Parkes
Centre for Materials and Catalysis Research,
School of Applied Sciences, University of Huddersfield,
Queensgate, Huddersfield HD1 3DH, UK

The technique was pioneered independently in the 1960s by Rouquerol in France who developed a method for use at reduced pressures called Constant Rate Thermal Analysis [2] and by the Pauliks in Hungary who introduced an approach called Quasi-Isothermal Quasi-Isobaric Thermal Analysis [3, 4]. In a later development, Sorensen established the Stepwise Isothermal Analysis method [5].

SCTA techniques have been based largely on the measurement of changes in gas concentration or in mass, although the temperature difference technique developed by Smith in 1940 [6] could be considered as the first SCTA method. This method generally referred to as "Smith Thermal Analysis" used a differential thermocouple to establish a constant temperature difference between the sample and furnace wall. It is still being employed in a modernised form to study alloy systems [7].

Paulik et al. [8] modified the Derivatograph simultaneous TG-DTA apparatus to enable the rate of the reaction to be controlled by the derivative of the DTA signal. They described the application of this technique to the study of a range of inorganic samples with the main emphasis on dehydration and decomposition reactions [9–12].

The aim of this study is to develop an apparatus to enable the advantages of SCTA to be applied to differential scanning calorimetry, which is the most powerful and widely used of the thermal analysis methods. The equipment is based on a Du Pont 910 DSC cell. This was chosen not only for its sensitivity and baseline stability but also for its ease of interfacing to the in-house control and data processing system.

Instrumentation

The SCDSC system is based on a Du Pont 910 DSC cell which uses a constant an heat flux plate and is shown

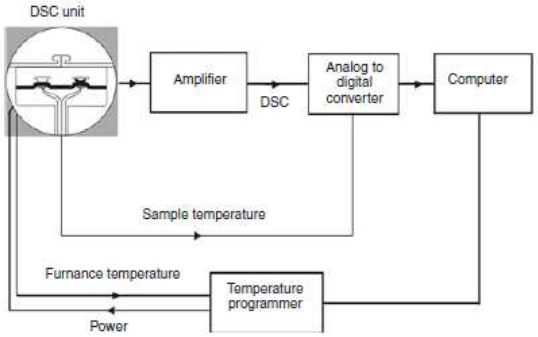

Fig. 1 Schematic diagram of SCDSC system

schematically in Fig. 1. The DSC signal is amplified using a microvolt DC-amplifier (Stanton Redcroft) and together with the sample, temperature is fed to a 22 bit USB analogue to digital converter (IOTech Data Shuttle USB/54) which also linearised the chromel–alumel sample temperature output. The furnace temperature is controlled by a digital temperature programmer (Eurotherm 818P) connected to the platinel control couple of the silver block DSC furnace. For sub-ambient work, a DSC refrigeration system has been used (TA Instrument RCS).

The data acquisition and control systems are a development of those used originally for sample controlled studies based on evolved gas techniques [13]. In addition to storing the DSC and sample temperatures, the reference temperature, furnace temperature and programmer set point temperature are also recorded.

The rate of heating is controlled directly from the DSC signal. A number of strategies relating the DSC signal to the rate of heating are available including constant reaction rate and stepwise isothermal analysis. For the initial experimental programme, an in-house technique called Proportional Heating has been used. The operation of the method depends on four main parameters. These are a maximum and minimum heating rate, a 'target' reaction rate and a function relating heating rate to reaction rate. When the reaction rate is zero, the heating rate is set to its maximum value. When the reaction rate is at, or above, the pre-set target level, heating rate is set to its minimum value. In between these limits, the heating rate is related to the reaction rate, by one of a number of possible functions. In this study, a linear relationship has been used with maximum and minimum heating rates of 5 and -5 °C min^{-1}. The choice of a negative value for the minimum heating rate means that the sample will be cooled if the specified target rate is exceeded.

The instrument was calibrated at a heating rate of 5 °C min^{-1} using the fusion of standard samples of *p*-nitrotoluene, benzil, indium, tin, lead and zinc (LGC Limited). The DSC signal was linearised for enthalpy by means of the in-house software. Regular calibration checks were made using indium. The DSC and SCDSC experiments were performed with the samples in open aluminium pans (TA Instrument Tzero) in an atmosphere of flowing nitrogen or air at a flow rate of 50 cm^3 min^{-1}. The samples were balanced for heat capacity with an equivalent amount of fused alumina powder in order to achieve minimum deflection on initial heating.

One problem with sample controlled techniques is the difficulty of making baseline corrections since the baseline for a given experiment is specific to both the sample and to the experimental conditions. The authors have addressed this by building in a facility to replay the temperature programme for an experiment. This enables a baseline to be determined under the same experimental conditions as for the sample. Thus, the experiment can be replayed with the reaction product or with empty pans.

Instrument performance and applications

The performance of the system is illustrated by studies on the thermal decomposition of sodium bicarbonate to form sodium carbonate. A typical DSC curve obtained at 5 °C min^{-1} is given in Fig. 2. The small peak preceding the main decomposition reaction has been attributed to the decomposition of surface bicarbonate [14]. Figure 3 shows an SCDSC experiment on sodium bicarbonate and illustrates the excellent temperature control obtained. It can be seen that after the onset of the main reaction, the sample initially had to be cooled to avoid exceeding the set reaction rate. This behaviour in sample controlled studies of decomposition reactions is considered to be typical of a nucleation and growth or autocatalytic mechanism [15]. Thus, sample controlled techniques can provide information on the nature of the reaction which cannot be deduced readily from thermal analysis curves obtained under linear heating conditions. The DSC and SC-DSC curves are

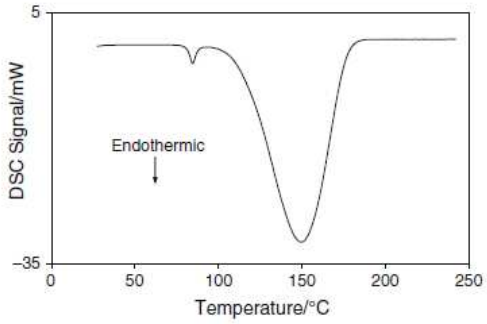

Fig. 2 DSC curve for sodium bicarbonate (Sample mass, 20 mg; heating rate, 5 °C min^{-1}; nitrogen atmosphere)

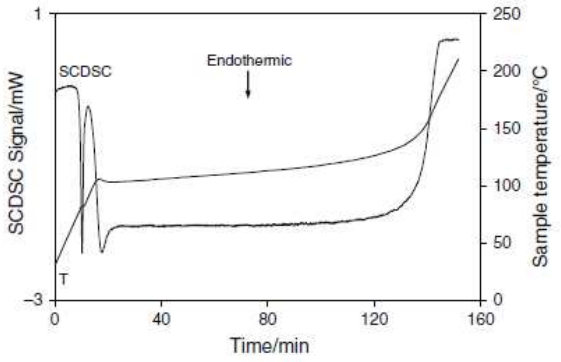

Fig. 3 SCDSC curve for sodium bicarbonate (Sample mass, 20 mg; heating rate, ± 5 °C min^{-1}; nitrogen atmosphere)

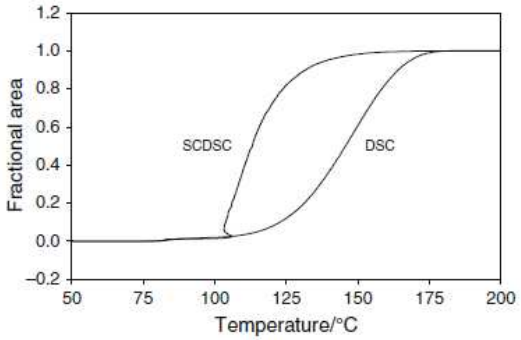

Fig. 4 Comparison of the fractional extent of reaction versus temperature plots for DSC and SCDSC experiments on sodium bicarbonate (sample mass, 20 mg; heating rate; DSC, 5 °C min^{-1}; SCDSC, ± 5 °C min^{-1}; nitrogen atmosphere)

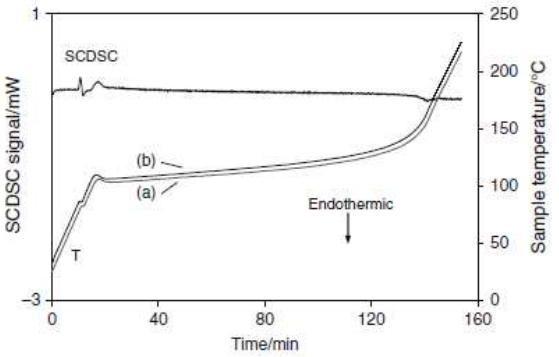

Fig. 5 SCDSC empty pan baseline obtained using replayed temperature profile from the sodium bicarbonate experiment shown in Fig. 3. *a* sodium bicarbonate SCDSC temperature profile. *b* replayed temperature profile (for clarity this has been displaced by +3 °C)

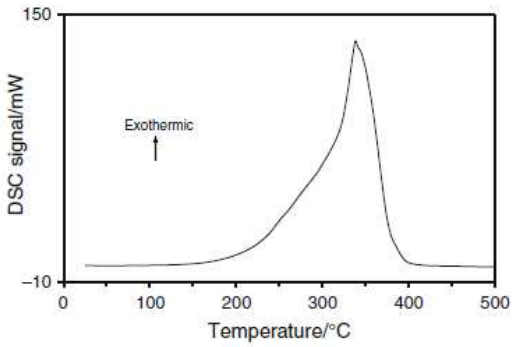

Fig. 6 DSC curve for a copper impregnated carbon (sample mass, 5 mg; heating rate, 5 °C min^{-1}; air atmosphere)

compared in Fig. 4 and show the significantly reduced temperature range over which decomposition takes place using SCDSC.

Figure 5 shows the temperature plot from the SCDSC experiment on sodium bicarbonate and the replayed temperature plot which can be seen to have closely followed the original. The DSC empty pan baseline obtained in the replayed experiment is also plotted and demonstrates the good baseline stability of the SCDSC system. This is particularly important since the heating programme is controlled by the magnitude of the deviation of the DSC signal from the baseline.

The second example is oxygen activation studies on a copper impregnated carbon formed by the pyrolysis of a copper doped carboxy methyl cellulose sample in nitrogen at 400 °C [16]. In common with a number of activated carbon precursors, this system is very reactive and gives rise to highly exothermic reactions when heated in air. This is illustrated by the DSC curve obtained using a sample mass of 5 mg (Fig. 6). The gasification reaction using aerial oxidation can therefore be difficult to control. This can result in overheating and excessive burn-off leading to a non uniform product [16].

An SCDSC experiment on the doped carbon in air is given in Fig. 7. This shows that a well controlled low temperature oxidation reaction has been obtained and that in order to achieve this, a low rate of heating has been used in the final stages. The chosen target rate has extended the oxidation reaction over a period of more than 2 h effectively eliminating self-heating problems. Thus, the technique offers the possibility of producing products of predetermined pore structure and surface area [16].

A major advantage of SCDSC is that it may be used to study reactions which take place without a mass change. This is illustrated in Fig. 8 which shows the curing of an epoxy resin with a polyaminoamide hardener (Araldite Precision) carried out under sample controlled conditions. This experiment is compared with a DSC experiment carried out on the same sample mass at 5 °C min^{-1} in Fig. 9 and again illustrates the reduced temperature range over

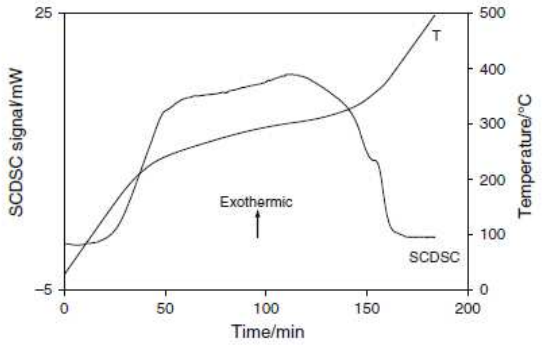

Fig. 7 SCDSC curve for a copper impregnated carbon (sample mass, 5 mg; heating rate, ± 5 °C min^{-1}; air atmosphere)

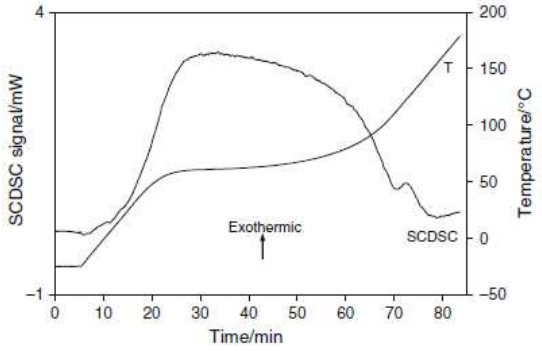

Fig. 8 SCDSC curve for an epoxy resin (sample mass, 33 mg; heating rate, ± 5 °C min^{-1}; nitrogen atmosphere)

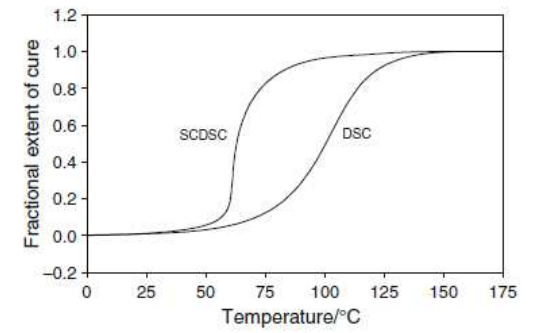

Fig. 9 Comparison of the fractional extent of cure versus temperature plots for DSC and SCDSC experiments on an epoxy resin (sample mass, 33 mg; heating rate; DSC, 5 °C min^{-1}; SCDSC, ± 5 °C min^{-1}; nitrogen atmosphere)

which a reaction takes place under sample controlled conditions. The use of SCDSC should allow the development of temperature profiles to enable samples to be cured at a selected rate.

Other areas for future study include investigation of the fusion of energy storage materials and pyrotechnic systems based on mixtures of metal powders and inorganic oxidants. In particular, work is being carried out on the very reactive zirconium-potassium perchlorate system where SCDSC has enabled the reaction to be studied at a slow controlled rate thus enabling samples to be extracted at intervals for chemical analysis.

Conclusions

A new system has been developed which for the first time has enabled the benefits of sample controlled thermal analysis to be extended to the widely used technique of DSC. This is based on a Du Pont 910 heat flux DSC cell which has been interfaced to an in-house control and data processing system. The rate of heating is controlled directly from the DSC signal and the excellent temperature control obtained using the new system is illustrated by studies on the decomposition of sodium bicarbonate and on the oxidation of a copper impregnated carbon.

The problem of making baseline corrections to sample controlled experiments has been addressed by the implementation of a facility to replay the temperature programme for an experiment. This enables a baseline to be determined under the same experimental conditions as for the sample. This facility will also be a value in enabling a suitable buoyancy correction to be applied in SCTG experiments.

The new technique has extended the range of reactions that fall within the scope of SCTA, particularly those taking place without a change in mass. This has been demonstrated by studies on the curing of an epoxy resin. It is anticipated that SCDSC will be of particular value in the study of metal-oxidant pyrotechnics where an ignition reaction can take place under linear heating conditions.

Acknowledgements The authors would like to thank Dr Steve Aubuchon of TA Instruments for the provision of a Tzero crucible press. The authors would also like to thank Dr Liz Dawson, School of Applied Sciences, University of Huddersfield, for supplying the sample of copper impregnated carbon and for helpful discussions.

References

1. Sørensen OT, Rouquerol J, editors. Sample Controlled Thermal Analysis. Dordrecht: Kluwer Academic Publishers; 2003.
2. Rouquerol J. Méthode d'analyse thermique sous faible pression et à vitesse de décomposition constante. Bull Soc Chim Fr. 1964;31–32.
3. Erdey L, Paulik F, Paulik J, Hungarian Patent No. 152197, registered October 1962, published December 1965.
4. Paulik J, Paulik F. Quasi-isothermal Thermogravimetry. Anal Chim Acta. 1971;56:328–31.

5. Sorensen OT. Thermogravimetric studies of non-stoichimetric cerium oxides under isothermal and quasi-isothermal conditions. Thermochim Acta. 1982;13:429–37.
6. Smith CS. A simple method of thermal analysis permitting quantitative measurements of specific and latent heats. Trans AIME. 1940;137:236–45.
7. Saccone A, Macchio D, Robinson JAJ, Hayes FH, Ferro R. Smith thermal analysis of selected Pr–Mg alloys. Thermochim Acta. 2001;317–318:497–502.
8. Paulik F, Bessenyey-Paulik E, Walther-Paulik K. Transformation-governed heating techniques in thermal analysis II. J Therm Anal Calorim. 1999;58:725–39.
9. Paulik F, Bessenyey-Paulik E, Walther-Paulik K. Differential thermal analysis under quasi-isothermal, quasi-isobaric conditions (Q-DTA). Examinations using "transformation-governed heating control" and "self-generated atmosphere" (TGHC-SGA). Thermochim Acta. 2003;402:105–16.
10. Paulik F, Bessenyey-Paulik E, Walther-Paulik K. Differential thermal analysis under quasi-isothermal, quasi-isobaric conditions (Q-DTA). Part II. Water evaporation and the decomposition mechanism of compounds with structural and crystal water. Thermochim Acta. 2004;424:75–82.
11. Paulik F, Bessenyey-Paulik E, Walther-Paulik K. Differential thermal analysis under quasi-isothermal, quasi-isobaric conditions (Q-DTA). Part III. Mechanism of congruent and incongruent phase transformations of salt hydrates. Thermochim Acta. 2005;430:59–65.
12. Paulik F, Bessenyey-Paulik E, Walther-Paulik K. Differential thermal analysis under quasi-isothermal, quasi-isobaric conditions (Q-DTA). Part IV. Latent error in the determination of the decomposition heat of salt hydrates decomposing congruently and incongruently. Thermochim Acta. 2005;438:76–82.
13. Barnes PA, Parkes GMB, Charsley EL. High performance evolved gas analysis system for catalyst characterization. Anal Chem. 1994;66:2226–31.
14. Dei L, Guarini GCT. The thermal decomposition of $NaHCO_3$. Renewed studies by DSC, SEM and FTIR. J Therm Anal. 1997;50:773–83.
15. Criado JM, Ortega A, Gotor F. Correlation between the shape of controlled-rate thermal analysis curves and the kinetics of solid-state reactions. Thermochim Acta. 1990;157:171–9.
16. Dawson EA, Parkes GMB, Barnes PA, Chinn MJ, Norman PR. A study of the activation of carbon using sample controlled thermal analysis. J Therm Anal Calorim. 1999;56:267–73.